SEMI-ANALYTICAL VIBRATION ANALYSIS OF AN ELASTICALLY CONNECTED NON-PRISMATIC DOUBLE-BEAM SYSTEM WITH A PASTERNAK MIDDLE LAYER

BY

AGBOOLA, OLASUNMBO OLAOLUWA
(CUGP080215)

MAY, 2017

SEMI-ANALYTICAL VIBRATION ANALYSIS OF AN ELASTICALLY CONNECTED NON-PRISMATIC DOUBLE-BEAM SYSTEM WITH A PASTERNAK MIDDLE LAYER

BY

AGBOOLA, OLASUNMBO OLAOLUWA
(CUGP080215)

MAY, 2017

SEMI-ANALYTICAL VIBRATION ANALYSIS OF AN ELASTICALLY CONNECTED NON-PRISMATIC DOUBLE-BEAM SYSTEM WITH A PASTERNAK MIDDLE LAYER

BY

AGBOOLA, OLASUNMBO OLAOLUWA
B.Sc (Ed) & M.Sc Mathematics (ILORIN)
(CUGP080215)

A THESIS SUBMITTED TO THE DEPARTMENT OF MATHEMATICS,
COLLEGE OF SCIENCE AND TECHNOLOGY, COVENANT UNIVERSITY, OTA,
OGUN STATE, NIGERIA
IN PARTIAL FULFILLMENT OF THE REQUIREMENTS FOR THE AWARD OF
DOCTOR OF PHILOSOPHY (Ph.D) DEGREE IN INDUSTRIAL MATHEMATICS

MAY, 2017

ACCEPTANCE

This is to attest that this thesis was accepted in partial fulfillment of the requirements for the award of Doctor of Philosophy (Ph.D) degree in Industrial Mathematics in the Department of Mathematics, College of Science and Technology, Covenant University, Ota, Ogun State, Nigeria.

John Ainwokhai Philip .....
(Secretary, School of Postgraduate Studies) Signature & Date

Prof. Samuel T. Wara .....
(Dean, School of Postgraduate Studies) Signature & Date

DECLARATION

I, AGBOOLA Olasunmbo Olaoluwa (CUGP080215) declare that this research was carried out by me under the supervision of Prof. Jacob A. Gbadeyan of the Department of Mathematics, University of Ilorin, Ilorin, Kwara State, Nigeria and Prof. Samuel A. Iyase of the Department of Mathematics, Covenant University, Ota, Ogun State, Nigeria. I attest that this thesis has not been presented either wholly or partly for the award of any degree elsewhere. All the sources of materials consulted in the course of this academic research are duly acknowledged.

Signed: _____ Date: _____

CERTIFICATION

We certify that this thesis titled "Semi-Analytical Vibration Analysis of an Elastically Connected Non-Prismatic Double-Beam System with a Pasternak Middle Layer" resulted from the original research carried out by AGBOOLA, Olasunmbo Olaoluwa (CUGP080215), in the Department of Mathematics, College of Science and Technology, Covenant University, Ota, Ogun State, Nigeria, under the supervision of Prof. Jacob A. Gbadeyan and Prof. Samuel A. Iyase. We have examined and found the work acceptable as part of the requirements for the award of Doctor of Philosophy (Ph.D) degree in Industrial Mathematics.

Prof. Jacob A. Gbadeyan .....
(Supervisor) Signature & Date

Prof. Samuel A. Iyase .....
(Co-Supervisor) Signature & Date

Dr. Timothy A. Anake .....
(Head of Department) Signature & Date

Prof. Folake O. Akinpelu .....
(External Examiner) Signature & Date

Prof. Samuel T. Wara .....
(Dean, School of Postgraduate Studies) Signature & Date

DEDICATION

To my father, *Moses Oladimeji Adetokunbo Agboola*,
whom I never knew
having died when I was barely 1 year, 3 months and 17 days old;
my grandmother, *Mrs. Olatunde Adeleye* (*Nee Talabi*);
my mother, who struggled hard to raise me and my siblings particularly after my father's death;
and to
all those good people, who in one way, or the other,
have helped me along, on my life's journey.

ACKNOWLEDGEMENTS

My deepest gratitude is due to God for seeing me through my doctorate degree training programme and making this thesis a reality. I could not have come this far without His enabling grace and favour! I would like to appreciate the Proprietor-base and the Management of Covenant University for the research facilities and the congenial work-environment provided.

I am heartily grateful to my supervisor, Prof. Jacob A. Gbadeyan, for his guidance and mentorship throughout the course of my doctoral programme. I am indebted to his wife, who constantly encouraged me and reminded me that I was always in her prayers. I also owe special thanks to my other supervisor, Prof. Samuel A. Iyase for his insightful comments. May God continually bless the works of their hands.

I wish to also thank the Acting Head of Department (HOD), Dr. Timothy A. Anake; the immediate-past Acting HOD, Dr. Enahoro A. Owoloko; the Departmental Postgraduate Coordinator, Dr. Sheila A. Bishop and other Departmental Examiners for their valuable comments on this thesis. Thanks are also due to Dr. Akindele Okedoye and all my colleagues in the Department for the assistance rendered. I acknowledge the assessors and the Panel of examiners for their constructive and helpful comments. I am equally grateful to the Departmental Officer, Mrs. Oluwaseun Amuleya; for assisting me in many ways and handling the paperwork.

I acknowledge the efforts of all my inspirational teachers right from my elementary school days till now. I sincerely appreciate the thoughtful gesture of Mr. & Mrs. Kolawole A. Oladimeji, Uncle Idowu Omoyele and Dr. Jimevwo G. Oghonyon. Also, I thank Dr. & Mrs. Olanrewaju Olotu (my host and hostess) for their hospitality.

I wish to gratefully thank my mother, whose toil has brought me thus far. My special gratitude goes to my wife, Olulayo, and our children– our God-given heritage for their sacrifices, unlimited tolerance and for bearing extra hardships so that I could work on this thesis. My brother and sisters also deserve many thanks for their encouragement.

TABLE OF CONTENTS

LIST OF TABLES

LIST OF FIGURES

LIST OF SYMBOLS

Symbol	Units	Description
$A_j(x)$	m^2	Area of cross-section of the jth beam at a distance x from its left-hand end
$A_j(\xi)$	$-$	non-dimensional area of cross-section of the jth beam at a distance ξ from the origin; $\xi \in [0, 1]$
$A_j(0)$	m^2	Area of cross-section of the jth beam at its left-hand end
$b_j(L)$	m	Breadth (width) of the jth beam
$b_j(x)$	m	Breadth (width) of the jth beam at a point x on the beam
$b_j(0)$	m	Breadth (width) of the jth beam at its left-hand end
E_j	$\mathrm{N\,m^{-2}}$	Young's modulus of elasticity of the jth beam
$E_jI_j(x)$	$\mathrm{N\,m^2}$	Bending stiffness of the jth beam at a distance x from its left-hand end
$G(x)$	$\mathrm{N\,m^{-2}}$	variable shear modulus of the elastic layer that connects upper and lower beams
$h_j(L)$	m	Height of the jth beam at its right-hand end
$h_j(x)$	m	Height of the jth beam at a point x on the beam
$h_j(0)$	m	Height of the jth beam at its left-hand end
$I_j(x)$	m^4	moment of inertia of the cross-section of the jth beam at a distance x from its left-hand end
$I_j(0)$	m^4	moment of inertia of the cross-section of the jth beam at its left-hand end
$I_j(\xi)$	$-$	non-dimensional moment of inertia of the cross-section of the jth beam at a distance ξ from its left-hand end
$K_{j,LR}$	$\mathrm{kg\,m^{-2}}$	stiffness of the rotational spring at the left-hand end of the jth beam
$K_{j,LT}$	$\mathrm{kg\,m^{-2}}$	stiffness of the translational spring at the left-hand end of the jth beam
$K_{j,RR}$	$\mathrm{kg\,m^{-2}}$	stiffness of the rotational spring at the right-hand end of the jth beam
$K_{j,RT}$	$\mathrm{kg\,m^{-2}}$	stiffness of the translational spring at the right-hand end of the jth beam
$k(x)$	$\mathrm{N\,m^{-2}}$	variable Winkler modulus of the elastic layer that connects upper and lower beams
L	m	length/span of each of the beams
x	m	spatial length coordinate or a position on the beam

t	s	time
$w_j(x,t)$	m	displacement of the jth beam at a distance x from its left-hand end and at time t
$Y_j(x)$	–	mode shape function of the jth beam
$Y_j(\xi)$	–	non-dimensional mode shape function of the jth beam
ξ	–	non-dimensional spatial length coordinate
ρ_j	$\mathrm{kg\,m^{-3}}$	mass density of the jth beam
$\rho_j A_j(x)$	$\mathrm{kg\,m^{-1}}$	Mass per unit length of the jth beam at a distance x from its left-hand end
$\rho_j I_j(x)$	$\mathrm{kg\,m^{3}}$	Rotatory inertia of cross-sectional area of the jth beam at a distance x from its left-hand end
$\Psi_{j,LR}$	–	non-dimensional parameter related to the stiffness of the rotational spring at the left-hand end of the jth beam
$\Psi_{j,LT}$	–	non-dimensional parameter related to the stiffness of the translational spring at the left-hand end of the jth beam
$\Psi_{j,RR}$	–	non-dimensional parameter related to the stiffness of the rotational spring at the right-hand end of the jth beam
$\Psi_{j,RT}$	–	non-dimensional parameter related to the stiffness of the translational spring at the right-hand end of the jth beam
ω_n	$\mathrm{rad\,s^{-1}}$	natural frequency for the nth mode of vibration

ABSTRACT

The analysis of free vibration characteristics of an elastically connected non-prismatic double-beam system based on both Euler-Bernoulli and Rayleigh beam theories was carried out in this study. The two beams are parallel and connected to each other by a Pasternak elastic medium which is characterized by Winkler modulus and shear modulus. For this analysis, arbitrary boundary conditions were assumed, and differential transformation method (DTM) was employed for the transformation of the coupled governing equations of motion yielding the eigenvalue problems. The natural frequencies and their corresponding mode shape functions for the system were calculated via some developed computer codes with implementation. The numerical results of the present method used were validated by comparing with the already existing ones in literature. Moreover, the effects on natural frequencies of the system produced by varying the taper ratio of the beams, Winkler modulus and shear modulus of the layer connecting the two beams as well as the mass and flexural rigidity of the upper beam were investigated in detail. It has been demonstrated that DTM can be used to analyse the free vibration of non-prismatic double-beam systems. It was found that the taper ratio of the beam, which accounts for non-uniformity of the beams in the system, had significant effects on the natural frequencies of the double-beam system. Also, it was observed that the effects on natural frequencies of the Winkler modulus and shear modulus of the Pasternak layer connecting the beams in the double-beam system largely depended on the type of the boundary conditions. Further more, it was found that all the lowest four natural frequencies of the non-prismatic double-beam system were very sensitive to the mass and the flexural rigidity of the upper beam. It is recommended, among others, that DTM can be extended to analyse free and forced vibrations of a non-prismatic double-beam system visco-elastically connected by a Pasternak layer.

Keywords: differential transformation method; double-beam system; Euler-Bernoulli beam; non-prismatic beam; Pasternak layer; Rayleigh beam.

CHAPTER ONE

INTRODUCTION

1.1 Background of the Study

Vibration is a natural phenomenon that is experienced on daily basis in our day-to-day activities. In simple terms, the "to-and-fro" or "back-and-forth" movement of an object from its normal stationary or equilibrium position is what is known as vibration. Many practical examples abound, for instance, movement of a pendulum bob, movement of a plucked guitar string, back-and-forth movement of a machine component and so on. Generally speaking, vibration concerns itself with the oscillatory motions of objects and the forces that are associated with these objects. Any object that, therefore, possesses mass and elasticity has the tendency of vibrating. For this reason, virtually all engineering structures undergo oscillatory motion to certain degrees (King, 2009).

Beams are the basic structural components in engineering which are used as simple and accurate model for complex engineering structural analysis. Vibration analysis of beams involves evaluation of their vibration characteristics, that is, natural frequencies and mode shapes. This is, therefore, important for better designing as well as to prevent resonance, which may lead to the collapse of the structure. It has been noted that carrying out preliminary dynamic analysis of beam structures will help to optimise the design and ultimately minimise future investments on repair to the barest minimum (Rezaiee-Pajand and Hozhabrossadati, 2016).

Quite a large number of investigations have been done on free and forced vibrations of single beams with uniform and non-uniform cross-section due to their useful applications in many fields of engineering. Prominent among these research endeavours are the studies done by Chun (1972), Grant (1975), Goel (1976a, 1976b), Maurizi *et al.* (1976), Hamada (1981), Kukla (1991), Gbadeyan and Oni (1994), Kukla and Posiadala

(1994), Esmailzadeh and Ghorashi (1995), Michaltsos *et al.* (1996), Wang and Lin (1996), Auciello and Maurizi (1997), Fung and Chen (1997), Foda and Abduljabbar (1998), Yeih *et al.* (1999), Rao (2000), Abu-Hilal and Mohsen (2000), Abu-Hilal and Zibdeh (2000), Kim and Kim (2001), Wu *et al.* (2001), Abu-Hilal (2003), Naguleswaran (2004), Mehri *et al.* (2009), Zamorska (2010) and Motaghian *et al.* (2011).

An extension of the concept of the single beam which is of great significance is that of the multiple or compound beam system, for instance double-beam system, triple-beam system and so on. The vibration problem of beam-type structures such as double-beam system whose members are elastically connected is still an important field of study to applied mathematicians and engineers because of its applications. The physical model of a double-beam system is usually composed of two parallel beams, prismatic (or non-prismatic as the case may be) coupled together by innumerable coupling springs (Abu-Hilal, 2006; Li and Hua, 2007).

The compound beam-type structures, one of which is double-beam system, have many applications in the engineering fields. They are extensively used to simulate bridges, guideways, railroads, overhead cranes, gun-tubes among many others. Specifically, an elastically connected double-beam system has been used to model a beam-type continuous dynamic vibration absorber (CDVA) usually used to control beam vibration. The beam-type dynamic vibration absorbing system is composed of the main beam and another beam (referred to as dynamic absorbing beam). The main and the dynamic absorbing beams are joined together by uniformly distributed springs and dampers. The dynamic absorbing beam together with the spring between the beams helps in reducing the vibratory motion undergone by the main beam of the system (Aida *et al.*, 1992; Oniszczuk, 2000; Stojanović and Kozić, 2012 and Şimşek and Cansiz, 2012).

The double-beam system has also been used to capture floating-slab railway tracks, which are widely used to control vibrations from underground trains. In this case, the

rail and the floating slab are represented by an upper and a lower beam respectively. Moreso, the railpads between the rails and the slab are simulated by a continuous layer of springs and dashpots (Hussein and Hunt, 2006). In addition, the mechanical behaviour of multi-walled carbon nanotubes in nanomechanics can also be modelled by a double-beam system (Kelly and Srinivas, 2009).

Considering the applications of the double-beam system in the fields of civil, aerospace and mechanical engineering, several studies have been carried out on problems concerning the vibration analysis of two parallel beams which are joined continuously by an elastic layer. These problems have received a significant amount of attention in the past and in recent years due to the fact that the dynamic analysis of structures helps to prevent component failure.

Researchers have used a lot of analytical and numerical methods to determine the vibration characteristics of the double-beam system. Approximate or numerical approaches are mostly used owing to difficulty posed when attempts are made to determine closed-form solutions for such structures. These methods include differential quadrature method (De Rosa and Lippiello, 2007; Arani and Amir, 2013; Arani, Amir, Dashti and Yousefi, 2014), Galerkin-type state-space method (Palmeri and Adhikari, 2011; Palmeri and Ntotsios, 2016), spectral element analysis (Li and Hua, 2007) and Adomian modified decomposition method (Mao, 2012; Mao and Wattanasakulpong, 2015). Other methods are dynamic stiffness method (Jun and Hongxing, 2008; Xiaobin *et al.*, 2014), transfer matrix method (Irie, Yamada and Kobayashi, 1982; Abbas *et al.*, 2013; 2015) and finite element method (Xin and Gao, 2011; Huang and Liu, 2013). Recently, Mirzabeigy *et al.* (2016) obtained a semi-analytical solution for free vibration analysis of two parallel and uniform (prismatic) beams connected together by variable stiffness Winkler-type elastic layer by means of differential transformation method.

In reality, it is often necessary to schematize certain structures which are used in

the field of engineering by means of non-prismatic beams in order to analyse their vibration characteristics effectively. This is very important in the modelling of real structures, especially where non-prismatic beams with variable characteristics of geometry is involved. It has been noted that non-prismatic beams, which are considered in this study, are widely used in buildings, bridges, aircraft structures and other fields of engineering in order to optimize weight, strength as well as satisfying different functional requirements (Attarnejad *et al.*, 2010).

1.2 Statement of the Problem

With respect to progress of research carried out on vibration analysis of double-beam systems so far, it is observed that researchers in the past have considered a system of elastically connected beams with a uniform cross-section where the elastic medium between the upper beam and the lower beam is simulated using Winkler model. However, based on the research report in the literature reviewed in the next chapter, and to the best of the Author's knowledge, no research has been reported on vibration analysis of double-beam system involving two non-prismatic beams which are elastically joined by a Pasternak elastic medium. It is worthy to note that Pasternak layer is more realistic than the Winkler layer in practical applications (Hamarat *et al.*, 2012).

To this end, the natural frequencies and the corresponding mode shapes of the coupled vibration of a system composed of two parallel and non-prismatic beams continuously joined by the elastic material of the Pasternak-type have been investigated in this study. The formulation of the governing equations of motion for the vibratory system is based on both Euler-Bernoulli and Rayleigh beam theories. The mathematical formulation of the problems described are presented in Chapter Three.

1.3 Aim and Objectives

The aim of this study was to present semi-analytical solutions for free vibration analysis of double-beam systems which are composed of two non-prismatic beams connected by an elastic medium simulated by a Pasternak foundation. Thus, the objectives of this study were to:

(i) determine the natural frequencies and associated mode shapes of an elastically connected non-prismatic double-beam system with a Pasternak middle layer based on Euler-Bernoulli and Rayleigh beam models;

(ii) investigate the effects on the vibration characteristics of the double-beam system described in (i) due to:

  (a) Winkler modulus and shear modulus of the layer connecting the two beams;

  (b) non-uniform cross-section parameter of the beams;

  (c) boundary conditions; and

  (d) mass and flexural rigidity of the upper beam; and

(iii) show that differential transformation method (DTM) has high precision and computational efficiency in vibration analysis of a system of two non-prismatic beams which are elastically connected by a Pasternak elastic layer.

1.4 Justification for the Study

This study is innovative in two aspects. First, unlike most studies, in which the beams were modelled as being uniform in cross-section, here due to the advantages of non-prismatic beams over prismatic beams, the former were considered. In addition, while most authors assumed Winkler model to simulate the layer connecting the two beams which is not realistic in practice, here, Pasternak model which accounts for interaction among the springs is assumed. The findings of this research would present information on free vibration of a double-beam system consisting of non-prismatic

beams coupled by Pasternak elastic medium for use as a useful reference for future study and design of such beam-type structures by structural engineers.

1.5 Significance of the Study

This study extended the frontiers of application of differential transformation method to vibration analysis of a complex structure that has practical engineering application to real-world challenges. The results of this study will be of specific interest to the engineering community. To the future researchers, this study can provide baseline information on the vibration problems undertaken in this thesis.

1.6 Scope of the Study

In structural engineering, the vibration characteristics of any structure can be defined by its modal properties which are natural frequency, mode shape, modal mass and modal damping. This study covered only two of the vibration characteristics of an elastically connected double-beam system coupled by a Pasternak elastic layer. These are the natural frequency and the mode shape of the double-beam system. Two of the vibration characteristics of the double-beam system, namely modal mass and modal damping were not considered in this study. The internal damping of the beams in the system and the layer damping were neglected. Again, this study was based on only Euler-Bernoulli and Rayleigh beam theories.

1.7 Limitation of the Study

Two of the vibration characteristics of the double-beam system, namely modal mass and modal damping were not considered in this study. In addition, this research did not investigate the forced vibration analysis of the system. Of note, the two beam models considered in this study neglected the contribution of shear deformation.

1.8 Definition of Terms

Some of the terms used in this study are adopted from Meirovitch (2001) and Rao (2004) as follows:

Definition 1.8.1. (Vibration). Vibration (also known as oscillation) is "any motion that repeats itself after an interval of time. Examples include the swinging of a pendulum and the motion of a plucked string".

Definition 1.8.2. (Prismatic beam). A prismatic beam is a beam with a uniform cross-section. It is also known as uniform beam.

Definition 1.8.3. (Non-prismatic beam). A non-prismatic beam, also referred to as a non-uniform beam, is a beam with a non-uniform cross-section.

Definition 1.8.4. (Free vibration). Free vibration is "a form of vibration that ensues if a system, after an initial disturbance, is left to vibrate on its own, without any external force acting on the system. The oscillation of a simple pendulum is an example of free vibration".

Definition 1.8.5. (Forced vibration). Forced vibration is "a form of vibration that occurs if a system is subjected to an external force", for example, a repeating type of force. For instance, the oscillation that arises in machines such as diesel engines.

Definition 1.8.6. (Out-of-phase vibration). Out-of-phase vibration is a situation when two parallel beams, coupled by a connector, vibrate asynchronously, that is in opposite direction. .

Definition 1.8.7. (In-phase vibration). In-phase vibration is a situation when both beams vibrate synchronously. As a result, the relative displacement between the two beams disappear.

Definition 1.8.8. (Amplitude). Amplitude of vibration of a vibrating body is "the maximum displacement of a vibrating body from its equilibrium position".

Definition 1.8.9. (Natural frequency). Natural frequency is the frequency at which a system vibrates in the absence of any external force.

Definition 1.8.10. (Mode shape). Mode shape of a given structure is the deformed shape that it would naturally exhibit at a particular frequency.

1.9 Organization of the Thesis

This thesis is organized into five chapters. This present introductory chapter gives the background of this study. Chapter Two presents a detailed survey of literature that bothers majorly on previous studies pertinent to the current research undertaken in this thesis. In Chapter Three, the fundamental principle of the method of solution applied in this study and the solution procedure for the vibration problems are described in detail. This covers the review of the basic notations, definitions and some theorems underlying the method. The mathematical formulation of the problems which are expressed by the equations of motion governing the vibration problems are also presented in this chapter. Chapter Four is devoted to the presentation and discussion of the research findings. Finally, Chapter Five presents a brief review of the objectives and contents of the research described in this thesis. It also features the conclusion drawn from the research based on the findings. Chapter Five also outlines the contributions of the study to knowledge in the field of vibration and recommendations for future research related to this study.

CHAPTER TWO

LITERATURE REVIEW

2.1 Introduction

In this chapter, an overview of previous studies which are relevant to the scope of this study is presented.

2.2 Survey of Related Previous Studies

The vibration problem of two beams which are elastically connected has wide application in many fields of engineering. As a result, different cases of the vibration of elastically connected double-beam systems have been studied by a number of investigators in the past. To start with, previous studies on free and forced vibrations of a single beam are first reviewed for comprehensiveness sake. The free vibration of a single beam under various supporting boundary conditions has been extensively studied for many years. Chun (1972) investigated the free vibration of a Bernoulli-Euler beam hinged at one end by a rotational spring with constant spring stiffness and with the other end free. Grant (1975) used the Newton-Raphson root finding method to solve the frequency equation for the normal modes of vibration of uniform beams with linear translational and rotational springs at one end and having a concentrated mass at the other free end. Maurizi et al. (1976) analysed the free vibration of a uniform beam hinged at one end by a rotational spring and subjected to the restraining action of a translational spring at the other end using exact expression of trigonometric and hyperbolic functions. Goel (1976) considered the vibration problem of a beam with an arbitrarily placed concentrated mass and elastically restrained against rotation at either end by using Laplace transforms. Kukla (1991) studied the free vibration of a beam supported on a stepped elastic foundation under various boundary conditions. Kukla and Posiadala (1994) also adopted the Green function to investi-

gate the free vibration of Euler-Bernoulli beams with many elastically mounted masses.

Wang and Lin (1996) investigated the dynamic analysis of beams with arbitrary boundary conditions using Fourier series. Fung and Chen (1997) studied the free and forced vibration of cantilever Euler-Bernoulli beam in contact with a rigid cylindrical foundation. Governing differential equations were developed through variational calculus and solution algorithm involved Runge-Kutta method. Yeih, *et al.* (1999) employed a dual multiple reciprocity method (MRM) to determine the natural frequencies and natural modes for an Euler-Bernoulli beam. Kim and Kim (2001) used Fourier series to obtain frequency expressions for uniform beams with generally restrained boundary conditions. An approximate solution to the transverse vibration of uniform Euler-Bernoulli beams under linearly varying axial force was presented in Naguleswaran (2004). He solved the mode shape differential equation using the method of Frobenius. Motaghian et al. (2011) developed closed form solutions to the free vibration problem of beams with mixed boundary conditions and resting on a partial elastic foundation of the Wınkler type by means of seperation of variables and Fourier series.

Hamada (1981) applied the double Laplace transformation with respect to both time and the length coordinate along the beam to solve the response problem of a simply supported and damped Euler-Bernoulli uniform beam of finite length traversed by a constant force moving at a uniform speed. He obtained an exact closed form solution for the dynamic deflection of the beam. Gbadeyan and Oni (1994) developed a theory concerning the dynamic response of Rayleigh beams and plates with arbitrary end supports and under an arbitrary number of moving concentrated masses by means of a technique based on modified generalized finite integral transform and the modified Struble's method. Esmailzadeh and Ghorashi (1995) investigated the dynamic behaviour of a beam under simply supported end boundary conditions carrying a uniform partially distributed moving mass or force. They employed the central difference expansions technique to solve the governing differential equation. Michaltsos *et al.*,

(1996) studied the linear dynamic response of a simply supported uniform beam under a moving load of constant magnitude and velocity, including the effect of its mass. Foda and Abduljabbar (1998) determined the dynamic deflection of an undamped simply supported Euler-Bernoulli beam of finite length under the action of a moving mass at constant speed using a Green function approach.

Abu-Hilal and Mohsen (2000) treated the transverse vibrations of homogeneous isotropic Euler-Bernoulli beams with general boundary conditions subjected to a constant force travelling with different types of motion. He studied the effects of boundary conditions, type of motion and damping on the response of the beams. In 2003, he used a Green function approach to determine the dynamic response of Euler-Bernoulli beam subjected to distributed and concentrated loads. Wu *et al.* (2001) used combined finite element and analytical methods to determine the dynamic responses of structures to moving bodies. The technique was used to study the response of a clamped-clamped beam subjected to a single mass moving along the beam. Mehri, *et al.* (2009) used a dynamic Green function to assess the effects of different boundary conditions, velocity of load and other parameters on the linear dynamic response of Euler-Bernoulli uniform beams excited by a moving load. Zamorska (2010) used the Green's function method to solve the free vibration problem of non-uniform Bernoulli-Euler beams. An approximate approach for the vibration problem of non-uniform Bernoulli-Euler beams had earlier been presented by Auciello and Maurizi (1997).

In the study carried out by Lee *et al.* (2014), the free vibrations of a prismatic beam resting on a Pasternak foundation were studied with emphasis placed on the bending-twist deformations of the beam. The analysis was carried out by combining both the Runge-Kutta and Regula-Falsi methods. The effects of the foundation stiffnesses, among other parameters, on the natural frequencies of the beam were investigated. It was found that the natural frequencies of the beam increase with the increase in the stiffnesses of Winkler and shear foundation. Ahmadi and Nikkhoo

(2014) studied the vibration behaviour of a non-uniform Euler-Bernoulli beam traversed by a moving load and a moving mass. The eigenfunction expansion method was used to transform the equations governing the motion of the beam into a system of linear time-varying ordinary differential equations. Thereafter, the authors made use of three function sets as the assumed vibration mode functions in determining the natural frequencies of the beam. These functions included, a set of mode shape functions of uniform beams with similar boundary conditions, a set of orthogonal polynomial functions, and a set of non-orthogonal polynomial functions. It was found that the values of natural frequencies obtained using non-orthogonal polynomials are the same with those obtained using non-orthogonal polynomials which implies that the orthogonalization of the beam's characteristic polynomials has no effect on the results. Abdelghany *et al.* (2015), in their study, used the differential transformation method to determine the natural frequencies and mode shapes of non-uniform circular beam. It was shown that variation of cross section has a substantial effect on the mode shapes of the circular beams as against the mode shapes of rectangular beams.

One of the earlier studies on double-beam systems was undertaken by Seelig and Hoppmann II (1964a), who presented the frequencies and associated mode shapes of a system of n elastically connected parallel beams having different support conditions. They used the result obtained for the general n-system to give detail analysis of the particular case of a two-beam system. Later, the authors in another research, developed and solved the differential equations of motion governing the vibration of an elastically connected double-beam system under the action of a spontaneous load. (Seelig and Hoppmann II, 1964b). Dublin and Friedrich (1956) and Osborne (1962), as cited in Seelig and Hoppmann II (1964b), had earlier studied the application of beam theory to the vibration of elastically coupled double-beam systems. The resonance conditions for an elastically double-beam system in which one of the beams is subjected to a moving point load oscillating longitudinally along the beam about a fixed point were derived by Kessel (1966). It was observed that an infinite number of load-movement

frequencies that will stimulate a given principal frequency of the double-beam system for the rth mode of vibration exists. Kessel and Raske (1967) examined the damped vibratory motion of an elastically connected double-beam system when it is disturbed by a moving point-load. The oscillation of the moving point-load is in the same direction as that of one of the members about a fixed point. The effects of damping, frequency of oscillation of load movement, amplitude of load movement, and modulus of the elastic connectors on the dynamic deflections of the system were assessed. Their results revealed that the double-beam system possesses the quality to function as an elastic vibration absorber.

Rao (1974) solved the differential equations governing the flexural vibrations of systems of elastically connected parallel bars to determine the natural frequencies and mode shapes of particular three- and two-beam systems. His analysis was based on the Timoshenko model and as such the effects of rotatory inertia and shear deformation were considered. Chonan (1976) investigated the dynamical responses of two beams connected with a set of independent springs and subjected to an impulsive load. The effect of the mass of the springs was taken into consideration. The method of the Laplace transformations with respect to both time and space variables was employed in solving the vibration problem. The numerical example considered to illustrate the theory involved application of a concentrated half—sine impulsive force to the mid-point of the upper beam of the system. The findings of the study indicated that the periods become longer and the amplitudes become smaller when the mass of the springs is increased. It was further found that an increase in the mass of the springs that connect the two beams make the difference in the response between the upper and the lower beams to be well pronounced, despite the fact that the amplitudes of both beams are nearly the same. Kukla and Skalmierski (1994) solved the problem of free vibration of a system of two prismatic Euler-Bernoulli beams which are coupled by a Winkler elastic layer. The solutions for different types of boundary conditions were presented.

Vu *et al.* (2000) utilized modal analysis to obtain a closed-form solution for the vibration of a damped uniform Euler-Bernoulli double-beam system. The system which consisted of a main beam, an auxiliary beam, with a distributed spring and dashpot in parallel between the two beams was subjected to harmonic excitation. It was found that each natural mode consists of two submodes namely the in-phase submode and the out-of-phase submode. The in-phase submode was described as the mode whose values of natural frequencies are not influenced by stiffness and damping. For the out-of-phase mode, increase in stiffness causes the natural frequencies to increase. Oniszczuk (2000) developed the free transverse theory of an elastically connected simply supported double-beam system continuously joined by a Winkler elastic layer. The motion of the system was solved using the Bernoulli-Fourier method. Oniszczuk (2003) used the modal expansion method to study the forced transverse vibration analysis of an elastically connected simply supported double-beam system. The excitation loadings considered included the stationary harmonic loads and moving concentrated forces. Abu-Hilal (2006) studied the dynamic response of a double-beam system subjected to a constant moving load under a simply supported end configuration. The influence of the moving speed of the load, the damping as well as the elasticity of the viscoelastic layer (used to join the two beams) on the dynamic responses of the two beams were determined.

Zhang *et al.* (2008a) studied the properties of free transverse vibration of a double beam system using Bernoulli–Euler beam model. The classical Bernoulli–Fourier method was used to formulate the equations governing the motion of the double-beam system with the assumption that both beams were simply supported and elastically connected by a Winkler-type layer. The authors also investigated the influence of compressive axial loading on the vibration characteristics of the system. Zhang *et al.* (2008b) studied the effects of compressive axial load on the forced vibrations of an elastically connected double-beam system. Their analysis was based on the

Bernoulli-Euler beam model having simply supported boundary conditions while the two beams of the system were connected by a Winkler elastic layer. It was found that the magnitudes of the steady-state vibration amplitudes of the two beams depend on the axial compression. Palmeri and Adhikari (2011) employed a Galerkin-type state-space technique to investigate the transverse vibrations of a system of two parallel Euler-Bernoulli elastic beams continuously joined by a Winkler-type viscoelastic layer. Ariaei *et al.* (2011) studied the dynamic response of an elastically connected multi-beam system using the Timoshenko beam theory. The authors employed change of variables to decouple the equations of motion and later used modal analysis to obtain the dynamic response of beams caused by a moving load. Then, the modal expansion method in conjunction with the transfer matrix method was used to obtain closed-form solution to the eigenvalue problem that arose from the vibration problem. The study involved identical prismatic beams with the restriction that the boundary conditions on the same side of the system must be similar. It was found that the maximum deflection of the multiple Timoshenko beam system is always lower than that of a single beam. It was also found that the values of the frequencies increase by increasing the stiffness of the springs, as expected.

Mao (2012) employed Adomian modified decomposition method to study the free vibrations of elastically connected beams under general conditions. The system considered was composed of uniform Euler-Bernoulli beams which are continuously joined by a Winkler-type elastic layer. Gbadeyan and Agboola (2012) applied the finite Fourier and Laplace integral transformations to analyse the dynamic behavior of a Rayleigh double-beam system traversed by a uniform partially distributed moving load. The system is made up of two identical, parallel simply-supported Rayleigh beams of equal length. The two beams are constant in cross-section and are continuously connected by a Winkler viscoelastic layer. It was found that increasing the value of the rotatory inertia caused the maximum displacement of the upper beam to also increase. Earlier, Gbadeyan *et al.* (2005) investigated dynamic behaviour of visco-elastically connected

double-beam system carrying uniform partially distributed moving masses based on Euler-Bernoulli theory.

The free and forced vibration analyses of two parallel prismatic beams connected to each other by uniformly distributed vertical springs were investigated by Huang and Liu (2013). The inner springs were also stimulated using Winkler model. Using finite element method for the analysis, it was found that the inner spring with large coefficient has a significant effect on the natural frequencies of out-of-phase vibration. Abbas *et al.* (2013) employed the transfer matrix method to determine the free vibration characteristics of a double-beam system composed of two identical, elastic and uniform Euler-Bernoulli beams coupled by a spring. It was observed that the two beams connected elastically by a spring show symmetric and anti-symmetric vibrations. Rezaiee-Pajand and Hozhabrossadati (2016) investigated the free vibration analysis of a double-beam system whereby the system was composed of two beams connected by a mass-spring device with each beam having elastic restraints at one end and free at the other end. The eigenvalue of the problem was obtained in the frequency domain by using Fourier transform.

Stojanović and Kozić (2012) studied the vibration characteristics of forced transverse vibration and buckling of an elastically connected simply supported double-beam system based on the Timoshenko beam theory, under compressive axial loading. The classical modal expansion method was used for the analysis. The influence of compressive axial load on the forced vibrations of the double-beam system were critically examined for three identified cases of excitation loadings namely stationary harmonic loads, uniformly distributed harmonic load and harmonic concentrated force. It was observed that the magnitudes of the steady-state vibration amplitudes of the two beams are dependent on the influence of rotary inertia and shear and axial compression. Specifically, it was found that the magnitudes of the steady-state vibration amplitudes of the two beams become larger as the axial compression increases and even larger

when the effect of rotary inertia and shear were taken into consideration. The authors argued that the Rayleigh and Timoshenko beam-type dynamic absorber could be used to reduce the incidence of excessive vibrations of corresponding beam systems.

Pavlović *et al.* (2012) used direct Lyapunov method to study the stability and instability of a prismatic Bernoulli-Euler double-beam system subjected to compressive axial loadings. The two beams in the system were both simply supported at their ends and continuously joined by a Winkler elastic layer. It was concluded that stability regions are almost identical for Gaussian and harmonic processes considered in the paper when the stiffness of the Winkler layer was increased while the uncertainty regions increased with increment of the Winkler layer stiffness. The free vibration and stability of a cantilever uniform double-beam system continuously joined by a Winkler-type elastic layer was investigated by Mao and Wattanasakulpong (2015) using the Adomian modified decomposition method. The free end of each beam in the system was restrained by a translational spring and subjected to a combination of compressive axial and follower loads. It was found that the natural frequencies tend to zero as the concentrated compressive loads increase and this situation was described as divergence instability of the system.

Recently, Li *et al.* (2016) used a semi-analytical method to obtain the natural frequencies and corresponding mode shapes of a double-beam system interconnected by a viscoelastic layer of the Winkler type. They further studied the effects of viscoelastic layer damping and Winkler layer on the vibration characteristics of the double-beam system. It was reported that the dynamic responses of upper beam decrease while the responses of lower beam increase with the increase in the stiffness of viscoelastic layer. It was also found that the dynamic responses of the lower beam decrease significantly with the increase of the mass of the upper beam. In addition, it is found that the dynamic responses of lower beam decrease while those of the upper beam increase with the increase of Winkler layer stiffness. Mirzabeigy *et al.* (2016)

used DTM to analyse free vibration of two identical parallel uniform beams attached together by variable stiffness Winkler-type elastic layer based on Euler–Bernoulli beam theory. It was found that odd mode frequencies of the two beams having the same boundary conditions remain constant for different values of stiffness of the Winkler layer that connects the two beams while the even mode frequencies were reported to be sensitive to variation of the stiffness of the connecting layer. Also, it was noted that the fundamental frequency of the system was not affected by distribution type of connecting layer when the total stiffness of connecting layer has a small value.

Virtually, all the above studies assumed that the two beams that make up the double-beam system are prismatic, having a uniform cross-section. An interesting research on double system is the investigation carried out by Frýba *et al.* (2007). A beam with an axial force and a pretensiled string coupled with by an elastic layer of Winkler type and subjected to a row of moving forces was used to model a prestressed bridge. The vibration problem was solved by using the Fourier and Laplace-Carson integral transformation methods. The authors noted that the prestressed bridges widely used for highway and railway bridges of small and medium spans, form naturally a double system with two elements namely beam and pretensiled strings which are bound together with an elastic layer and dampers to diminish the dynamic response.

The recent study on vibration analysis of Rayleigh double-beam system which used the Pasternak model to simulate the elastic layer that connects the two beams was reported by Mohammadi and Nasirshoaibi (2015). They used the modal expansion method for the analysis and studied the effects of Pasternak layer on the forced vibrations of the double-beam system for the case of simply supported boundary conditions for the two beams. It was found that the magnitudes of the steady-state vibration's amplitudes become smaller when the shear Pasternak modulus increases. This reportedly implies that a Pasternak layer has the ability to reduce the magnitudes of the steady-state vibration's amplitudes more than a Winkler elastic layer. The

forced transverse vibration analysis of a closed double single-walled carbon nanotube system containing a fluid, based on the Rayleigh beam theory was carried out by Nasirshoaibi *et al.* (2015) in a later study. The authors assumed that the two single-walled carbon nanotubes are continuously joined by a Pasternak layer and the effect of compressive axial load on the forced vibrations of the double-nanotube system was investigated. It was found that the magnitudes of the steady-state vibration amplitude of the upper and lower nanotubes that make up the system decrease and increase, respectively when the axial compression becomes larger. It was also reported that the amplitudes of the steady-state vibration of the two beams decrease with the increase of shear modulus of the Pasternak layer for different axial compression ratios. It was noted that Mohammadi and Nasirshoaibi together with their co-authors assumed that the cross-section of the two beams was uniform. Mirzabeigy *et al.* (2017) used the Bernoulli-Fourier method to analyse the free vibration of a double-beam system which is elastically connected by a Winkler-type layer. The authors based their solutions on the assumption that the two beams are uniform and that they can have different cross sections or made from different materials. Also, the analysis required that the boundary conditions of both the upper and lower beams must be the same.

From an overall point of view, it has been observed from the above literature that no research has been done to investigate the free vibration analysis of a system of two non-prismatic beams coupled by a Pasternak elastic layer. To the best of author's knowledge, no report has been published in the literature in this perspective. Thus in this thesis, the free vibration of a non-prismatic double-beam system connected by a Pasternak elastic layer under different boundary conditions is reported.

CHAPTER THREE

METHODOLOGY

3.1 Introduction

This chapter discusses the methodology of the research presented in this thesis. Firstly, the basic idea and principles of the method of solution employed in solving the vibration problems are provided. Vibration analysis of systems involving uniform beams can be done using analytical methods. However, it often becomes difficult, if not impossible to find a suitable analytical method when the cross-section of the beam is non-prismatic along its length. In this chapter, a semi-analytical technique known as differential transformation method is presented for solving the vibration problems proposed in Chapter One. The subsequent sections explicate the mathematical formulation of the vibration problems and the implementation of the solution procedures.

3.2 Description of Method of Solution: Differential Transformation Method (DTM)

The goal of this section is to recall notations, definitions and review some theorems of the DTM that were used in this study. These are comprehensively discussed in Chen and Ho (1996, 1999), Hassan (2002, 2008), Ayaz (2004), Ho and Chen (1998) and Ozgumus and Kaya (2006). Also, the main steps of implementing the DTM in solving differential equations will be highlighted.

Meanwhile, different types of solution procedures have been used to solve eigenvalue problem which results from vibration analysis and other classes of problems. Among the methods that have been used in the previous studies reported in the available literature include the finite element method, the Frobenius method of series (Naguleswaran, 1991 and 2004), variational techniques such as Rayleigh Ritz and

Galerkin methods, generalized method of finite integral transformation, the Laplace transformation, the classical Bernoulli Fourier method, the classical modal expansion method, an exact dynamic stiffness method, the finite difference method, the perturbation technique, Adomian decomposition method, Modified Adomian Decomposition Method (Hsu *et al.*, 2008), He's variational iteration method (Liu and Gurram, 2009), singular value decomposition method (Yieh *et al.*, 1999) etc, may be found in literature. The existing techniques have difficulties in relation to the size of computational work, especially when the system has several partial differential equations.

The differential transformation method (DTM) is a semi-analytical technique that is based on the well-known Taylor series expansion. The method was first introduced and used by Zhou in 1986 to study electrical circuits (Chen and Ho, 1996; Ho and Chen, 1998; Malik and Dang, 1998). Some of the advantages of the DTM are that it is very simple to implement and also has a high level of accuracy (Kaya, 2006). It has also been noted that DTM yields an analytical solution to given problem in the form of a polynomial. One of the major differences between DTM and the traditional higher order Taylor series method is that it does not require the symbolic computation of derivatives of the data functions.

The methodology has been organized into the following stages:

(i) First, obtain the non-dimensional form of the governing equations of motion and the boundary equations;

(ii) Use the definition and properties of the differential transformation to transform the non-dimensional form of both the governing equations and the boundary conditions;

(iii) Obtain the recurrence relations of the non-dimensional governing equations and combine them with the boundary conditions to obtain the transformed solution to the vibration problem; and

(iv) Finally, obtain the inverse of the transformed solution.

DTM involves applying some transformation rules to the governing differential equations together with the boundary conditions associated with them. By so doing, we obtain a set of algebraic equations in terms of the differential transforms of the original functions and the desired solution is obtained by solving these algebraic equations. An important merit that DTM has over Taylor series method is that it does not require symbolic computation of derivatives which might be very expensive when large orders are involved.

The differential transformation of the rth derivative of a function, $y(\xi)$, is defined as follows: (Chen and Ho, 1996; Ho and Chen, 1998; Arikoglu and Ozkol, 2005; Abazari and Abazari, 2009 and other references)

$$\bar{Y}(r) = \frac{1}{r!}\left[\frac{d^r y(\xi)}{d\xi^r}\right]_{\xi=0} \tag{3.1}$$

where $y(\xi)$ is the original function and $\bar{Y}(r)$ is the rth order differential transformation of $y(\xi)$. The inverse differential transformation of $\bar{Y}(r)$ is defined as follows:

$$y(\xi) = \sum_{r=0}^{\infty} \xi^r \bar{Y}(r) \tag{3.2}$$

Substituting equation (3.1) into equation (3.2), we have

$$y(\xi) = \sum_{r=0}^{\infty} \frac{\xi^r}{r!}\left[\frac{d^r y(\xi)}{d\xi^r}\right]_{\xi=0} \tag{3.3}$$

which is the Taylor series of $y(\xi)$ at $\xi = 0$. Equation (3.3) implies that the concept of differential transformation is obtained from the Taylor series expansion. However, it is important to remark that DTM does not require the symbolic calculation of the derivatives. This is one of the advantages that DTM holds over higher-order Taylor series method. In practical applications, the function, $y(\xi)$, is often expressed by the

finite-term series

$$y(\xi) = \sum_{r=0}^{M} \xi^r \bar{Y}(r) \tag{3.4}$$

where the value of M is determined by the convergence of the natural frequencies. Equation (3.4) implies that

$$\sum_{r=M+1}^{\infty} \xi^r \bar{Y}(r)$$

is very small so that its value can be neglected.

The fundamental theorems (proofs included) of the dimensional transform which are veritable tools used for the transformation of the governing equations and the associated boundary conditions are as listed below: (Arikoglu and Ozkol, 2005; Mirzabeigy, 2014).

Theorem 3.2.1. If $f(\xi) = g(\xi) \pm h(\xi)$, then

$$\bar{F}(r) = \bar{G}(r) \pm \bar{H}(r). \tag{3.5}$$

Proof. From the definition (3.1), we can write

$$\bar{G}(r) = \frac{1}{r!}\left[\frac{d^r g(\xi)}{d\xi^r}\right]_{\xi=0}, \tag{3.6}$$

and

$$\bar{H}(r) = \frac{1}{r!}\left[\frac{d^r h(\xi)}{d\xi^r}\right]_{\xi=0}. \tag{3.7}$$

Suppose that

$$f(\xi) = g(\xi) + h(\xi). \tag{3.8}$$

Therefore,

$$\bar{F}(r) = \frac{1}{r!}\left\{\frac{d^r}{d\xi^r}\left[g(\xi)+h(\xi)\right]\right\}\Big|_{\xi=0}, \tag{3.9}$$

which can be put in the form

$$\bar{F}(r) = \frac{1}{r!}\left[\frac{d^r g(\xi)}{d\xi^r}\right]_{\xi=0} + \frac{1}{r!}\left[\frac{d^r h(\xi)}{d\xi^r}\right]_{\xi=0}. \tag{3.10}$$

Hence, by equations (3.6) and (3.7), it follows that

$$\bar{F}(r) = \bar{G}(r) + \bar{H}(r). \tag{3.11}$$

Similarly, it can be proved that

$$\bar{F}(r) = \bar{G}(r) - \bar{H}(r). \tag{3.12}$$

for

$$f(\xi) = g(\xi) - h(\xi). \tag{3.13}$$

Hence,

$$\bar{F}(r) = \bar{G}(r) \pm \bar{H}(r),$$

as required. □

Theorem 3.2.2. If $f(\xi) = \lambda g(\xi)$, then

$$\bar{Y}(r) = \lambda \bar{G}(r), \tag{3.14}$$

where λ is an arbitrary constant.

Proof. Suppose that

$$f(\xi) = \lambda g(\xi). \tag{3.15}$$

Thus,

$$\bar{F}(r) = \frac{1}{r!}\left\{\frac{d^r}{d\xi^r}\left[\lambda g(\xi)\right]\right\}\Big|_{\xi=0} \tag{3.16}$$

or

$$\bar{F}(r) = \lambda\frac{1}{r!}\left[\frac{d^r g(\xi)}{d\xi^r}\right]_{\xi=0} \tag{3.17}$$

Using equation (3.6) in (3.17), one obtains

$$\bar{F}(r) = \lambda\bar{G}(r). \tag{3.18}$$

This completes the proof. □

Theorem 3.2.3. If $f(\xi) = \dfrac{dg(\xi)}{d\xi}$, then

$$\bar{F}(r) = (r+1)\bar{G}(r+1). \tag{3.19}$$

Proof. Given that

$$f(\xi) = \frac{dg(\xi)}{d\xi}. \tag{3.20}$$

Thus,

$$\bar{F}(r) = \frac{1}{r!}\left\{\frac{d^r}{d\xi^r}\left[\frac{dg(\xi)}{d\xi}\right]\right\}\Big|_{\xi=0}, \tag{3.21}$$

which is equivalent to

$$\bar{F}(r) = \frac{1}{r!}\left[\frac{d^{r+1}g(\xi)}{d\xi^{r+1}}\right]_{\xi=0}. \tag{3.22}$$

From the definition (3.1), we have

$$\left.\frac{d^r y(\xi)}{d\xi^r}\right|_{\xi=0} = r!\bar{Y}(r) \tag{3.23}$$

which implies that

$$\left.\frac{d^{r+1} g(\xi)}{d\xi^{r+1}}\right|_{\xi=0} = (r+1)!\bar{G}(r+1). \tag{3.24}$$

Using equation (3.24) in (3.22) gives

$$\bar{F}(r) = \frac{(r+1)!}{r!}\bar{G}(r+1). \tag{3.25}$$

Equation (3.25) reduces to

$$\bar{F}(r) = (r+1)\bar{G}(r+1). \tag{3.26}$$

The result follows. □

Theorem 3.2.4. If $f(\xi) = \dfrac{d^2 g(\xi)}{d\xi^2}$, then

$$\bar{F}(r) = (r+1)(r+2)\bar{G}(r+2). \tag{3.27}$$

Proof. Given that

$$f(\xi) = \frac{d^2 g(\xi)}{d\xi^2}. \tag{3.28}$$

Thus,

$$\bar{F}(r) = \frac{1}{r!}\left\{\frac{d^r}{d\xi^r}\left[\frac{d^2 g(\xi)}{d\xi^2}\right]\right\}\Bigg|_{\xi=0}$$

$$= \frac{1}{r!}\left[\frac{d^{r+2} g(\xi)}{d\xi^{r+2}}\right]_{\xi=0}.$$

From the definition (3.1), we have

$$\left.\frac{d^r y(\xi)}{d\xi^r}\right|_{\xi=0} = r!\bar{Y}(r) \tag{3.29}$$

Thus,

$$\bar{F}(r) = \frac{(r+2)!}{r!}\bar{G}(r+2), \tag{3.30}$$

or

$$\bar{F}(r) = (r+1)(r+2)\bar{G}(r+2). \tag{3.31}$$

This completes the proof. □

Theorem 3.2.5. If $f(\xi) = \dfrac{d^n g(\xi)}{d\xi^n}$, then

$$\bar{F}(r) = (r+1)(r+2)\dots(r+n)\bar{G}(r+n). \tag{3.32}$$

Proof. The proof of this theorem follows analogously from the proofs of theorems 3.2.3 and 3.2.4. □

Theorem 3.2.6. If $f(\xi) = g(\xi)h(\xi)$, then

$$\bar{F}(r) = \sum_{s=0}^{r} \bar{G}(s)\bar{H}(r-s), \tag{3.33}$$

or

$$\bar{F}(r) = \sum_{s=0}^{r} \bar{G}(r-s)\bar{H}(s). \tag{3.34}$$

Proof. Given that

$$f(\xi) = g(\xi)h(\xi). \tag{3.35}$$

Thus,

$$\bar{F}(r) = \frac{1}{r!} \left\{ \frac{d^r}{d\xi^r} \left[g(\xi) h(\xi) \right] \right\} \Big|_{\xi=0} \tag{3.36}$$

By using Leibniz's formula for the rth derivative of a product of functions, the expression in the parentheses of equation (3.36) can be expressed as

$$\frac{d^r}{d\xi^r} \left[g(\xi) h(\xi) \right] = \sum_{s=0}^{r} \binom{r}{s} \frac{d^s}{d\xi^s} \left[g(\xi) \right] \frac{d^{r-s}}{d\xi^{r-s}} \left[h(\xi) \right], \tag{3.37}$$

where

$$\binom{r}{s} = \frac{r!}{s!\,(r-s)!} \tag{3.38}$$

is the binomial coefficient.

Thus,

$$\left[\frac{d^r}{d\xi^r} \left[g(\xi) h(\xi) \right] \right]_{\xi=0} = \sum_{s=0}^{r} \binom{r}{s} \left[s! \bar{G}(s) \right] \left[(r-s)! \bar{H}(r-s) \right], \tag{3.39}$$

noting that

$$\left[\frac{d^s g(\xi)}{d\xi^s} \right]_{\xi=0} = s! \bar{G}(s), \tag{3.40}$$

and

$$\left[\frac{d^{e-s} h(\xi)}{d\xi^{r-s}} \right]_{\xi=0} = (r-s)! \bar{H}(r-s). \tag{3.41}$$

Equation (3.39) can be expressed as

$$\left[\frac{d^r}{d\xi^r} \left[g(\xi) h(\xi) \right] \right]_{\xi=0} = \sum_{s=0}^{r} \binom{r}{s} s!(r-s)! \bar{G}(s) \bar{H}(r-s), \tag{3.42}$$

which, after simplification, becomes

$$\left[\frac{d^r}{d\xi^r} \left[g(\xi) h(\xi) \right] \right]_{\xi=0} = \sum_{s=0}^{r} r! \bar{G}(s) \bar{H}(r-s). \tag{3.43}$$

Using equation (3.43) in equation (3.36), we have

$$\bar{F}(r) = \sum_{s=0}^{r} \bar{G}(s)\bar{H}(r-s). \tag{3.44}$$

as required. □

Theorem 3.2.7. If $f(\xi) = g(\xi)\dfrac{d^2h(\xi)}{d\xi^2}$, then

$$\bar{F}(r) = \sum_{s=0}^{r} \bar{G}(r-s)(s+1)(s+2)\bar{H}(s+2). \tag{3.45}$$

Proof. The result of this theorem can be established by using theorems 3.2.5 and 3.2.6. □

Theorem 3.2.8. If $f(\xi) = g(\xi)\dfrac{d^nh(\xi)}{d\xi^n}$, then

$$\bar{F}(r) = \sum_{s=0}^{r} \bar{G}(s-r)(s+1)(s+2)\dots(s+n)\bar{H}(s+n). \tag{3.46}$$

Proof. Similar to the proof of theorem 3.2.7. □

Theorem 3.2.9. If $f(\xi) = \dfrac{d^mg(\xi)}{d\xi^m}\dfrac{d^nh(\xi)}{d\xi^n}$, then

$$\bar{F}(r) = \sum_{s=0}^{r} (r-s+1)(r-s+2)\dots(r-s+m)\bar{G}(r-s+m)(s+1)(s+2)\dots(s+n)\bar{H}(s+n). \tag{3.47}$$

Proof. The proof is analogous to that of theorem 3.2.6. □

Theorem 3.2.10. If $f(\xi) = \xi^n$, then

$$\bar{F}(r) = \delta(r-n) = \begin{cases} 0 & \text{if } r \neq n; \\ 1 & \text{if } r = n. \end{cases} \tag{3.48}$$

The above-listed theorems are often used in the transformation of the equations of

motion as used in this analysis. In a similar manner, some of the basic theorems (with their proofs) that are used in the transformation of the boundary conditions are as follows (Arikoglu and Ozkol, 2005):

Theorem 3.2.11. If $f(0) = 0$, then

$$\bar{F}(0) = 0. \tag{3.49}$$

Proof. From the definition (3.1), it follows that

$$\bar{F}(r) = \frac{1}{r!}\left[\frac{d^r f(\xi)}{d\xi^r}\right]_{\xi=0}. \tag{3.50}$$

Thus,

$$\begin{aligned}\bar{F}(0) &= \frac{1}{0!}\left[\frac{d^0 f(\xi)}{d\xi^0}\right]_{\xi=0} \\ &= [f(\xi)]_{\xi=0} \\ &= 0,\end{aligned}$$

as required. □

Theorem 3.2.12. If $\left.\frac{df(\xi)}{d\xi}\right|_{\xi=0} = 0$, then

$$\bar{F}(1) = 0. \tag{3.51}$$

Proof. Putting $r = 1$ in (3.50), we have

$$\begin{aligned}\bar{F}(1) &= \frac{1}{1!}\left[\frac{df(\xi)}{d\xi}\right]_{\xi=0} \\ &= \left[\frac{df(\xi)}{d\xi}\right]_{\xi=0} \\ &= 0.\end{aligned}$$

□

Theorem 3.2.13. If $\left.\dfrac{d^2 f(\xi)}{d\xi^2}\right|_{\xi=0} = 0$, then

$$\bar{F}(2) = 0. \tag{3.52}$$

Proof. From equation (3.50), we have

$$\begin{aligned}
\bar{F}(2) &= \frac{1}{2!}\left[\frac{d^2 f(\xi)}{d\xi^2}\right]_{\xi=0} \\
&= \frac{1}{2}\left[\frac{d^2 f(\xi)}{d\xi^2}\right]_{\xi=0} \\
&= 0.
\end{aligned}$$

□

Theorem 3.2.14. If $\left.\dfrac{d^3 f(\xi)}{d\xi^3}\right|_{\xi=0} = 0$, then

$$\bar{F}(3) = 0. \tag{3.53}$$

Proof. Substituting $r = 3$ into equation (3.50) yields

$$\begin{aligned}
\bar{F}(3) &= \frac{1}{3!}\left[\frac{d^3 f(\xi)}{d\xi^3}\right]_{\xi=0} \\
&= \frac{1}{6}\left[\frac{d^3 f(\xi)}{d\xi^3}\right]_{\xi=0} \\
&= 0.
\end{aligned}$$

□

Theorem 3.2.15. If $f(1) = 0$, then

$$\sum_{r=0}^{\infty} \bar{F}(r) = 0. \tag{3.54}$$

Proof. By equation (3.2), we have

$$f(\xi) = \sum_{r=0}^{\infty} \xi^r \bar{F}(r). \tag{3.55}$$

Plugging $\xi = 1$ in equation (3.55) gives

$$f(1) = \sum_{r=0}^{\infty} \bar{F}(r). \tag{3.56}$$

So,

$$\sum_{r=0}^{\infty} \bar{F}(r) = 0. \tag{3.57}$$

□

Theorem 3.2.16. If $\left.\frac{df(\xi)}{d\xi}\right|_{\xi=1} = 0$, then

$$\sum_{r=0}^{\infty} r\bar{F}(r) = 0. \tag{3.58}$$

Proof. Differentiating equation (3.55) with respect to ξ once yields

$$\frac{df(\xi)}{d\xi} = \sum_{r=0}^{\infty} r\xi^{r-1}\bar{F}(r). \tag{3.59}$$

Evaluating equation (3.59) at $\xi = 1$, one obtains

$$\left.\frac{df(\xi)}{d\xi}\right|_{\xi=1} = \sum_{r=0}^{\infty} r\bar{F}(r). \tag{3.60}$$

Hence,

$$\sum_{r=0}^{\infty} r\bar{F}(r) = 0. \tag{3.61}$$

□

Theorem 3.2.17. If $\left.\frac{d^2f(\xi)}{d\xi^2}\right|_{\xi=1} = 0$, then

$$\sum_{r=0}^{\infty} r(r-1)\bar{F}(r) = 0. \tag{3.62}$$

Proof. Differentiating equation (3.59) again with respect to ξ gives

$$\frac{d^2 f(\xi)}{d\xi^2} = \sum_{r=0}^{\infty} r\,(r-1)\,\xi^{r-2}\bar{F}(r). \tag{3.63}$$

Now, evaluating equation (3.63) at $\xi = 1$, one obtains

$$\left.\frac{d^2 f(\xi)}{d\xi^2}\right|_{\xi=1} = \sum_{r=0}^{\infty} r\,(r-1)\,\bar{F}(r). \tag{3.64}$$

This implies that

$$\sum_{r=0}^{\infty} r\,(r-1)\,\bar{F}(r) = 0. \tag{3.65}$$

□

Theorem 3.2.18. If $\left.\frac{d^3 f(\xi)}{d\xi^3}\right|_{\xi=1} = 0$, then

$$\sum_{r=0}^{\infty} r(r-1)(r-2)\bar{F}(r) = 0. \tag{3.66}$$

Proof. Differentiating equation (3.63) again with respect to ξ produces

$$\frac{d^3 f(\xi)}{d\xi^3} = \sum_{r=0}^{\infty} r\,(r-1)\,(r-2)\,\xi^{r-3}\bar{F}(r). \tag{3.67}$$

Now, evaluation of equation (3.63) at $\xi = 1$ gives

$$\left.\frac{d^3 f(\xi)}{d\xi^3}\right|_{\xi=1} = \sum_{r=0}^{\infty} r\,(r-1)\,(r-2)\,\bar{F}(r). \tag{3.68}$$

This implies that

$$\sum_{r=0}^{\infty} r\,(r-1)\,(r-2)\,\bar{F}(r) = 0. \tag{3.69}$$

□

3.3 Mathematical Formulation of the Problems

The mathematical formulation of the vibration problems considered in this thesis in terms of a pair of coupled partial differential equations and the associated boundary conditions are presented in this section.

3.3.1 Mathematical models for the two vibration problems

The double-beam system shown in Figure 3.1 is composed of two parallel, non-prismatic and homogeneous beams, which have the same length and are continuously joined by an elastic Pasternak layer characterised by Winkler modulus, $k(x)$ and shear modulus, $G(x)$. The two tapered beams that make up the double-beam system are either Rayleigh or Euler-Bernoulli beams depending on the effects of the parameters considered.

The top beam and the bottom beam were designated as the upper beam and lower beam, respectively. In this study, it was assumed that the material properties of both beams, that is, Young's modulus of elasticity E_j, and mass density ρ_j, were constants. However, the geometric properties of the beams, that is, the area of cross-section, $A_j(x)$ and moment of inertia of the cross-section , $I_j(x)$, of both beams, vary continuously along the length of each of the beams. The subscript j took the value 1 for the upper beam and 2 for the lower beam. Euler-Bernoulli and Rayleigh beam theories for transverse vibration were adopted in this study. It was also generally assumed that the two beams were not identical in terms of their material and geometric properties. Since free vibration was considered, it was assumed that no external force acted on the upper beam.

Consider first the Rayleigh beam theory. The governing differential equations of motion and boundary conditions of the elastically connected double-beam system can be derived in two ways, namely the Newtonian approach and the extended Hamilton's

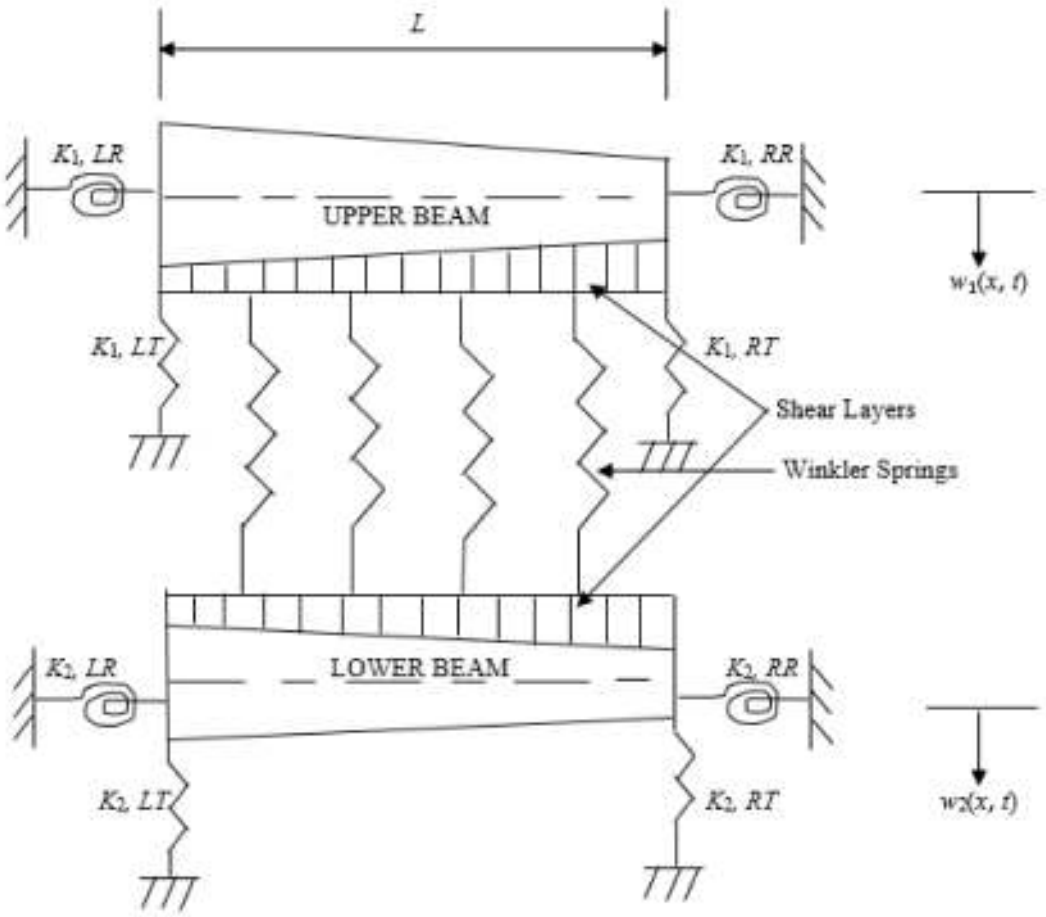

Figure 3.1: The structural model of a system of two non-prismatic beams elastically connected with a Pasternak elastic layer

variational principle (Meirovitch, 2001). By using Newtonian approach, the governing differential equation of motion for free vibration of a Rayleigh beam could be easily obtained as:

$$\frac{\partial^2}{\partial x^2}\left[EI(x)\frac{\partial^2 w(x,t)}{\partial x^2}\right]+\rho A(x)\frac{\partial^2 w(x,t)}{\partial t^2}-\frac{\partial}{\partial x}\left[\rho I(x)\frac{\partial}{\partial x}\left(\frac{\partial^2 w(x,t)}{\partial t^2}\right)\right]=0, \quad (3.70)$$

where $w(x,t)$ denotes the displacement, $EI(x)$ the flexural rigidity, $\rho A(x)$ the mass per unit length and $\rho I(x)$ is the rotatory inertia of the cross-sectional area of the beam (Bottega, 2006).

Using $w_j(x,t)$ to denote the deflection of the jth beam at a distance x from its left-hand end at time t, then the deflections of the upper beam ($j=1$) and lower beam ($j=2$) can be written, respectively as $w_1(x,t)$ and $w_2(x,t)$.

Assume that there is no connection between the two beams such that they vibrate independently. Then, based on this assumption and using the above notations, the equations governing the motion of the upper and the lower beams can be written respectively as:

$$\begin{aligned}\frac{\partial^2}{\partial x^2}\left[E_1 I_1(x)\frac{\partial^2 w_1(x,t)}{\partial x^2}\right] &+\rho_1 A_1(x)\frac{\partial^2 w_1(x,t)}{\partial t^2}\\ &-\frac{\partial}{\partial x}\left[\rho_1 I_1(x)\frac{\partial}{\partial x}\left(\frac{\partial^2 w_1(x,t)}{\partial t^2}\right)\right]=0,\end{aligned} \quad (3.71)$$

and

$$\begin{aligned}\frac{\partial^2}{\partial x^2}\left[E_1 I_2(x)\frac{\partial^2 w_1(x,t)}{\partial x^2}\right] &+\rho_2 A_2(x)\frac{\partial^2 w_2(x,t)}{\partial t^2}\\ &-\frac{\partial}{\partial x}\left[\rho_1 I_2(x)\frac{\partial}{\partial x}\left(\frac{\partial^2 w_2(x,t)}{\partial t^2}\right)\right]=0.\end{aligned} \quad (3.72)$$

Next, it is assumed that the elastic layer which continuously connects the upper and the lower beams together is of the Pasternak type characterised by $k(x)$, the variable Winkler modulus of the elastic layer (springs) that connects the two beams together and $G(x)$, the variable shear modulus that accounts for the shear interaction among the springs. So, the restoring forces from the Pasternak elastic layer are expressed as:

$$F_1 = \left(k(x) - G(x)\frac{\partial^2}{\partial x^2}\right)\left[w_1(x,t) - w_2(x,t)\right], \tag{3.73}$$

and

$$F_2 = \left(k(x) - G(x)\frac{\partial^2}{\partial x^2}\right)\left[w_2(x,t) - w_1(x,t)\right], \tag{3.74}$$

for the upper and lower beams respectively.

As a result of the restoring forces from the Pasternak elastic layer, the coupled governing partial differential equations for transverse vibrations of the double-beam system whose structural model is shown in Figure 3.1 can be stated in the form:

$$\begin{aligned}
&\frac{\partial^2}{\partial x^2}\left[E_1 I_1(x)\frac{\partial^2 w_1(x,t)}{\partial x^2}\right] + \rho_1 A_1(x)\frac{\partial^2 w_1(x,t)}{\partial t^2} \\
&\quad - \frac{\partial}{\partial x}\left[\rho_1 I_1(x)\frac{\partial}{\partial x}\left(\frac{\partial^2 w_1(x,t)}{\partial t^2}\right)\right] \\
&\quad + \left(k(x) - G(x)\frac{\partial^2}{\partial x^2}\right)\left[w_1(x,t) - w_2(x,t)\right] = 0,
\end{aligned} \tag{3.75}$$

and

$$\begin{aligned}
&\frac{\partial^2}{\partial x^2}\left[E_2 I_2(x)\frac{\partial^2 w_2(x,t)}{\partial x^2}\right] + \rho_2 A_1(x)\frac{\partial^2 w_2(x,t)}{\partial t^2} \\
&\quad - \frac{\partial}{\partial x}\left[\rho_2 I_2(x)\frac{\partial}{\partial x}\left(\frac{\partial^2 w_2(x,t)}{\partial t^2}\right)\right] \\
&\quad + \left(k(x) - G(x)\frac{\partial^2}{\partial x^2}\right)\left[w_2(x,t) - w_1(x,t)\right] = 0,
\end{aligned} \tag{3.76}$$

where E_1, E_2, ρ_1, ρ_2, $A_1(x)$, $A_2(x)$, $I_1(x)$ and $I_2(x)$ have their usual meanings as earlier defined. It should be noted that the products $E_jI_j(x)$ and $\rho_jA_j(x)$, for $j = 1, 2$ respectively represents the flexural rigidity (also called flexural stiffness) and mass per unit length (also known as the beam mass intensity) of the jth beam. Also, $\rho_jI_j(x)$, for $j = 1, 2$ is the rotatory inertia term of the jth beam. It is informative to point out that the corresponding governing equations for Euler-Bernoulli beams can be obtained as a special case of the Rayleigh beams' equations if the rotatory inertia term, $\rho_jI_j(x)$, is neglected. This is equivalent to setting the term involving $\rho_jI_j(x)$ in equations (3.75) and (3.76) to zero. Equations (3.75) and (3.76), together with an appropriate set of boundary and initial conditions, define the free vibration problem of the elastically connected non-prismatic Rayleigh double-beam system with Pasternak middle layer.

3.3.2 Boundary Conditions

In order to solve equations (3.75) and (3.76), eight boundary conditions were required. These were obtained by specifying two boundary conditions at the left-hand end, $x = 0$ and two boundary conditions at the right-hand end, $x = L$ of each beam. On the basis of arbitrary boundary conditions at each end of the beams, the two beams in the double-beam system were assumed, in this study, to be elastically restrained by means of translational and rotational springs as shown in Figure 3.1. Now the boundary conditions at the ends of the jth beam associated with a general elastically end restrained non-prismatic Rayleigh double-beam system are given as follows: (Ho and Chen, 1998; Hsu *et al.*, 2008)

$$E_jI_j\frac{\partial^2 w_j(x,t)}{\partial x^2} - k_{j,LR}\frac{\partial w_j(x,t)}{\partial x} = 0, \tag{3.77}$$

$$\frac{\partial}{\partial x}\left[E_jI_j(x)\frac{\partial^2 w_j(x,t)}{\partial x^2}\right] + \rho_jI_j(x)\frac{\partial^3 w_j(x,t)}{\partial x\partial t^2} + k_{j,LT}\frac{\partial w_j(x,t)}{\partial x} = 0, \tag{3.78}$$

at the left-hand end of the beam, and

$$E_j I_j(x)\frac{\partial^2 w_j(x,t)}{\partial x^2} + k_{j,RR}\frac{\partial w_j(x,t)}{\partial x} = 0, \tag{3.79}$$

$$\frac{\partial}{\partial x}\left[E_j I_j(x)\frac{\partial^2 w_j(x,t)}{\partial x^2}\right] + \rho_j I_j(x)\frac{\partial^3 w_j(x,t)}{\partial x \partial t^2} - k_{j,RT} w_j(x,t) = 0, \tag{3.80}$$

at the right-hand end of the beam, for $j = 1,\ 2$,

where $k_{j,LR}$ and $k_{j,LT}$ are the stiffnesses of the rotational and translational springs at the left-hand end of the jth beam respectively, and $k_{j,RR}$ and $k_{j,RT}$ are the corresponding spring stiffnesses at its right-hand end (see Han *et al.*, 1999, Li *et al.*, 2013). Equations (3.75)–(3.80) constitute the first vibration problem that is solved. It is remarked, at this juncture, that the corresponding governing equations of motion and associated boundary conditions for the second problem based on Euler-Bernoulli beam theory, are obtained by setting the $\rho_j I_j(x)$ term in equations (3.75)–(3.80) to zero.

3.4 Application of Differential Transformation Method

3.4.1 Assumed Solution (Modal Analysis)

An exact solution for the vibration characteristics of the vibration problem in this study is intractable because of the nature of the pair of coupled governing equations of motion having variable coefficients. This is why a recourse is made to approximate solution which is obtained using the method earlier described.

The free vibration solution of the system under consideration (whose schematic diagram is shown in Figure 3.1) can be obtained by assuming harmonic motion (the simplest type of periodic motion) and applying the relevant boundary conditions. This allows the transverse displacement of each beam, that is, $w_j(x,t)$ to be separable in space and time (as the product of functions) and as such can be assumed to take the

form (using complex-variable representation):

$$w_j(x,t) = Y_j(x)e^{i\omega t}, \quad j = 1,\ 2, \tag{3.81}$$

where $Y_j(x)$ is the mode shape function of the jth beam, $e^{i\omega t}$ is a harmonic function of time t with ω as the angular natural frequency of the double-beam system's structure. Also, $i = \sqrt{-1}$ is the conventional imaginary unit. As a matter of fact, the solution is in the form of a sinusoidal variation of $w_j(x,t)$ with the natural frequency ω. By introducing the assumed solution (3.81) into equations (3.75) and (3.76) and after necessary factorization, one obtains the time independent governing equations of motion as follows:

$$\begin{aligned}\frac{d^2}{dx^2}\left[E_1I_1(x)\frac{d^2Y_1}{dx^2}\right] &- \rho_1A_1(x)\omega^2Y_1(x) + \frac{d}{dx}\left[\rho_1I_1(x)\omega^2\frac{dY_1(x)}{dx}\right] \\ &+ k(x)\left[Y_1(x) - Y_2(x)\right] - G(x)\frac{d^2}{dx^2}\left[Y_1(x) - Y_2(x)\right] = 0,\end{aligned} \tag{3.82}$$

and

$$\begin{aligned}\frac{d^2}{dx^2}\left[E_2I_2(x)\frac{d^2Y_2}{dx^2}\right] &- \rho_2A_2(x)\omega^2Y_2(x) + \frac{d}{dx}\left[\rho_2I_2(x)\omega^2\frac{dY_2(x)}{dx}\right] \\ &+ k(x)\left[Y_2(x) - Y_1(x)\right] - G(x)\frac{d^2}{dx^2}\left[Y_2(x) - Y_1(x)\right] = 0.\end{aligned} \tag{3.83}$$

Equations (3.82) and (3.83) are fourth order ordinary differential equations with variable coefficients. Their solutions depend mainly on the distribution functions representing the actual non-uniformity characteristics of the beams. To obtain the boundary conditions for the modal functions, we substitute the assumed harmonic response in equation (3.81) into equations (3.77)–(3.80) to get the boundary conditions as follows:

$$E_jI_j(x)\frac{d^2Y_j(x)}{dx^2} - K_{j,LR}\frac{dY_j}{dx} = 0, \tag{3.84}$$

$$\frac{d}{dx}\left[E_j I_j(x)\frac{d^2Y_j(x)}{dx^2}\right] + \rho_j I_j(x)\omega^2\frac{dY_j(x)}{dx} + K_{j,LT}Y_j(x) = 0, \tag{3.85}$$

at $x = 0$, and

$$E_j I_j(x)\frac{d^2Y_j(x)}{dx^2} + K_{j,RR}\frac{dY_j}{dx} = 0, \tag{3.86}$$

$$\frac{d}{dx}\left[E_j I_j(x)\frac{d^2Y_j(x)}{dx^2}\right] + \rho_j I_j(x)\omega^2\frac{dY_j(x)}{dx} - K_{j,RT}Y_j(x) = 0, \tag{3.87}$$

at $x = L$.

3.4.2 Non-dimensionalization of the governing equations and boundary conditions

The ordinary differential governing equations of motion, (3.82) and (3.83), are not convenient for the analysis since they include many parameters. Without any loss of generality and in order to facilitate the general analysis, the following dimensionless variables and parameters are introduced:

$$\xi = \frac{x}{L},\ y_j(\xi) = \frac{Y_j(x)}{L},\ I_j(\xi) = \frac{I_j(x)}{I_j(0)},\ A_j(\xi) = \frac{A_j(x)}{A_j(0)},\ j = 1\ ,2 \tag{3.88}$$

where ξ_j, $y_j(\xi)$, $I_j(\xi)$, and $A_j(\xi)$ are the non-dimensional parameters for the length, deflection, moment of inertia of the cross-section and cross-sectional area of the jth beam respectively. In addition, $I_j(0)$ and $A_j(0)$ are the moment of inertia of the cross-section and cross-sectional area of the jth beam at the left-hand end ($x = 0$).

Using the non-dimensional quantities stated in equations (3.88) in equations (3.82) and (3.83) one can obtain:

$$\frac{d^2}{d(L\xi)^2}\left[E_1I_1(0)I_1(\xi)\frac{d^2\{Ly_1(\xi)\}}{d(L\xi)^2}\right] - \rho_1A_1(0)A_1(\xi)\omega^2Ly_1(\xi)$$
$$+ \frac{d}{d(L\xi)}\left[\rho_1I_1(0)I_1(\xi)\omega^2\frac{d\{Ly_1(\xi)\}}{d(L\xi)}\right] + k(x)[Ly_1(\xi) - Ly_2(\xi)] \tag{3.89}$$
$$- G(x)\frac{d^2}{d(L\xi)^2}\left[Ly_1(\xi) - Ly_2(\xi)\right] = 0,$$

and

$$\frac{d^2}{d(L\xi)^2}\left[E_2I_2(0)I_2(\xi)\frac{d^2\{Ly_2(\xi)\}}{d(L\xi)^2}\right] - \rho_2A_2(0)A_2(\xi)\omega^2Ly_2(\xi)$$
$$+ \frac{d}{d(L\xi)}\left[\rho_2I_2(0)I_2(\xi)\omega^2\frac{d\{Ly_2(\xi)\}}{d(L\xi)}\right] + k(x)[Ly_2(\xi) - Ly_1(\xi)] \tag{3.90}$$
$$- G(x)\frac{d^2}{d(L\xi)^2}\left[Ly_2(\xi) - Ly_1(\xi)\right] = 0,$$

respectively.

Equations (3.89) and (3.90), after necessary simplification, become

$$\frac{d^2}{d\xi^2}\left[\frac{E_1I_1(0)}{L^3}I_1(\xi)\frac{d^2y_1(\xi)}{d\xi^2}\right] - \rho_1A_1(0)A_1(\xi)\omega^2Ly_1(\xi)$$
$$+ \frac{d}{d(L\xi)}\left[\rho_1I_1(0)I_1(\xi)\omega^2\frac{d\{Ly_1(\xi)\}}{d(L\xi)}\right] + k(x)[Ly_1(\xi) - Ly_2(\xi)] \tag{3.91}$$
$$- G(x)\frac{d^2}{d(L\xi)^2}\left[Ly_1(\xi) - Ly_2(\xi)\right] = 0,$$

and

$$\frac{d^2}{d\xi^2}\left[\frac{E_2I_2(0)}{L^3}I_2(\xi)\frac{d^2y_2(\xi)}{d\xi^2}\right] - \rho_2A_2(0)A_2(\xi)\omega^2Ly_2(\xi)$$
$$+ \frac{d}{d(L\xi)}\left[\rho_2I_2(0)I_2(\xi)\omega^2\frac{d\{Ly_2(\xi)\}}{d(L\xi)}\right] + k(x)[Ly_2(\xi) - Ly_1(\xi)] \tag{3.92}$$
$$- G(x)\frac{d^2}{d(L\xi)^2}\left[Ly_2(\xi) - Ly_1(\xi)\right] = 0,$$

respectively.

Multiplying equations (3.91) and (3.92) through by $\frac{L^3}{E_1I_1(0)}$ and $\frac{L^3}{E_2I_2(0)}$ respectively,

one obtains

$$\begin{aligned}
&\frac{d^2}{d\xi^2}\left[I_1(\xi)\frac{d^2y_1(\xi)}{d\xi^2}\right] - \frac{\rho_1 A_1(0)\omega^2 L^4}{E_1 I_1(0)} A_1(\xi) y_1(\xi) \\
&\quad + \frac{d}{d\xi}\left[\frac{\rho_1 I_1(0)\omega^2 L^2}{E_1 I_1(0)} I_1(\xi)\frac{dy_1(\xi)}{d\xi}\right] + \frac{k(x)L^4}{E_1 I_1(0)}\left[y_1(\xi) - y_2(\xi)\right] \\
&\quad - \frac{G(x)L^2}{E_1 I_1(0)}\frac{d^2}{d\xi^2}\Big[y_1(\xi) - y_2(\xi)\Big] = 0,
\end{aligned} \tag{3.93}$$

and

$$\begin{aligned}
&\frac{d^2}{d\xi^2}\left[I_2(\xi)\frac{d^2y_2(\xi)}{d\xi^2}\right] - \frac{\rho_2 A_2(0)\omega^2 L^4}{E_2 I_2(0)} A_2(\xi) y_2(\xi) \\
&\quad + \frac{d}{d\xi}\left[\frac{\rho_2 I_2(0)\omega^2 L^2}{E_2 I_2(0)} I_2(\xi)\frac{dy_2(\xi)}{d\xi}\right] + \frac{k(x)L^4}{E_2 I_2(0)}\left[y_2(\xi) - y_1(\xi)\right] \\
&\quad - \frac{G(x)L^2}{E_2 I_2(0)}\frac{d^2}{d\xi^2}\Big[y_2(\xi) - y_1(\xi)\Big] = 0,
\end{aligned} \tag{3.94}$$

which can be put in the forms

$$\begin{aligned}
&\frac{d^2}{d\xi^2}\left[I_1(\xi)\frac{d^2y_1(\xi)}{d\xi^2}\right] - \frac{\rho_1 A_1(0)\omega^2 L^4}{E_1 I_1(0)} A_1(\xi) y_1(\xi) \\
&\quad + \frac{d}{d\xi}\left[\frac{\rho_1 A_1(0)\omega^2 L^4}{E_1 I_1(0)}\frac{I_1(0)}{A_1(0)L^2} I_1(\xi)\frac{dy_1(\xi)}{d\xi}\right] + \frac{k(x)L^4}{E_1 I_1(0)}\left[y_1(\xi) - y_2(\xi)\right] \\
&\quad - \frac{G(x)L^2}{E_1 I_1(0)}\frac{d^2}{d\xi^2}\Big[y_1(\xi) - y_2(\xi)\Big] = 0,
\end{aligned} \tag{3.95}$$

and

$$\begin{aligned}
&\frac{d^2}{d\xi^2}\left[I_2(\xi)\frac{d^2y_2(\xi)}{d\xi^2}\right] - \frac{\rho_2 A_2(0)\omega^2 L^4}{E_2 I_2(0)} A_2(\xi) y_2(\xi) \\
&\quad + \frac{d}{d\xi}\left[\frac{\rho_2 A_2(0)\omega^2 L^4}{E_2 I_2(0)}\frac{I_2(0)}{A_2(0)L^2} I_2(\xi)\frac{dy_2(\xi)}{d\xi}\right] + \frac{k(x)L^4}{E_2 I_2(0)}\left[y_2(\xi) - y_1(\xi)\right] \\
&\quad - \frac{G(x)L^2}{E_2 I_2(0)}\frac{d^2}{d\xi^2}\Big[y_2(\xi) - y_1(\xi)\Big] = 0,
\end{aligned} \tag{3.96}$$

respectively.

The governing differential equations (3.82) and (3.83) can be written in the following dimensionless forms:

$$\frac{d^2}{d\xi^2}\left[I_1(\xi)\frac{d^2y_1(\xi)}{d\xi^2}\right] - \lambda_1^2\omega^2 A_1(\xi)y_1(\xi) + \frac{d}{d\xi}\left[r_1^2\lambda_1^2 I_1(\xi)\frac{dy_1(\xi)}{d\xi}\right] + \kappa_1(\xi)\left[y_1(\xi) - y_2(\xi)\right] - g_1(\xi)\frac{d^2}{d\xi^2}\left[y_1(\xi) - y_2(\xi)\right] = 0, \tag{3.97}$$

and

$$\frac{d^2}{d\xi^2}\left[I_2(\xi)\frac{d^2y_2(\xi)}{d\xi^2}\right] - \lambda_2^2\omega^2 A_2(\xi)y_2(\xi) + \frac{d}{d\xi}\left[r_2^2\lambda_2^2 I_2(\xi)\frac{dy_2(\xi)}{d\xi}\right] + \kappa_2(\xi)\left[y_2(\xi) - y_1(\xi)\right] - g_2(\xi)\frac{d^2}{d\xi^2}\left[y_2(\xi) - y_1(\xi)\right] = 0, \tag{3.98}$$

where

$$\kappa_j(\xi) = \frac{k(x)L^4}{E_jI_j(0)},\ \lambda_j^2 = \frac{\rho_j A_j(0)L^4}{E_jI_j(0)},\ g_j(\xi) = \frac{G(x)L^2}{E_jI_j(0)},\ r_j^2 = \frac{I_j(0)}{L_j^2A_j(0)} \tag{3.99}$$

for $j = 1,\ 2$.

Following similar argument, the boundary conditions in equations (3.84)–(3.87) can be rewritten in the following non-dimensional form:

$$\frac{d^2y_j(\xi)}{d\xi^2} - \Psi_{j,LR}\frac{dy_j(\xi)}{d\xi} = 0, \tag{3.100}$$

$$\frac{d^3y_j(\xi)}{d\xi^3} + \frac{dI_j(\xi)}{d\xi}\frac{d^2y_j(\xi)}{d\xi^2} + r_j^2\lambda_j^2\omega^2\frac{dy_j(\xi)}{d\xi} + \Psi_{j,LT}y_j(\xi) = 0, \tag{3.101}$$

at $\xi = 0$,

and

$$\frac{d^2y_j(\xi)}{d\xi^2} + \Psi_{j,RR}\frac{dy_j(\xi)}{d\xi} = 0, \tag{3.102}$$

$$\frac{d^3y_j(\xi)}{d\xi^3} + \eta_j \frac{d^2y_j(\xi)}{d\xi^2} + r_j^2\lambda_j^2\omega^2 \frac{dy_j(\xi)}{d\xi} - \Psi_{j,RT}y_j(\xi) = 0, \tag{3.103}$$

at $\xi = 1$, in which

$$\begin{aligned} &\Psi_{j,LR} = \frac{K_{j,LR}L}{E_jI_j(0)},\ \Psi_{j,LT} = \frac{K_{j,LT}L^3}{E_jI_j(0)},\ \Psi_{j,RR} = \frac{K_{j,RR}L}{E_jI_j(L)}, \\ &\Psi_{j,RT} = \frac{K_{j,RT}L^3}{E_jI_j(L)},\ \eta_j = \frac{1}{I_j(\xi)}\frac{dI_j(\xi)}{d\xi}\bigg|_{\xi=1}, \end{aligned} \tag{3.104}$$

for $j = 1,\ 2$,

where $\Psi_{j,LT}$, $\Psi_{j,RT}$ are the dimensionless parameters related to the stiffnesses of the translational springs, and $\Psi_{j,LR}$, $\Psi_{j,RR}$ are the dimensionless parameters related to the stiffnesses of the rotational springs at the left and right-hand ends for the jth beam respectively.

3.4.3 DTM Formulation and the Desired Solution

Now, the method already alluded to is applied to solve the problem in this Section. The fundamental principle of the DTM is to transform the governing equations of motion and the boundary conditions into a set of algebraic equations by using the differential transformation rules and the theorems appropriately.

3.4.4 Differential Transformation of Governing equations of motion

By applying product rule of differentiation appropriately to equations (3.97) and (3.98), we get

$$\begin{aligned} I_1(\xi)\frac{d^4y_1(\xi)}{d\xi^4} + 2\frac{dI_1(\xi)}{d\xi}\frac{d^3y_1(\xi)}{d\xi^3} + \frac{d^2I_1(\xi)}{d\xi^2}\frac{d^2y_1(\xi)}{d\xi^2} - \lambda_1^2\omega^2A_1(\xi)y_1(\xi) \\ + r_1^2\lambda_1^2\omega^2\left[I_1(\xi)\frac{d^2y_1(\xi)}{d\xi^2} + \frac{dI_1(\xi)}{d\xi}\frac{dy_1(\xi)}{d\xi}\right] \\ + \kappa_1(\xi)\left[y_1(\xi) - y_2(\xi)\right] - g_1(\xi)\frac{d^2}{d\xi^2}\left[y_1(\xi) - y_2(\xi)\right] = 0, \end{aligned} \tag{3.105}$$

and

$$
\begin{aligned}
I_1(\xi)\frac{d^4y_2(\xi)}{d\xi^4} + 2\frac{dI_2(\xi)}{d\xi}\frac{d^3y_2(\xi)}{d\xi^3} + \frac{d^2I_2(\xi)}{d\xi^2}\frac{d^2y_2(\xi)}{d\xi^2} - \lambda_2^2\omega^2 A_2(\xi)y_2(\xi) \\
+ r_2^2\lambda_2^2\omega^2\left[I_2(\xi)\frac{d^2y_2(\xi)}{d\xi^2} + \frac{dI_2(\xi)}{d\xi}\frac{dy_2(\xi)}{d\xi}\right] \\
+ \kappa_2(\xi)\left[y_2(\xi) - y_1(\xi)\right] - g_2(\xi)\frac{d^2}{d\xi^2}\left[y_2(\xi) - y_1(\xi)\right] = 0,
\end{aligned} \tag{3.106}
$$

respectively.

Using Theorems 3.2.1 through 3.2.10 appropriately, the differential transforms of equations (3.97) and (3.98), are obtained as:

$$
\begin{aligned}
&\sum_{s=0}^{r}\bar{I}_1(r-s)(s+1)(s+2)(s+3)(s+4)\bar{Y}_1(s+4) \\
&+ 2\sum_{s=0}^{r}(r-s+1)\bar{I}_1(r-s+1)(s+1)(s+2)(s+3)\bar{Y}_1(s+3) \\
&+ \sum_{s=0}^{r}(r-s+1)(r-s+2)\bar{I}_1(r-s+2)(s+1)(s+2)\bar{Y}_1(s+2) \\
&- \lambda_1^2\omega^2\sum_{s=0}^{r}\bar{A}_1(r-s)\bar{Y}_1(s) + r_1^2\lambda_1^2\omega^2\left[\sum_{s=0}^{r}\bar{I}_1(r-s)(s+1)(s+2)\bar{Y}_1(s+2)\right. \\
&\left.+ \sum_{s=0}^{r}(r-s+1)\bar{I}_1(r-s+1)(s+1)\bar{Y}_1(s+1)\right] \\
&+ \sum_{s=0}^{r}\bar{K}_1(r-s)[\bar{Y}_1(s) - \bar{Y}_2(s)] \\
&- \sum_{s=0}^{r}\bar{G}_1(r-s)(s+1)(s+2)\left[\bar{Y}_1(s+2) - \bar{Y}_2(s+2)\right] = 0,
\end{aligned} \tag{3.107}
$$

and

$$
\begin{aligned}
&\sum_{s=0}^{r}\bar{I}_2(r-s)(s+1)(s+2)(s+3)(s+4)\bar{Y}_2(s+4) \\
&+ 2\sum_{s=0}^{r}(r-s+1)\bar{I}_2(r-s+1)(s+1)(s+2)(s+3)\bar{Y}_2(s+3) \\
&+ \sum_{s=0}^{r}(r-s+1)(r-s+2)\bar{I}_2(r-s+2)(s+1)(s+2)\bar{Y}_2(s+2) \\
&- \lambda_2^2\omega^2\sum_{s=0}^{r}\bar{A}_2(r-s)\bar{Y}_2(s) + r_2^2\lambda_2^2\omega^2\left[\sum_{s=0}^{r}\bar{I}_2(r-s)(s+1)(s+2)\bar{Y}_2(s+2)\right.
\end{aligned}
$$

$$
\begin{aligned}
&+\sum_{s=0}^{r}(r-s+1)\bar{I}_2(r-s+1)(s+1)\bar{Y}_2(s+1)\Bigg] \\
&+\sum_{s=0}^{r}\bar{K}_2(r-s)[\bar{Y}_2(s)-\bar{Y}_1(s)] \\
&-\sum_{s=0}^{r}\bar{G}_2(r-s)(s+1)(s+2)\left[\bar{Y}_2(s+2)-\bar{Y}_1(s+2)\right]=0,
\end{aligned}
\tag{3.108}
$$

where $\bar{I}_j(r)$, $\bar{A}_j(r)$ and $\bar{Y}_j(r)$, $j = 1,\ 2$ are the transformed functions of $I_j(\xi), A_j(\xi)$ and $y_j(\xi)$ respectively.

3.4.5 DTM Transformation of Boundary Conditions

In a similar fashion, Theorems 3.2.11-3.2.18 are appropriately applied to the boundary conditions presented in equations (3.100)–(3.103). Thus, the transformed boundary conditions at both ends of each beam in the double-beam system are obtained as:

$$
2!\bar{Y}_j(2)-\Psi_{j,LR}\bar{Y}_j(1)=0, \tag{3.109}
$$

$$
6\bar{Y}_j(3)+2\frac{d\bar{I}_j(0)}{d\xi}\bar{Y}_j(2)+r_j^2\lambda_j^2\omega^2\bar{Y}_j(1)+\Psi_{j,LT}\bar{Y}_j(0)=0, \tag{3.110}
$$

at $\xi = 0$, and

$$
\sum_{r=0}^{M}r(r-1)\bar{Y}_j(r)+\Psi_{j,RR}\sum_{r=0}^{M}r\bar{Y}_j(r)=0, \tag{3.111}
$$

$$
\begin{aligned}
\sum_{r=0}^{M}(r+1)(r+2)(r+3)\bar{Y}_j(r+3)+\eta_j\sum_{r=0}^{M}r(r-1)\bar{Y}_j(r) \\
+r_j^2\lambda_j^2\omega^2\sum_{r=0}^{M}r\bar{Y}_j(r)-\Psi_{j,RT}\sum_{r=0}^{M}\bar{Y}_j(r)=0,
\end{aligned}
\tag{3.112}
$$

at $\xi = 1$.

3.4.6 Evaluation of Natural Frequencies and Mode Shapes

The values of $\bar{Y}_1(0),\ \bar{Y}_2(0),\ \bar{Y}_1(1)$ and $\bar{Y}_2(1)$ are unknown. So, they are set as unknowns such as:

$$\begin{aligned}
\bar{Y}_1(0) &= c_1, \\
\bar{Y}_1(1) &= c_2, \\
\bar{Y}_2(0) &= c_3, \\
\bar{Y}_2(1) &= c_4.
\end{aligned} \tag{3.113}$$

Solving equations (3.109) and (3.110) for $\bar{Y}_1(2),\ \bar{Y}_2(2),\ \bar{Y}_1(3)$ and $\bar{Y}_2(3)$, we get

$$\bar{Y}_1(2) = \frac{\Psi_{1,LR}}{2} c_2, \tag{3.114}$$

$$\bar{Y}_2(2) = \frac{\Psi_{2,LR}}{2} c_4, \tag{3.115}$$

$$\bar{Y}_1(3) = -\frac{\Psi_{1,LT}}{6} c_1 - \frac{1}{6}\left[\Psi_{1,LR}\frac{dI_1(0)}{d\xi} + r_1^2\lambda_1^2\omega^2\right] c_2, \tag{3.116}$$

and

$$\bar{Y}_2(3) = -\frac{\beta_{2,LT}}{6} c_3 - \frac{1}{6}\left[\Psi_{2,LR}\frac{dI_2(0)}{d\xi} + r_2^2\lambda_2^2\omega^2\right] c_4. \tag{3.117}$$

In order to get $\bar{Y}_1(4)$ and $\bar{Y}_2(4)$, equations (3.112)-(3.117) are used appropriately in equations (3.106) and (3.107). Following similar recursive procedure, the values of $\bar{Y}_1(r)$ and $\bar{Y}_2(r)$ for $r = 5,\ 6, \ldots, M$ (where M is to be decided by the convergence of the natural frequency) can be determined in terms of constants c_1, c_2, c_3 and c_4.

Substituting $\bar{Y}_1(r)$ and $\bar{Y}_2(r)$ for $r = 0,\ 1, 2, \ldots,\ M$ into equations (3.111) and

(3.112) yields the following equation:

$$f_{\iota 1}^{(M)}(\omega)c_1 + f_{\iota 2}^{(M)}(\omega)c_2 + f_{\iota 3}^{(M)}(\omega)c_3 + f_{\iota 4}^{(M)}(\omega)c_4 = 0, \quad \iota = 1,\ 2,\ 3,\ 4, \tag{3.118}$$

such that $f_{\iota 1}^{(M)}(\omega),\ f_{\iota 2}^{(M)}(\omega),\ f_{\iota 3}^{(M)}(\omega),\ f_{\iota 4}^{(M)}(\omega)$ are polynomial functions of ω corresponding to M. The system of equations in (3.118) can be expressed in the following matrix form:

$$\begin{pmatrix} f_{11}^{(M)}(\omega) & f_{12}^{(M)}(\omega) & f_{13}^{(M)}(\omega) & f_{14}^{(M)}(\omega) \\ f_{21}^{(M)}(\omega) & f_{22}^{(M)}(\omega) & f_{23}^{(M)}(\omega) & f_{24}^{(M)}(\omega) \\ f_{31}^{(M)}(\omega) & f_{32}^{(M)}(\omega) & f_{33}^{(M)}(\omega) & f_{34}^{(M)}(\omega) \\ f_{41}^{(M)}(\omega) & f_{42}^{(M)}(\omega) & f_{43}^{(M)}(\omega) & f_{44}^{(M)}(\omega) \end{pmatrix} \begin{bmatrix} c_1 \\ c_2 \\ c_3 \\ c_4 \end{bmatrix} = \begin{bmatrix} 0 \\ 0 \\ 0 \\ 0 \end{bmatrix}. \tag{3.119}$$

In order to obtain the frequency equation for computing ω, we invoke the condition that the determinant of the coefficient matrix of equation (3.119) must be equal to zero. That is,

$$\begin{vmatrix} f_{11}^{(M)}(\omega) & f_{12}^{(M)}(\omega) & f_{13}^{(M)}(\omega) & f_{14}^{(M)}(\omega) \\ f_{21}^{(M)}(\omega) & f_{22}^{(M)}(\omega) & f_{23}^{(M)}(\omega) & f_{24}^{(M)}(\omega) \\ f_{31}^{(M)}(\omega) & f_{32}^{(M)}(\omega) & f_{33}^{(M)}(\omega) & f_{34}^{(M)}(\omega) \\ f_{41}^{(M)}(\omega) & f_{41}^{(M)}(\omega) & f_{43}^{(M)}(\omega) & f_{44}^{(M)}(\omega) \end{vmatrix} = 0. \tag{3.120}$$

From the foregoing, the frequencies are calculated by solving equation (3.120). The non-trivial solution of equation (3.120) is simply a polynomial root finding problem. The roots of the above frequency equation can be determined by using techniques like Newton's method, Laguerre's method and so on. However, in this study, Student-

Linear Algebra which is a built-in function in Maple 18 was used to develop a computer programme code in accordance with Theorems 3.2.1-3.2.18 with a view to computing the roots which are the eigenvalues. The programme codes can be found in Appendices I and II.

Solving the frequency determinant equation (3.120), one gets

$$\omega = \omega_n^{(M)}, \quad n = 1,\ 2, \ldots, \tag{3.121}$$

where $\omega_n^{(M)}$ is the nth estimated eigenvalue (natural frequency) corresponding to the nth mode of vibration. The value of M will be decided by the convergence of the natural frequency expressed by the following inequality:

$$|\omega_n^{(M)} - \omega_n^{(M-1)}| \leq \varepsilon, \tag{3.122}$$

where $\omega_n^{(M)}$ is the Mth estimated natural frequency corresponding to M and ε is the error tolerance parameter (allowable error). In this study, the error tolerance parameter was taken as $\varepsilon = 0.0001$.

If inequality (3.122) is satisfied, then we get the nth modal natural frequency, ω_n of the structure. Generally, ω_n is a complex number of the form $\omega_n = a + ib$. The imaginary component of ω_n is the nth natural frequency of the double-beam system. Without mincing words, the first of ω's which approximately satisfies equation (3.122) is the first natural frequency of the double-beam system.

The mode shape functions of the upper and lower beams can be obtained by setting c_4 to unity in equation (3.119) so that the values of the remaining unknown constants, c_1, c_2 and c_3 are determined. Setting $c_4 = 1$ in equation (3.119), we have the following

system of equations:

$$\begin{aligned} f_{11}^{(M)}(\omega)\cdot c_1 + f_{12}^{(M)}(\omega)\cdot c_2 + f_{13}^{(M)}(\omega)\cdot c_3 &= f_{14}^{(M)}, \\ f_{21}^{(M)}(\omega)\cdot c_1 + f_{22}^{(M)}(\omega)\cdot c_2 + f_{23}^{(M)}(\omega)\cdot c_3 &= f_{24}^{(M)}, \\ f_{31}^{(M)}(\omega)\cdot c_1 + f_{32}^{(M)}(\omega)\cdot c_2 + f_{33}^{(M)}(\omega)\cdot c_3 &= f_{34}^{(M)}. \end{aligned} \tag{3.123}$$

Solving the above equations for c_1, c_2 and c_3 by Cramer's rule, one obtains

$$c_1 = \frac{det(A_1)}{det(A)}, \tag{3.124}$$

$$c_2 = \frac{det(A_2)}{det(A)}, \tag{3.125}$$

and

$$c_3 = \frac{det(A_3)}{det(A)}, \tag{3.126}$$

provided that $det(A) \neq 0$,

where

$$det(A) = \begin{vmatrix} f_{11}^{(M)}(\omega) & f_{12}^{(M)}(\omega) & f_{13}^{(M)}(\omega) \\ f_{21}^{(M)}(\omega) & f_{22}^{(M)}(\omega) & f_{23}^{(M)}(\omega) \\ f_{31}^{(M)}(\omega) & f_{32}^{(M)}(\omega) & f_{33}^{(M)}(\omega) \end{vmatrix}, \tag{3.127}$$

$$det(A_1) = \begin{vmatrix} -f_{14}^{(M)}(\omega) & f_{12}^{(M)}(\omega) & f_{13}^{(M)}(\omega) \\ -f_{24}^{(M)}(\omega) & f_{22}^{(M)}(\omega) & f_{23}^{(M)}(\omega) \\ -f_{34}^{(M)}(\omega) & f_{32}^{(M)}(\omega) & f_{33}^{(M)}(\omega) \end{vmatrix}, \tag{3.128}$$

$$det(A_2) = \begin{vmatrix} f_{11}^{(M)}(\omega) & -f_{14}^{(M)}(\omega) & f_{13}^{(M)}(\omega) \\ f_{21}^{(M)}(\omega) & -f_{24}^{(M)}(\omega) & f_{23}^{(M)}(\omega) \\ f_{31}^{(M)}(\omega) & -f_{34}^{(M)}(\omega) & f_{33}^{(M)}(\omega) \end{vmatrix}, \tag{3.129}$$

and

$$det(A_3) = \begin{vmatrix} f_{11}^{(M)}(\omega) & f_{12}^{(M)}(\omega) & -f_{14}^{(M)}(\omega) \\ f_{21}^{(M)}(\omega) & f_{22}^{(M)}(\omega) & -f_{24}^{(M)}(\omega) \\ f_{31}^{(M)}(\omega) & f_{32}^{(M)}(\omega) & -f_{34}^{(M)}(\omega) \end{vmatrix}. \tag{3.130}$$

Thus, the mode shape functions corresponding to any modal vibration frequency for both upper and lower beams can be expressed as:

$$y_1(\xi) = \sum_{r=0}^{M} \xi^r \bar{Y}_1(r), \tag{3.131}$$

and

$$y_2(\xi) = \sum_{r=0}^{M} \xi^r \bar{Y}_2(r), \tag{3.132}$$

respectively.

By normalizing equations (3.131) and (3.132), we obtain the normalized mode shape functions for the upper and lower beams as follows: (Hsu *et al.*, 2008)

$$\bar{y}_1(\xi) = \frac{y_1(\xi)}{\sqrt{\int_0^1 [y_1(\xi)]^2 \, d\xi}}, \tag{3.133}$$

and

$$\bar{y}_2(\xi) = \frac{y_2(\xi)}{\sqrt{\int_0^1 [y_2(\xi)]^2 \, d\xi}}. \tag{3.134}$$

Usually, there are two types of tapers in non-prismatic beam classification namely single taper and double taper. The single taper is obtained when only the beam depth (thickness) varies linearly along the beam axis. On the other hand, double taper arises when the beam width and depth are varied linearly along the beam axis. In the literature, the variation of the geometric properties of a non-prismatic beam has been assumed using many distributions such as algebraic polynomials, exponential functions, trigonometric series or their combinations. Abrate (1995) and Ozgumus and Kaya (2006) used power functions to represent the distribution of the non-prismatic characteristics of the beams which were adopted in this study. Following the assumption in their research, polynomial functions of the position are used to represent the cross-sectional area and the moment of inertia of the cross-section of the beams. The general expressions for the breadth, $b_j(x)$, the height, $h_j(x)$, the cross-sectional area, $A_j(x)$, and the moment inertia of cross-section, $I_j(x)$ of the jth beam are given by the following expressions: (Tang *et al.*, 2015)

$$b_j(x) = b_j(0)\left(1 - c_{b_j}\frac{x}{L}\right)^p, \tag{3.135}$$

$$h_j(x) = h_j(0)\left(1 - c_{h_j}\frac{x}{L}\right)^q, \tag{3.136}$$

$$A_j(x) = b_j(x)h_j(x) = A_j(0)\left(1 - c_{b_j}\frac{x}{L})^p(1 - c_{h_j}\frac{x}{L}\right)^q, \tag{3.137}$$

and

$$I_j(x) = \frac{b_j(x)h_j^3(x)}{3} = I_j(0)(1 - c_{b_j}\frac{x}{L})^p(1 - c_{h_j}\frac{x}{L})^{3q}, \tag{3.138}$$

such that

$$A_j(0) = b_j(0)h_j(0), \tag{3.139}$$

and

$$I_j(0) = \frac{b_j(0)\left[h_j(0)\right]^3}{12}, \tag{3.140}$$

where $A_j(0)$, $I_j(0)$, $b_j(0)$ and $h_j(0)$ are the cross-sectional area, moment of inertia of the cross-section, width and height of the jth beam at its left-hand end ($x = 0$). In equations (3.135)–(3.138), c_{b_j} and c_{h_j} which represent the breadth and height taper ratios of the jth beam respectively, are defined as follows:

$$c_{b_j} = 1 - \frac{b_j(L)}{b_j(0)}, \tag{3.141}$$

and

$$c_{h_j} = 1 - \frac{h_j(L)}{h_j(0)}, \tag{3.142}$$

which satisfy $0 \leq c_{b_j} < 1,\ 0 \leq c_{h_j} < 1$, p and q are the constants used to describe the profile of various cross-sections. $b_j(L)$ and $h_j(L)$ are the width and height of the jth beam at the right-hand end, $x = L$ (Ozgumus and Kaya, 2006).

Taking different combined values of p and q will give various shapes of the cross-section. It is easy to see that one can recover the prismatic beams by simply setting $p = q = 0$ or just putting the taper ratio, $c_{b_j} = c_{h_j} = 0$. Non-negative integers such as 0, 1 or 2 are usually chosen for p and q when considering most regular situations for non-prismatic beams in practice (Tang *et al.*, 2015).

For the purpose of analysis in this study, attention is restricted to a beam pair with constant width and linearly varying depth. This can be obtained by setting $p = 0$ and $q = 1$ in equations (3.135)–(3.138) to obtain the following expressions:

$$b_j(x) = b_j(0), \tag{3.143}$$

$$h_j(x) = h_j(0)\left(1 - c_{h_j}\frac{x}{L}\right), \tag{3.144}$$

$$A_j(x) = A_j(0)\left(1 - c_{h_j}\frac{x}{L}\right), \tag{3.145}$$

and

$$I_j(x) = I_j(0)\left(1 - c_{h_j}\frac{x}{L}\right)^3. \tag{3.146}$$

For simplicity, let us write $\beta_j = c_{h_j}$ henceforth. Thus, the cross-sectional area and the moment of inertia of the cross-section of the jth beam in equations (3.145) and (3.146) become:

$$A_j(x) = A_j(0)\left(1 - \beta_j\frac{x}{L}\right); \quad j = 1,\ 2, \tag{3.147}$$

and

$$I_j(x) = I_j(0)\left(1 - \beta_j\frac{x}{L}\right)^3; \quad j = 1,\ 2, \tag{3.148}$$

where $A_j(0)$ and $I_j(0)$ have their usual meanings for the jth beam at its left-hand end $x = 0$, β_j is the taper ratio for the jth beam which satisfies $0 \leq \beta_j < 1$. The cross-sectional area and moment of inertia of the cross-section of the jth beam, in

dimensionless form, can now be written as

$$A_j(\xi) = \frac{A_j(x)}{A_j(0)} = 1 - \beta_j \frac{x}{L} = 1 - \beta_j \xi, \quad j = 1,\ 2, \tag{3.149}$$

and

$$I_j(\xi) = \frac{I_j(x)}{I_j(0)} = \left(1 - \beta_j \frac{x}{L}\right)^3 = (1 - \beta_j \xi)^3, \quad j = 1,\ 2, \tag{3.150}$$

respectively.

Substituting equations (3.149) and (3.150) into equations (3.105) and (3.106), one obtains

$$\begin{aligned}
&(1-\beta_1\xi)^3 \frac{d^4 y_1(\xi)}{d\xi^4} + 2\frac{d[(1-\beta_1\xi)^3]}{d\xi}\frac{d^3 y_1(\xi)}{d\xi^3} + \frac{d^2[(1-\beta_1\xi)^3]}{d\xi^2}\frac{d^2 y_1(\xi)}{d\xi^2} \\
&- \lambda_1^2\omega^2(1-\beta_1\xi)y_1(\xi) + r_1^2\lambda_1^2\omega^2\left[(1-\beta_1\xi)^3\frac{d^2 y_1(\xi)}{d\xi^2} + \frac{d(1-\beta_1\xi)^3}{d\xi}\frac{dy_1(\xi)}{d\xi}\right] \\
&+ k_1(\xi)\left[y_1(\xi) - y_2(\xi)\right] - g_1(\xi)\frac{d^2}{d\xi^2}\left[y_1(\xi) - y_2(\xi)\right] = 0,
\end{aligned} \tag{3.151}$$

and

$$\begin{aligned}
&(1-\beta_2\xi)^3 \frac{d^4 y_4(\xi)}{d\xi^4} + 2\frac{d[(1-\beta_2\xi)^3]}{d\xi}\frac{d^3 y_2(\xi)}{d\xi^3} + \frac{d^2[(1-\beta_2\xi)^3]}{d\xi^2}\frac{d^2 y_2(\xi)}{d\xi^2} \\
&- \lambda_2^2\omega^2(1-\beta_2\xi)y_2(\xi) + r_2^2\lambda_2^2\omega^2\left[(1-\beta_2\xi)^3\frac{d^2 y_2(\xi)}{d\xi^2} + \frac{d(1-\beta_2\xi)^3}{d\xi}\frac{dy_2(\xi)}{d\xi}\right] \\
&+ k_2(\xi)\left[y_2(\xi) - y_1(\xi)\right] - g_2(\xi)\frac{d^2}{d\xi^2}\left[y_2(\xi) - y_1(\xi)\right] = 0,
\end{aligned} \tag{3.152}$$

respectively.

These can be further simplified to give

$$\begin{aligned}
&(1-3\beta_1\xi + 3\beta_1^2\xi^2 - \beta_1^3\xi^3)\frac{d^4 y_1(\xi)}{d\xi^4} - 6\beta_1\left(1 - 2\beta_1\xi + \beta_1^2\xi^2\right)\frac{d^3 y_1(\xi)}{d\xi^3} \\
&+ 6\beta_1^2\left(1-\beta_1\xi\right)\frac{d^2 y_1(\xi)}{d\xi^2} - \lambda_1^2\omega^2(1-\beta_1\xi)y_1(\xi) \\
&+ r_1^2\lambda_1^2\omega^2\Bigg[(1 - 3\beta_1\xi + 3\beta_1^2\xi^2 - \beta_1^3\xi^3)\frac{d^2 y_1(\xi)}{d\xi^2} - 3\beta_1(1 - 2\beta_1\xi \\
&+ \beta_1^2\xi^2)\frac{dy_1(\xi)}{d\xi}\Bigg] + k_1(\xi)\left[y_1(\xi) - y_2(\xi)\right] - g_1(\xi)\frac{d^2}{d\xi^2}\left[y_1(\xi) - y_2(\xi)\right] = 0,
\end{aligned} \tag{3.153}$$

and

$$
\begin{aligned}
&(1-3\beta_2\xi+3\beta_2^2\xi^2-\beta_2^3\xi^3)\frac{d^4y_2(\xi)}{d\xi^4}-6\beta_2\left(1-2\beta_2\xi+\beta_2^2\xi^2\right)\frac{d^3y_2(\xi)}{d\xi^3}\\
&\quad+6\beta_2^2\left(1-\beta_2\xi\right)\frac{d^2y_2(\xi)}{d\xi^2}-\lambda_2^2\omega^2(1-\beta_2\xi)y_2(\xi)\\
&\quad+r_2^2\lambda_2^2\omega^2\Bigg[(1-3\beta_2\xi+3\beta_2^2\xi^2-\beta_2^3\xi^3)\frac{d^2y_2(\xi)}{d\xi^2}-3\beta_2(1-2\beta_2\xi\\
&\quad+\beta_2^2\xi^2)\frac{dy_2(\xi)}{d\xi}\Bigg]+k_2(\xi)\left[y_2(\xi)-y_1(\xi)\right]-g_2(\xi)\frac{d^2}{d\xi^2}\Bigg[y_2(\xi)-y_1(\xi)\Bigg]=0,
\end{aligned}
\tag{3.154}
$$

respectively.

Applying Theorems 3.2.1-3.2.10 appropriately to equations (3.153) and (3.154) yields

$$
\begin{aligned}
&\sum_{s=0}^{r}\left[\delta(r-s)-3\beta_1\delta(r-s-1)+3\beta_1^2\delta(r-s-2)-\beta_1^3\delta(r-s-3)\right]\\
&\times(s+1)(s+2)(s+3)(s+4)\bar{Y}_1(s+4)\\
&-6\beta_1\sum_{s=0}^{r}\left[\delta(r-s)-2\beta_1\delta(r-s-1)+\beta_1^2\delta(r-s-2)\right]\\
&\times(s+1)(s+2)(s+3)\bar{Y}_1(s+3)\\
&+6\beta_1^2\sum_{s=0}^{r}\left[\delta(r-s)-\beta_1\delta(r-s-1)\right](s+1)(s+2)\bar{Y}_1(s+2)\\
&-\lambda_1^2\omega^2\sum_{s=0}^{r}\left[\delta(r-s)-\beta_1\delta(r-s-1)\right]\bar{Y}_1(s+2)\\
&+r_1^2\lambda_1^2\omega^2\Bigg\{\sum_{s=0}^{r}\Bigg[\delta(r-s)-3\beta_1\delta(r-s-1)+3\beta_1^2\delta(k-r-2)\\
&-\beta_1^3\delta(r-s-3)\Bigg]\times(s+1)(s+2)\bar{Y}_1(s+2)-3\beta_1\sum_{r=0}^{k}\Bigg[\delta(r-s)\\
&-2\beta_1\delta(r-s-1)+\beta_1^2\delta(r-s-2)\Bigg](s+1)\bar{Y}_1(s+1)\Bigg\}\\
&+\bar{K}_1(r-s)\left[\bar{Y}_1(s)-\bar{Y}_2(s)\right]\\
&-\bar{G}_1(r-s)(s+1)(s+2)\left[\bar{Y}_1(s+2)-\bar{Y}_2(s+2)\right]=0,
\end{aligned}
\tag{3.155}
$$

and

$$
\begin{aligned}
&\sum_{s=0}^{r}\left[\delta(r-s)-3\beta_2\delta(r-s-1)+3\beta_2^2\delta(r-s-2)-\beta_2^3\delta(r-s-3)\right]\\
&\times(s+1)(s+2)(s+3)(s+4)\bar{Y}_2(s+4)\\
&-6\beta_2\sum_{s=0}^{r}\left[\delta(r-s)-2\beta_2\delta(r-s-1)+\beta_2^2\delta(r-s-2)\right]\\
&\times(s+1)(s+2)(s+3)\bar{Y}_2(s+3)\\
&+6\beta_2^2\sum_{s=0}^{r}\left[\delta(r-s)-\beta_2\delta(r-s-1)\right](s+1)(s+2)\bar{Y}_2(s+2)\\
&-\lambda_2^2\omega^2\sum_{s=0}^{r}\left[\delta(r-s)-\beta_2\delta(r-s-1)\right]\bar{Y}_2(s+2)\\
&+r_2^2\lambda_2^2\omega^2\Bigg\{\sum_{s=0}^{r}\Bigg[\delta(r-s)-3\beta_2\delta(r-s-1)+3\beta_2^2\delta(k-r-2)\\
&-\beta_2^3\delta(r-s-3)\Bigg]\times(s+1)(s+2)\bar{Y}_2(s+2)-3\beta_2\sum_{r=0}^{k}\Bigg[\delta(r-s)\\
&-2\beta_2\delta(r-s-1)+\beta_2^2\delta(r-s-2)\Bigg](s+1)\bar{Y}_2(s+1)\Bigg\}\\
&+\bar{K}_2(r-s)\left[\bar{Y}_2(s)-\bar{Y}_1(s)\right]\\
&-\bar{G}_2(r-s)(s+1)(s+2)\left[\bar{Y}_2(s+2)-\bar{Y}_1(s+2)\right]=0,
\end{aligned}
\tag{3.156}
$$

respectively.

Equations (3.155) and (3.156) are the recurrence relations for the vibration problem of elastically connected non-prismatic Rayleigh double-beam system with Pasternak middle layer. It is assumed that both the upper beam and the lower beam have a constant width and linearly varying depth.

It is remarked that, the corresponding recurrence relations for the vibration problem based on Euler-Bernoulli beam theory can be derived by setting r_j, for $j = 1,\ 2$ in

equations (3.155) and (3.156) to zero. To this end, we obtain

$$
\begin{aligned}
&\sum_{s=0}^{r}\left[\delta(r-s)-3\beta_1\delta(r-s-1)+3\beta_1^2\delta(r-s-2)-\beta_1^3\delta(r-s-3)\right]\\
&\times(s+1)(s+2)(s+3)(s+4)\bar{Y}_1(s+4)\\
&-6\beta_1\sum_{s=0}^{r}\left[\delta(r-s)-2\beta_1\delta(r-s-1)+\beta_1^2\delta(r-s-2)\right]\\
&\times(s+1)(s+2)(s+3)\bar{Y}_1(s+3)\\
&+6\beta_1^2\sum_{s=0}^{r}\left[\delta(r-s)-\beta_1\delta(r-s-1)\right](s+1)(s+2)\bar{Y}_1(s+2)\\
&-\lambda_1^2\omega^2\sum_{s=0}^{r}\left[\delta(r-s)-\beta_1\delta(r-s-1)\right]\bar{Y}_1(s+2)\\
&+\bar{K}_1(r-s)\left[\bar{Y}_1(s)-\bar{Y}_2(s)\right]\\
&-\bar{G}_1(r-s)(s+1)(s+2)\left[\bar{Y}_1(s+2)-\bar{Y}_2(s+2)\right]=0,
\end{aligned}
\tag{3.157}
$$

and

$$
\begin{aligned}
&\sum_{s=0}^{r}\left[\delta(r-s)-3\beta_2\delta(r-s-1)+3\beta_2^2\delta(r-s-2)-\beta_2^3\delta(r-s-3)\right]\\
&\times(s+1)(s+2)(s+3)(s+4)\bar{Y}_2(s+4)\\
&-6\beta_2\sum_{s=0}^{r}\left[\delta(r-s)-2\beta_2\delta(r-s-1)+\beta_2^2\delta(r-s-2)\right]\\
&\times(s+1)(s+2)(s+3)\bar{Y}_2(s+3)\\
&+6\beta_2^2\sum_{s=0}^{r}\left[\delta(r-s)-\beta_2\delta(r-s-1)\right](s+1)(s+2)\bar{Y}_2(s+2)\\
&-\lambda_2^2\omega^2\sum_{s=0}^{r}\left[\delta(r-s)-\beta_2\delta(r-s-1)\right]\bar{Y}_2(s+2)\\
&+\bar{K}_2(r-s)\left[\bar{Y}_2(s)-\bar{Y}_1(s)\right]\\
&-\bar{G}_2(r-s)(s+1)(s+2)\left[\bar{Y}_2(s+2)-\bar{Y}_1(s+2)\right]=0,
\end{aligned}
\tag{3.158}
$$

respectively.

CHAPTER FOUR

RESULTS AND DISCUSSION

4.1 Introduction

A theoretical model for free vibration analysis of a system of two beams with variable cross-section and moment of inertia of the cross-section which are continuously coupled by Pasternak elastic layer has been formulated in the preceding chapter. In this chapter, numerical computations were first carried out to show the efficiency of the proposed method. The research findings are thereafter presented and discussed in relation to relevant previous research on vibration of elastically connected double-beam systems. These results are conveniently presented in tables and figures.

4.2 Verification and Numerical Examples

Firstly, in order to validate the results obtained from the present model, the natural frequencies of a prismatic Euler-Bernoulli double-beam system whereby the two beams are continuously connected by a Winkler-type elastic layer are compared with the results available in the literature. Both cases of the two beams being identical and non-identical are considered. Secondly, numerical examples on a non-prismatic double-beam system whereby the two beams are connected by a Pasternak-type elastic layer are considered. The effects of the taper ratio of the beams, stiffness of the springs, the stiffness of the shear layer and boundary conditions on the natural frequencies of the system are investigated. MAPLE 18 was used for all the computations.

Results Validation: A comparison of the results for a prismatic double-beam system

Example 4.1: As the first example, we consider the free vibration of a simply supported prismatic Euler-Bernoulli double-beam system elastically coupled by an elastic

layer of the Winkler type in order to validate the present method in this thesis. The two beams were assumed to be identical in both material and geometric properties. In this example, both upper and lower beams are homogeneous and simply supported at their two ends (that is, SS-SS). Their material and geometric properties are:

$E_1 = E_2 = 1 \times 10^{10}$ N m^{-2}, $I_1(0) = I_2(0) = I = 4 \times 10^{-4}$ m^4,

$\rho_1 = \rho_2 = 2 \times 10^3$ kg m^{-3}, $A_1(0) = A_2(0) = A = 5 \times 10^{-2}$ m^2,

$L_1 = L_2 = L = 10$ m.

The above properties were adopted from the studies of Oniszczuk (2000) and Huang and Liu (2013).

For convenience and purpose of comparison, the values of Winkler and shear moduli of the Pasternak layer were assumed uniform. The Winkler modulus of the springs is changed in the interval $k = (0 \sim 5) \times 10^5$ N m^{-2}. The above system has already been solved by both Oniszczuk (2000) and Huang and Liu (2013) using the classical modal expansion method and finite element method respectively.

It is to be noted that any type of classical boundary conditions can be easily achieved by setting the boundary spring stiffness to be either infinite (a very large number) or zero. For example, the clamped boundary condition is obtained by setting both the stiffness of the translational and rotational springs to a very large number, (1×10^{18}) is used in this study). In a similar manner, assigning an extremely large number (say, 1×10^{18}) and zero to the stiffness of the translational spring and rotational spring, respectively will yield the simply supported boundary condition. Moreover, setting both the stiffness of the translational and rotational springs to zero leads to free boundary condition (Mao, 2012). In identifying the boundary conditions, letters S, C and F have been used respectively to indicate the simply supported, clamped and free boundary condition. Further more, the values of shear modulus of the Pasternak layer and taper ratio (non-uniformity parameter of the beams) were set to zero since Winkler elastic layer was considered by Oniszczuk (2000) and Huang and Liu (2013).

The results of the calculations which yielded the first five natural frequencies of the system with the stated material properties using the present semi-analytical procedure known as DTM are reported in Table 4.1. The results are compared with those reported by Oniszczuk (2000) and Huang and Liu (2013) who used different approaches, as earlier stated.

Table 4.1: Comparison by methods of the first five natural frequencies of a prismatic Euler-Bernoulli double-beam system elastically connected by Winkler layer with simply supported boundary conditions (SS-SS)

ω_n		$k \times 10^5$ N m^{-2}					
n		0	1	2	3	4	5
	Oniszczuk (2000)	19.7	19.7	19.7	19.7	19.7	19.7
1	Huang & Liu (2013)	19.7	19.7	19.7	19.7	19.7	19.7
	DTM (Present)	19.7392	19.7392	19.7392	19.7392	19.7392	19.7392
	Oniszczuk (2000)	79.0	48.9	66.3	79.0	79.0	79.0
2	Huang & Liu (2013)	79.0	48.9	66.3	79.0	79.0	79.0
	DTM (Present)	78.9568	48.8839	66.2543	78.9568	78.9568	78.9568
	Oniszczuk (2000)	177.7	79.0	79.0	79.9	91.6	101.9
3	Huang & Liu (2013)	177.7	79.0	79.0	79.9	91.6	101.9
	DTM (Present)	177.6529	78.9568	78.9568	79.9532	91.5950	101.9296
	Oniszczuk (2000)	315.8	90.7	101.2	110.6	119.3	127.4
4	Huang & Liu (2013)	315.8	90.7	101.2	110.6	119.3	127.4
	DTM (Present)	315.8273	90.7424	101.1641	110.6082	119.3071	127.4134
	Oniszczuk (2000)	493.5	177.7	177.7	177.7	177.7	177.7
5	Huang & Liu (2013)	493.5	177.7	177.7	177.7	177.7	177.7
	DTM (Present)	493.4802	177.6529	177.6529	177.6529	177.6529	177.6529

It is seen from Table 4.1 that the results yielded by differential transformation method (DTM) are in excellent agreement with the values reported by Oniszczuk (2000) and Huang and Liu (2013) in their respective studies.

Example 4.2: For the purpose of numerical validation, the DTM is next used to calculate the natural frequencies of a double-beam system, with the two beams having the same mechanical parameters. Here, we consider a prismatic double-beam system with two physically and geometrically identical Euler-Bernoulli beams under different vibrating configurations.The two beams are connected by a continuous linear elastic layer of the Winkler-type (in the absence of shearing layer).

The material and geometric properties used here are the same as those for the system previously examined in example 4.1. The Wınkler modulus of the springs is $k = 2 \times 10^5$ Nm^{-2}. The first three natural frequencies for the system with different boundary conditions are listed in Table 4.2. The values reported by Huang and Liu (2013) are recalled for the purpose of comparison.

Table 4.2: Comparison of DTM with Finite element method (FEM) for a prismatic Euler-Bernoulli double-beam system composed of two beams (with identical material and geometric properties) elastically connected by Winkler layer

Boundary conditions		Methods	ω_1	ω_2	ω_3
Upper beam	Lower beam				
S-S	S-S	FEM (Huang & Liu,2013)	19.7392	66.2543	78.9568
		DTM (Present)	19.7392	66.2543	78.9568
S-S	C-C	FEM (Huang & Liu,2013)	32.6046	72.9636	88.4699
		DTM (Present)	32.6046	72.9636	88.4699
C-C	C-C	FEM (Huang & Liu,2013)	44.7466	77.4742	123.3456
		DTM (Present)	44.7465	77.4742	123.3456

From Table 4.2, it is obvious that the present results for the prismatic double-beam system are also in excellent agreement with those obtained using finite element method. These two examples show that the DTM is highly efficient and accurate. This again shows the versatility of DTM.

Example 4.3: In this last stage of validation, a double-beam system comprised of two prismatic Euler-Bernoulli beams having different material and geometric parameters and under different combinations of boundary conditions is considered. The double-beam system studied by Mao (2012) is restudied here to further check the accuracy and effectiveness of DTM. In this case, the length of each beam is $L = 10$ m, while the material and geometric properties of the upper beam are:

$E_1 = 1 \times 10^{10}$ Nm^{-2}, $A_1(0) = A_1 = 5 \times 10^{-2}$ m^2,
$I_1(0) = I_1 = 4 \times 10^{-4}$ m^4, $\rho_1 = 2 \times 10^3$ kg m^{-3}.

For the lower beam, the flexural stiffness and the mass per unit length are as follows: $E_2I_2 = 2 \times E_1I_1$ and $\rho_2A_2 = 2 \times \rho_1A_1$, respectively. This shows that the upper beam is lighter and more flexible than the lower. The Winkler modulus of the inner springs used for the computation is $k = 1 \times 10^5$ kg m^{-3}. By using these values, the natural frequencies are calculated and the results are shown in Table 4.3. These calculated results are compared with the ones listed in Mao (2012) via Adomian Modified Decomposition method (AMDM).

The results in Table 4.3 also show that there is a close agreement between DTM and Adomian Modified Decomposition Method (AMDM). The excellent agreement between DTM results and the ones obtained via other methods motivated the author to apply DTM to vibration analysis of non-prismatic double-beam system elastically connected by a Pasternak layer.

Table 4.3: Comparison of the first three natural frequencies by methods for a prismatic Euler-Bernoulli double-beam system composed of non-identical beams elastically connected by Winkler layer

Boundary conditions		Methods	ω_1	ω_2	ω_3
Upper beam	Lower beam				
S-S	S-S	AMDM (Mao, 2012)	19.7392	43.4699	78.9568
		DTM (Present)	19.7392	43.4699	78.9568
C-C	C-C	AMDM (Mao, 2012)	44.7466	59.1799	123.3456
		DTM (Present)	44.7645	59.1799	123.3456
C-C	C-F	AMDM (Mao, 2012)	21.6179	46.0571	58.2712
		DTM (Present)	21.6179	46.0571	58.2712
C-F	C-F	AMDM (Mao, 2012)	7.0320	39.3630	44.0690
		DTM (Present)	7.0320	39.3630	44.0690

4.3 Vibration characteristics of non-prismatic Euler-Bernoulli (EB) double-beam system elastically connected by a Pasternak layer

Next, the numerical results for free vibration analysis of non-prismatic EB double-beam system connected by a Pasternak layer for fixed values of Winkler modulus and shear modulus of the Pasternak layer are presented in this Section. Also, the effects of the Winkler modulus and shear modulus of the connecting medium on the natural frequencies of the system are explored. Here, a non-prismatic double-beam system when the two beams have identical material and geometric properties is first considered. The material and geometric properties of the beams are given as follows:

$E_1 = E_2 = 1 \times 10^{10}$ N m^{-2}, $I_1(0) = I_2(0) = 4 \times 10^{-4}$ m^4,

$\rho_1 = \rho_2 = 2 \times 10^3$ kg m^{-3}, $A_1(0) = A_2(0) = 5 \times 10^{-2}$ m^2,

$k = 2 \times 10^5$ N m^{-2}, $G = 100$ N m^{-2}, $\beta_1 = \beta_2 = \beta$, and $L_1 = L_2 = L = 10$ m.

4.3.1 Natural Frequencies of Non-prismatic EB double-beam system composed of identical beams for different boundary conditions

Table 4.4 lists the first four natural frequencies of non-prismatic EB double-beam system composed of identical beams for different boundary conditions with various

values of taper ratio (β). The cases of the boundary conditions considered are:

(i) both ends of the two beams are simply supported (SS-SS);

(ii) both ends of the two beams are clamped (CC-CC);

(iii) both ends of the upper beam are simply supported; while both ends of the lower beam are clamped (SS-CC);

(iv) both ends of the upper beam are simply supported; while both ends of the lower beam are free (SS-FF);

(v) both ends of the upper beam are simply supported; while the lower beam is clamped- free (SS-CF);

(vi) both ends of the upper beam are clamped; while the lower beam is clamped-free (CC-CF);

(vii) both ends of the upper beam are simply supported; while the lower beam is clamped- free (SS-CF);

(viii) upper beam clamped-free, lower beam clamped-free beam (CF-CF).

Table 4.4: Variation of the first four natural frequencies of a non-prismatic Euler-Bernoulli double-beam system composed of identical beams elastically coupled by Pasternak layer with various values of taper ratio (non-uniformity parameter) under different boundary conditions (Winkler modulus, $k = 2 \times 10^5$ N m^{-2}; shear modulus, $G = 100$ N m^{-2}

Taper ratio (β)	Freq.	Boundary conditions						
		SS-SS	CC-CC	SS-CC	SS-FF	SS-CF	CC-CF	CF-CF
$\beta = 0$ (prismatic)	ω_1	19.7392	44.7466	32.6049	16.9751	23.1918	35.1206	7.0320
$\beta = 0.25$		17.1544	38.9673	29.2081	15.3121	21.7654	32.9477	7.2725
$\beta = 0.50$		14.2431	32.6712	25.1394	13.1731	19.7984	29.0730	7.6476
$\beta = 0$ (prismatic)	ω_2	66.2558	77.4758	72.9650	40.2520	50.8642	53.9764	44.0690
$\beta = 0.25$		68.8124	78.2058	74.2198	40.6190	52.6751	56.3064	40.5078
$\beta = 0.50$		57.9037	80.9705	69.1299	39.4515	52.9992	61.1684	36.6345
$\beta = 0$ (prismatic)	ω_3	78.9568	123.3460	88.4713	57.9528	70.5884	75.9423	63.6352
$\beta = 0.25$		69.7946	107.3940	79.9916	58.2069	72.9462	77.2142	70.9496
$\beta = 0.50$		74.3212	89.9613	78.7660	58.3934	76.1885	80.4525	79.1401
$\beta = 0$ (prismatic)	ω_4	101.1680	138.6180	132.7366	68.3761	90.4711	124.5378	77.0866
$\beta = 0.25$		96.7666	127.0700	120.4750	70.5954	84.4139	110.4539	80.0853
$\beta = 0.50$		95.3683	117.1053	110.2125	74.5137	83.1926	96.9528	88.5552

)

It has, however, been demonstrated in Table 4.4 that DTM can be used to obtain natural frequencies of non-prismatic elastically connected double-beam system for any combination of end configurations for the beams that made up the system.

4.3.2 Effect of taper ratio on the natural frequencies of identical Euler-Bernoulli double-beam system with Pasternak middle layer

The effects of the taper ratio on the first four natural frequencies of an elastically connected non-prismatic double-beam system composed of two identical Euler-Bernoulli (EB) beams attached together by a Pasternak elastic medium are graphically shown in set of Figures 4.1– 4.4. The physical properties of the beams used for the calculations are the ones stated earlier.

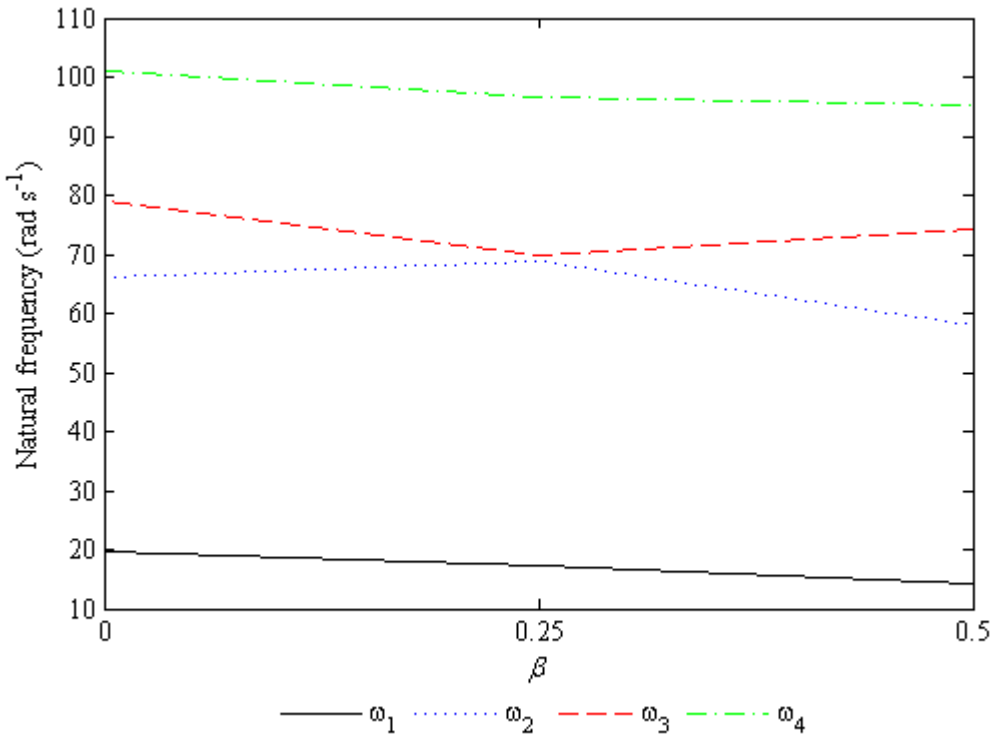

Figure 4.1: Effect of taper ratio on the first four natural frequencies for a pair of identical Euler-Bernoulli beams with Pasternak middle layer for simply supported boundary conditions

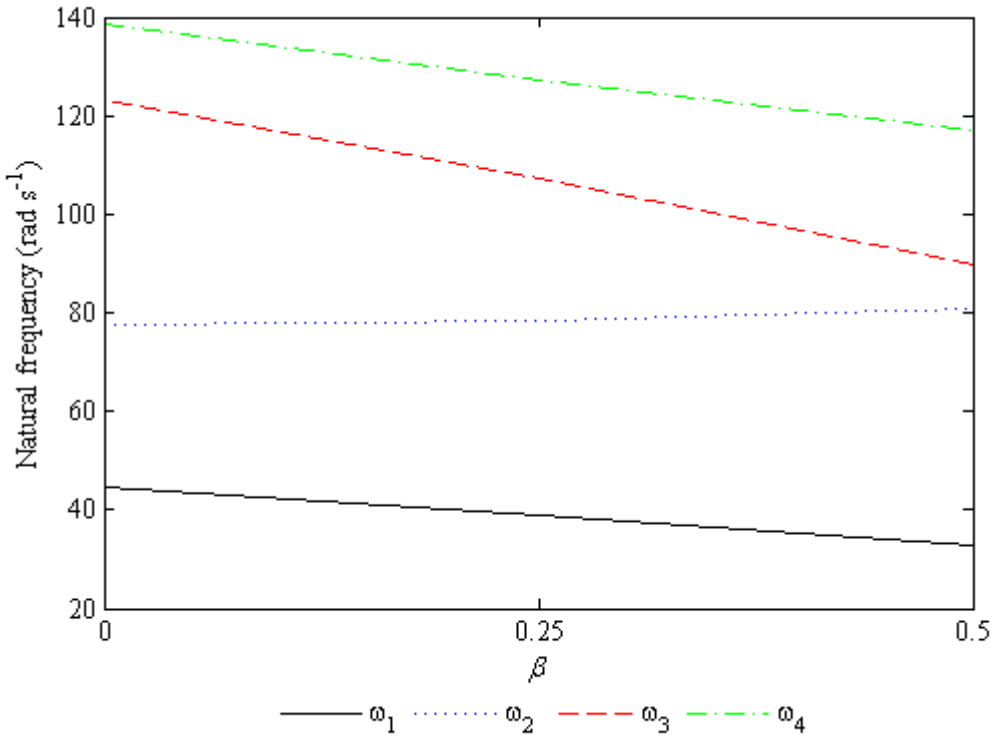

Figure 4.2: Effect of the taper ratio on the first four natural frequencies for CC-CC (clamped-clamped upper beam, clamped-clamped lower beam) for a pair of identical non-prismatic Euler-Bernoulli beams with Pasternak middle layer

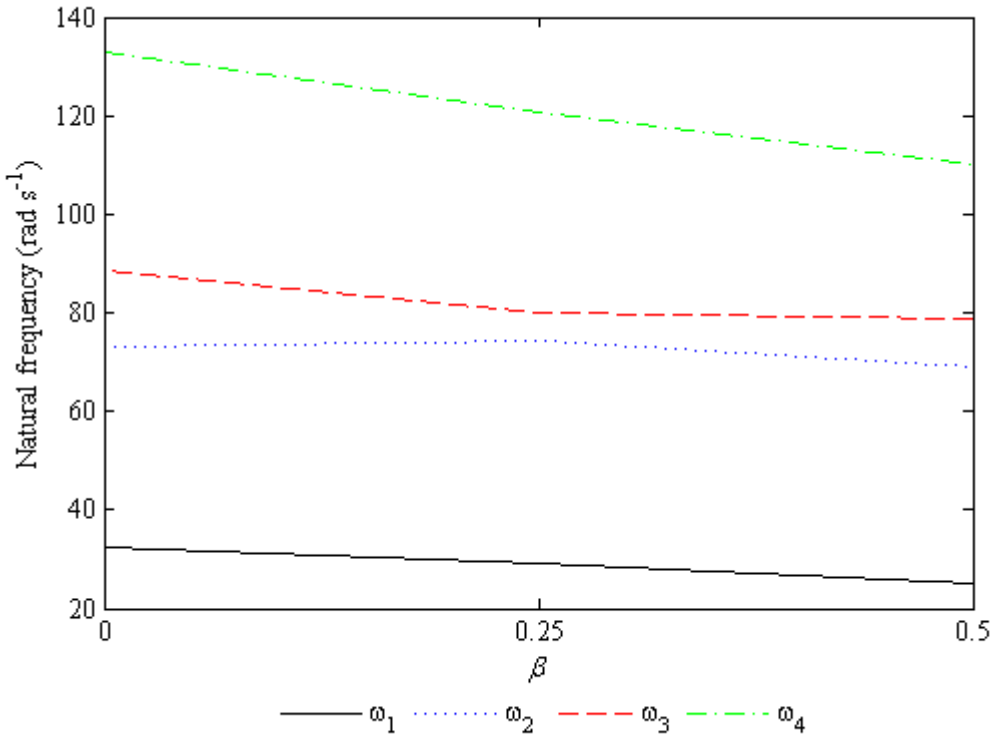

Figure 4.3: Effect of the taper ratio on first four natural frequencies for SS-CC (upper beam simply supported at both ends, lower beam clamped at both ends) for a pair of identical Euler-Bernoulli beams with Pasternak middle layer

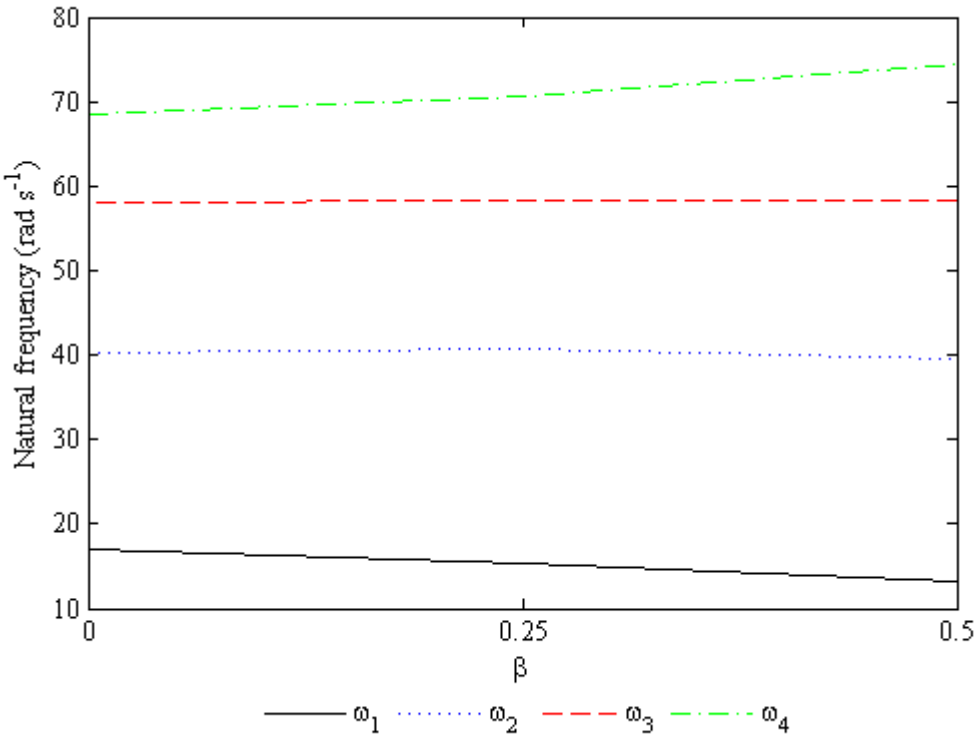

Figure 4.4: Effect of the taper ratio on first four natural frequencies for SS-FF (simply supported-simply supported upper beam, free-free lower beam) for a pair of identical non-prismatic EB beams

It is seen that for simply supported boundary conditions as shown in Figure 4.1, the first and fourth natural frequencies decrease by increasing the value of the taper ratio. However, the second natural frequency initially increases until a certain value is attained after which its trend is reversed. On the contrary, the third natural frequency initially decreases and later increases after reaching a particular value. The case of the first and fourth natural frequencies decreasing with the taper ratio might be due to the softening effect resulting from the decrease of the area of cross-section of the beams.

From Figure 4.2 which shows the influence of taper ratio on the vibration frequencies of a double-beam system consisting a pair of identical Euler-Bernoulli beams with CC-CC boundary condition, it is observed that the first, third and fourth natural frequencies decrease with the increase in the taper ratio, while the taper ratio has a slight increasing effect on the second natural frequency.

From Figure 4.3, it can be seen that increasing the taper ratio has a decreasing effect on all the natural frequencies, except for the second natural frequency which initially increases and later decreases.

Figure 4.4 illustrates the influence of the taper ratio for the SS-FF case. It is obvious that the first natural frequency decreases with the increase of the taper ratio. It is also observed that the third and fourth natural frequencies increase as the taper ratio increases for the end configuration being considered.

Obviously, the taper ratio has a decreasing effect on the fundamental (first) natural frequency of the double-beam system for all the boundary conditions treated. As earlier noted, this behaviour might have occurred because of the softening effect owing to the decrease of the cross-sectional area of the beams.

4.3.3 Effect of Winkler modulus and shear modulus of the Pasternak layer on the natural frequencies of non-prismatic EB double-beam system

The influence of Winkler modulus of the springs and shear modulus of the Pasternak layer in between the two beams is studied in this example for SS-SS, CC-CC and SS-CC boundary conditions. The two beams that make up the system have identical material and geometric properties given as follows:

$E_1 = E_2 = 1 \times 10^{10}$ N m^{-2}, $I_1(0) = I_2(0) = 4 \times 10^{-4}$ m^4,
$\rho_1 = \rho_2 = 2 \times 10^3$ kg m^{-3}, $A_1(0) = A_2(0) = 5 \times 10^{-2}$ m^2, $G = 100$ N m^{-2},
$L_1 = L_2 = 10$ m, and $\beta_1 = \beta_2 = \beta = 0.5$

4.3.3.1 Effect of Winkler modulus on the natural frequencies

The Winkler modulus of the springs that connect the upper beam and lower beam is an important parameter in the vibration analysis of the double-beam system. Thus, its effect on the natural frequencies of the double-beam system is examined. In Figures 4.5 – 4.7, the variation of the first four natural frequencies of the system described in the last Section is plotted with respect to the Winkler modulus of the springs connecting the two identical beams at a fixed value of shear modulus for different boundary conditions previously stated. The material and geometric parameters of the beams used in the previous Section are used here with three different values of Winkler modulus, that is, $k = 1 \times 10^5, 2 \times 10^5, 3 \times 10^5$ N m^{-2}. The value of shear modulus, $G = 100$ N m^{-2}.

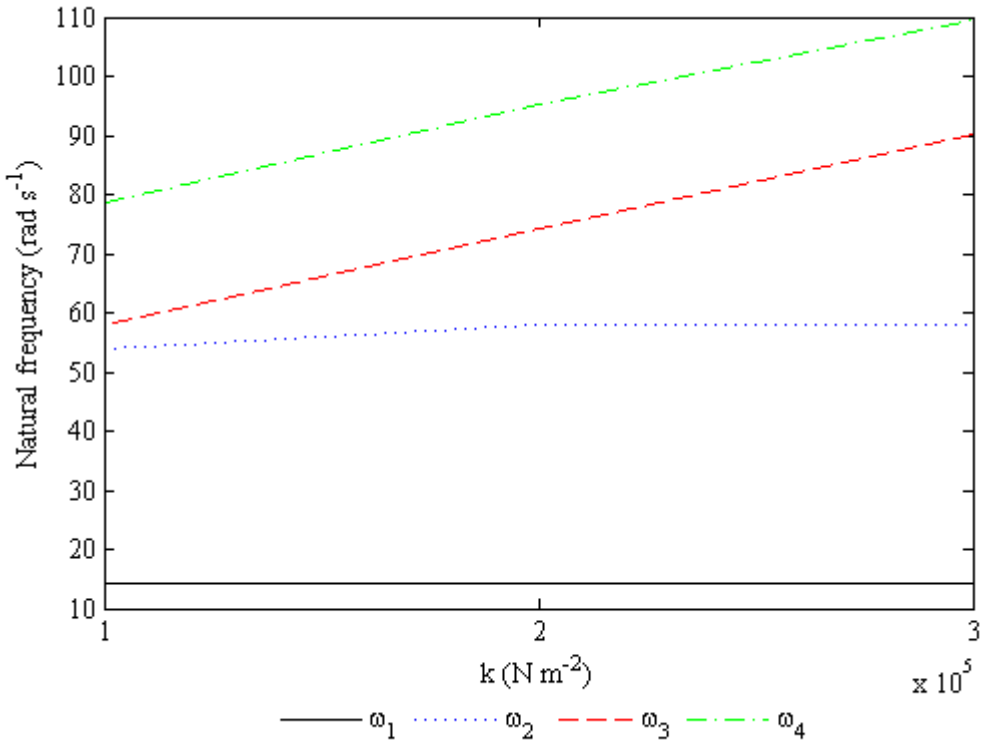

Figure 4.5: Effect of Winkler modulus on the first four natural frequencies of the non-prismatic EB double-beam system composed of two identical beams under simply-supported boundary condition ($G = 100$ N m^{-2})

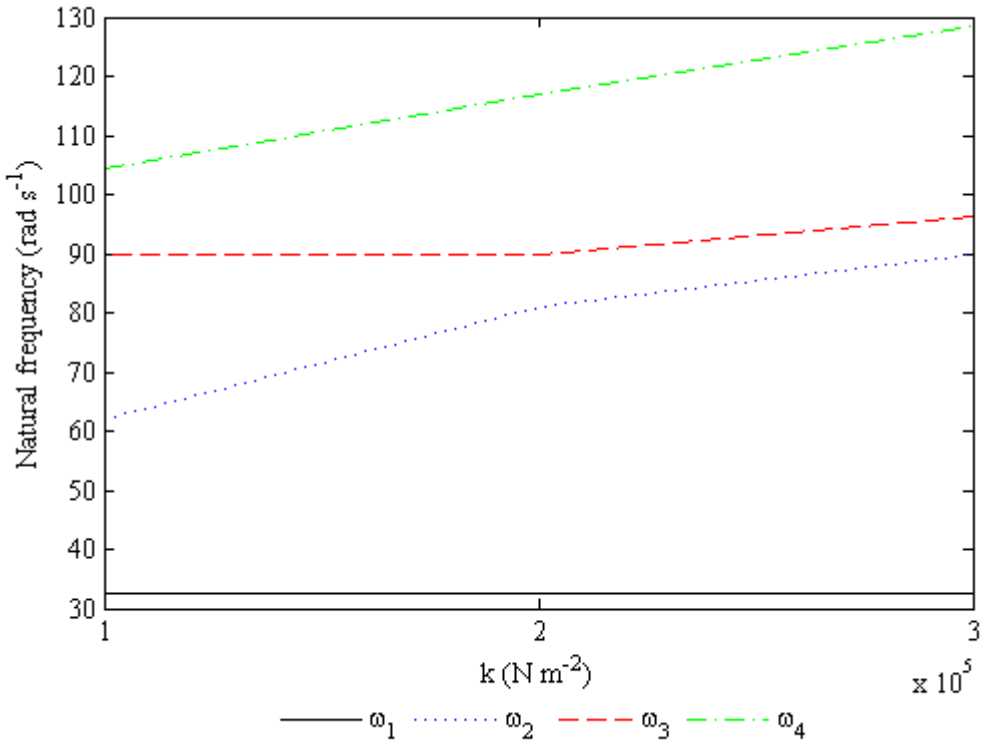

Figure 4.6: Effect of Winkler modulus on the first four natural frequencies of the non-prismatic EB double-beam system composed of two identical beams under CC-CC boundary condition ($G = 100\ \mathrm{N\,m^{-2}}$)

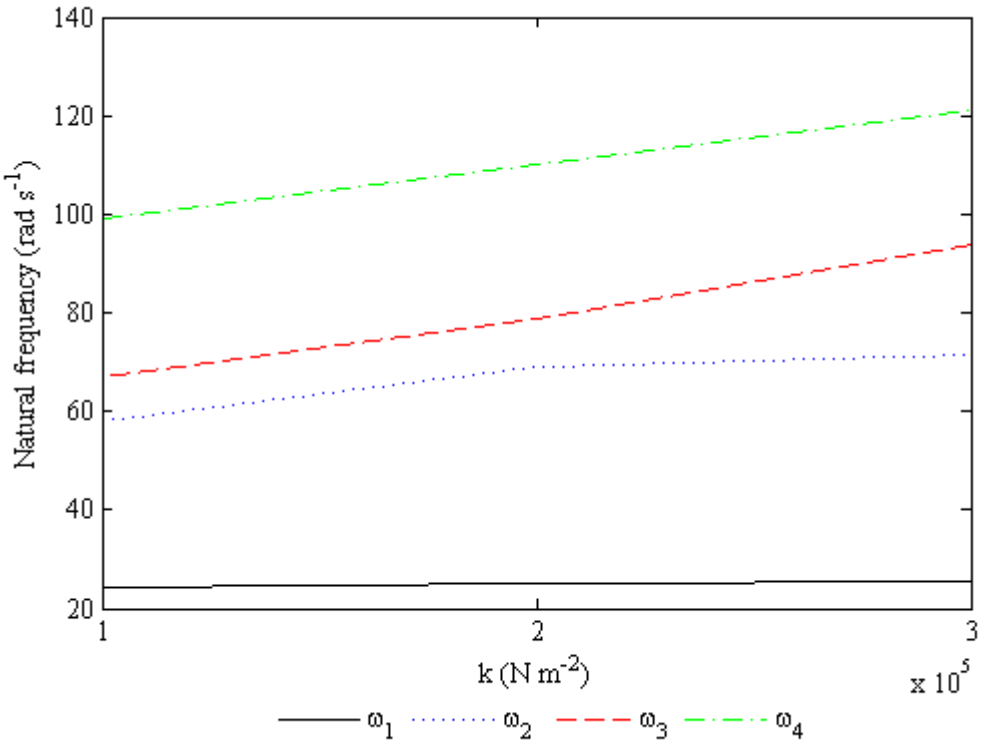

Figure 4.7: Effect of Winkler modulus on the first four natural frequencies of the non-prismatic EB double-beam system composed of two identical beams under SS-CC boundary condition ($G = 100$ N m^{-2})

Figure 4.6 illustrates the effect of the Winkler modulus of the springs on the lowest four frequencies of the double-beam system composed of two non-prismatic identical beams under CC-CC boundary condition ($G = 100\ \mathrm{N\,m^{-2}}$). The influence of the Winkler layer of the springs on the first four natural frequencies of the double-beam system composed of two non-prismatic identical EB beams for SS-CC boundary condition ($G = 100\ \mathrm{N\,m^{-2}}$) is shown in Figure 4.7. It is observed from Figure 4.5 that the first natural frequency for the double-beam system under SS-SS remains constant in spite of the increase in the value of k. Also, the effect of Winkler modulus, k on the second natural frequency is such that as k increases the natural frequency increases slightly. However, it is observed that the third and fourth natural frequencies increase linearly with an increase in the Winkler modulus.

With reference to Figure 4.6, it is obvious that increasing the Winkler modulus has little or no effect on the first natural frequency. It is however, noticed that the Winkler modulus has increasing effect on the third and fourth natural frequencies of the system being considered for CC-CC case when the shear modulus, $G = 100\ \mathrm{N\,m^{-2}}$. It is obvious in Figure 4.7 that the first four natural frequencies for the system are increasing with an increase in the Winkler modulus of the springs between the two beams.

4.3.3.2 Effect of Shear modulus of the Pasternak layer on the natural frequencies of non-prismatic EB double-beam system

The influence of shear modulus of the Pasternak layer in between the two beams is next studied for SS-SS, CC-CC and SS-CC cases. The values of the parameters of the beams used for the analysis are as given here:

$E_1(0) = E_2(0) = 1 \times 10^{10}\ \mathrm{N\,m^{-2}}$, $I_1(0) = I_2(0) = 4 \times 10^{-4}\ \mathrm{m^4}$,
$\rho_1 = \rho_2 = 2 \times 10^{3}\ \mathrm{kg\,m^{-3}}$, $A_1(0) = A_2(0) = 5 \times 10^{-2}\ \mathrm{m^2}$,
$k = 2 \times 10^{5}\ \mathrm{N\,m^{-2}}$, $L_1 = L_2 = L = 10\ \mathrm{m}$, and $\beta_1 = \beta_2 = \beta = 0.5$.
The results of the calculations are shown in Tables 4.5–4.7.

Table 4.5: The first four natural frequencies of a non-prismatic EB double-beam system composed of two identical beams elastically connected by Pasternak layer for different values of shear modulus under simply supported boundary condition (Winkler modulus, $k = 2 \times 10^5$ N m^{-2}, $\beta = 0.50$)

Natural Frequencies	Shear Modulus (N m^{-2})			
	$G = 0$	$G = 100$	$G = 200$	$G = 300$
ω_1	14.2431	14.2431	14.2431	14.2431
ω_2	57.9037	57.9037	57.9037	57.9037
ω_3	74.3194	74.3212	74.3230	74.3248
ω_4	95.3624	95.3684	95.3744	95.3803

Table 4.6: The first four natural frequencies of a non-prismatic EB double-beam system composed of two identical beams elastically connected by Pasternak layer for different values of shear modulus under CC-CC boundary condition (Winkler modulus, $k = 2 \times 10^5$ N m^{-2}, $\beta = 0.50$)

Natural Frequencies	Shear Modulus (N m^{-2})			
	$G = 0$	$G = 100$	$G = 200$	$G = 300$
ω_1	32.6712	32.6712	32.6712	32.6712
ω_2	80.9684	80.9704	80.9725	80.9747
ω_3	89.9613	89.9614	89.9614	89.9613
ω_4	117.0995	117.1051	117.1109	117.1167

It can be observed from Table 4.5 that the influence of shear modulus of the Pasternak layer connecting the two beams is not the same for all the natural frequencies. Specifically, it has no effect on the lowest two natural frequencies of the system. Whereas, magnitudes of the third and fourth frequencies of the system become larger when the value of the shear modulus of the Pasternak layer increases. The insensitivity of the first and the second natural frequencies for simply-supported boundary condition can be explained by their associated mode shapes in Figure 5.8 where the two beams appear to vibrate as a single beam.

As shown in Table 4.6, the first and third natural frequencies for the double-beam system on CC-CC boundary condition have little or no sensitivity to the shear modulus of the Pasternak layer connecting them. However, there is a tendency for the natural frequency for the second and fourth modes of vibration to increase when the shear modulus of the Pasternak layer is increased, though the increment noticed is not well

Table 4.7: The first four natural frequencies of a non-prismatic EB double-beam system composed of two identical beams elastically connected by Pasternak layer for different values of shear modulus under SS-CC boundary condition (Winkler modulus, $k = 2 \times 10^5$ N m^{-2}, $\beta = 0.50$)

Natural Frequencies	Shear Modulus (N m^{-2})			
	$G = 0$	$G = 100$	$G = 200$	$G = 300$
ω_1	25.1392	25.1394	25.1397	25.1399
ω_2	69.1288	69.1299	69.1311	69.1322
ω_3	78.7643	78.7660	78.7678	78.7696
ω_4	110.2076	110.2125	110.2171	110.2219

pronounced.

As depicted in Table 4.7, it is noted that increment of the shear modulus for the case of SS-CC boundary condition has small increasing effect on all the lowest four natural frequencies of the double-beam system.

4.3.4 Mode shapes of a non-prismatic EB double-beam system composed of two identical beams elastically connected by Pasternak layer for different boundary conditions (Winkler modulus, $k = 2 \times 10^5$ N m^{-2}, $\beta_1 = \beta_2 = \beta = 0.50$)

The first four mode shapes for SS-SS, CC-CC and SS-CC boundary conditions are shown in Figures 4.8–4.10.

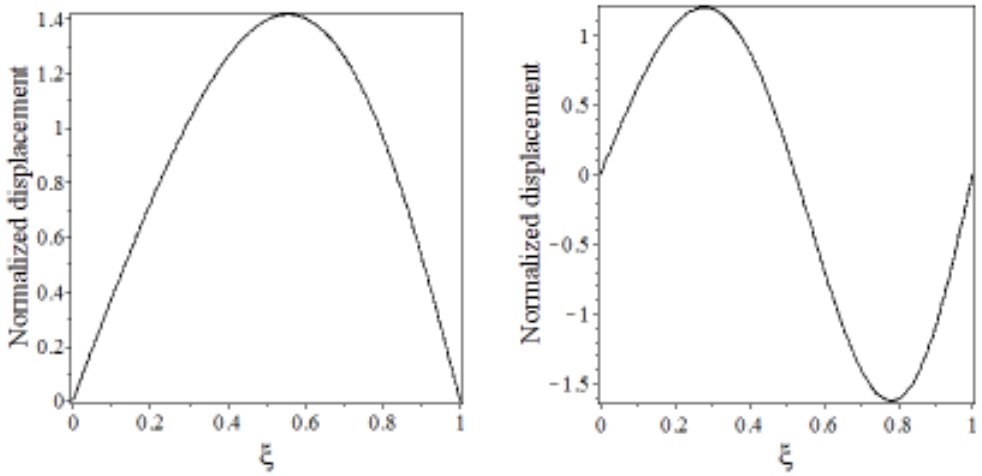

(a) 1st Mode shape: $\omega_1 = 14.2431$

(b) 2nd Mode shape: $\omega_2 = 57.9037$

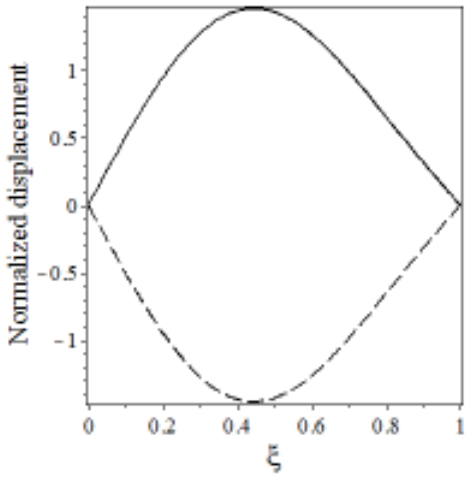

(c) 3rd Mode shape: $\omega_3 = 74.3212$

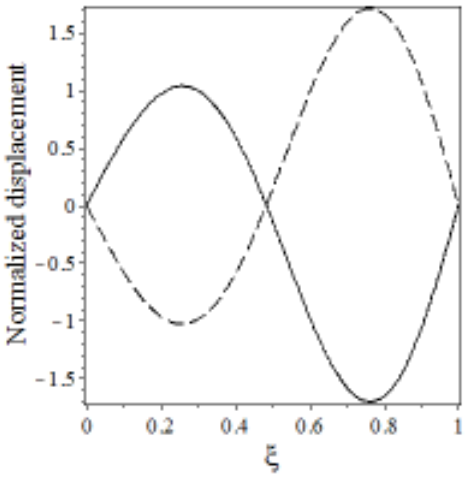

(d) 4th Mode shape: $\omega_4 = 95.3683$

Figure 4.8: The first four mode shapes of the non-prismatic simply supported-simply supported (SS-SS) double-beam system composed of a pair of identical EB beams: $\beta_1 = \beta_2 = \beta = 0.5$, $k = 2 \times 10^5$ N m^{-2}, $G = 100$ N m^{-2}; upper beam (solid line), lower beam (dash)

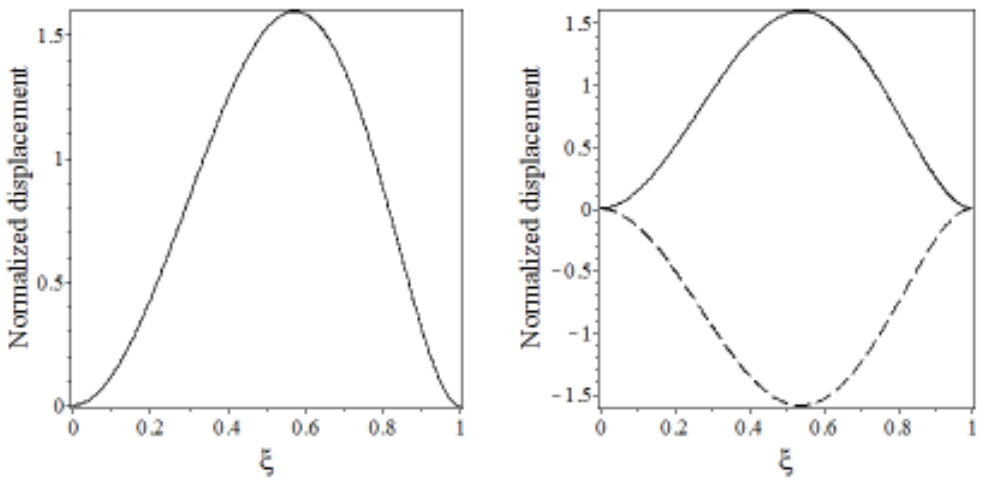

(a) 1st Mode shape: $\omega_1 = 32.6712$

(b) 2nd Mode shape: $\omega_2 = 80.9705$

(c) 3rd Mode shape: $\omega_3 = 89.9613$

(d) 4th Mode shape: $\omega_4 = 117.1053$

Figure 4.9: The four mode shapes of the non-prismatic double-beam system composed of a pair of identical EB beams under CC-CC boundary condition: $\beta_1 = \beta_2 = \beta = 0.5$, $k = 2 \times 10^5$ N m^{-2}, $G = 100$ N m^{-2}; upper beam (solid line), lower beam (dash)

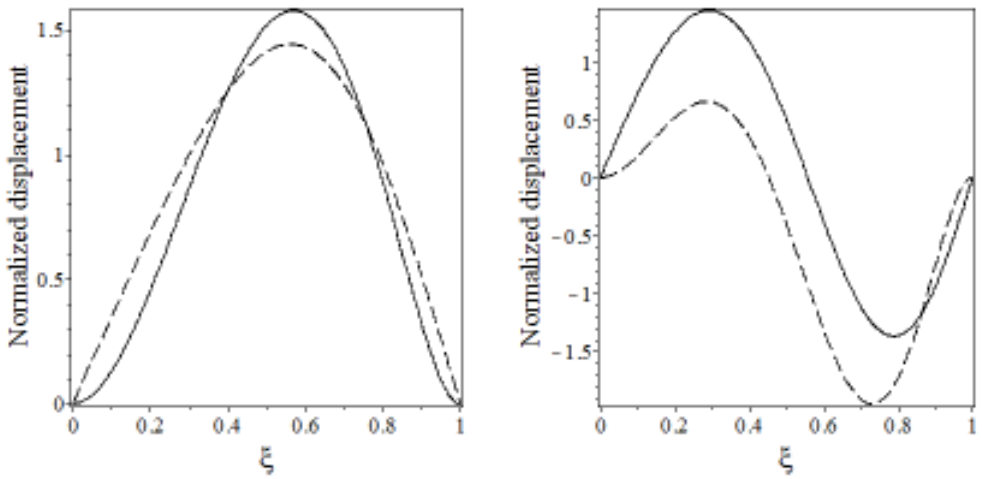

(a) 1st Mode shape: $\omega_1 = 25.1394$ (b) 2nd Mode shape: $\omega_2 = 69.1299$

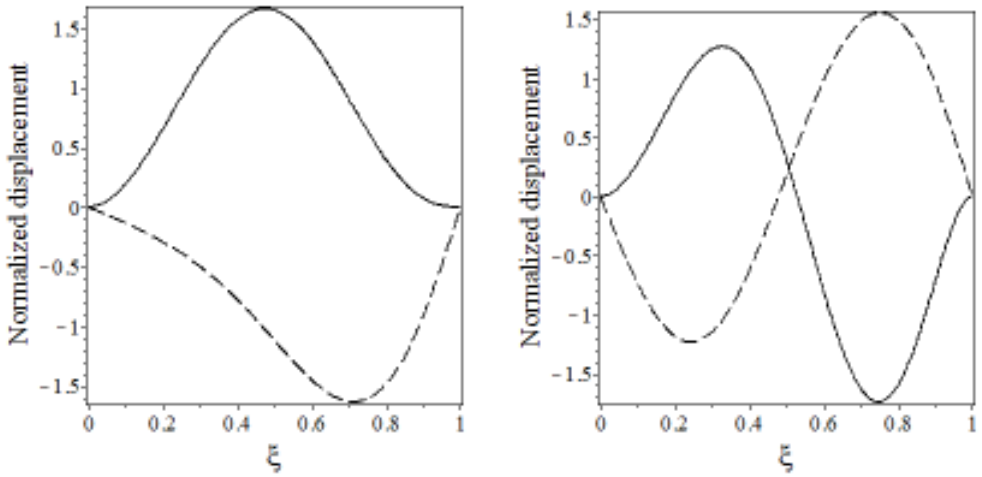

(c) 3rd Mode shape: $\omega_3 = 78.7660$ (d) 4th Mode shape: $\omega_4 = 110.2125$

Figure 4.10: The first four mode shapes of the non-prismatic double-beam system composed of a pair of identical EB beams under SS-CC boundary condition: $\beta_1 = \beta_2 = \beta = 0.5$, $k = 2 \times 10^5$ N m^{-2}, $G = 100$ N m^{-2}; upper beam (solid line), lower beam (dash)

4.3.5 Non-identical beams case

The natural frequencies of a non-prismatic EB double-beam composed of two non-identical beams elastically connected by a Pasternak layer for fixed values of Winkler modulus of the springs and shear modulus of the Pasternak layer are presented here.

The two beams in this case are non-identical in terms of their material and geometric properties. The properties of the beams are given as follows:

$E_1 = E_2 = 1 \times 10^{10}\ \mathrm{N\,m^{-2}}$, $I_1(0) = 4 \times 10^{-4}\ \mathrm{m^4}$, $I_2(0) = 2 \times I_1(0)$,
$\rho_1 = \rho_2 = 2 \times 10^{3}\ \mathrm{kg\,m^{-3}}$, $A_1(0) = 5 \times 10^{-2}\ \mathrm{m^2}$, $A_2(0) = 2 \times A_1(0)$,
$k = 2 \times 10^{5}\ \mathrm{N\,m^{-2}}$, $G = 100\ \mathrm{N\,m^{-2}}$, and $L_1 = L_2 = L = 10\ \mathrm{m}$

In Table 4.8, the first four natural frequencies for a non-prismatic Euler-Bernoulli (EB) double-beam system having Pasternak middle layer under various combinations of boundary conditions for various values of taper ratio (non-uniformity parameter) of the beams on the free vibration frequencies of the system are presented.

Table 4.8: The first four natural frequencies of a non-prismatic EB double-beam system elastically connected by Pasternak layer for different values of taper ratio under different boundary conditions (non-identical case)

Freq.	Taper Ratio (β)	Boundary conditions					
		SS-SS	CC-CC	SS-CC	SS-CF	CC-CF	CF-CF
ω_1	$\beta = 0$	19.7392	44.7466	35.5935	20.6665	27.5341	7.0320
	$\beta = 0.25$	17.1544	38.9673	32.0082	20.2971	27.6686	7.2725
	$\beta = 0.50$	14.2431	32.6712	27.5406	19.3127	26.1178	7.6476
ω_2	$\beta = 0$	58.2219	70.7279	64.2078	44.5054	48.4489	44.0690
	$\beta = 0.25$	61.0686	70.4800	64.9492	44.8169	47.3715	40.5078
	$\beta = 0.50$	57.9037	72.0574	66.5313	45.3763	48.8670	36.6345
ω_3	$\beta = 0$	78.9568	123.3456	89.4528	62.0779	69.6474	55.2217
	$\beta = 0.25$	68.8124	107.3941	81.4525	63.7103	69.7477	61.6178
	$\beta = 0.50$	64.9313	89.9613	73.8008	66.5642	71.6508	69.3678
ω_4	$\beta = 0$	96.0977	134.9624	128.2406	90.4147	124.1014	70.3013
	$\beta = 0.25$	90.5810	122.4463	114.4671	83.6147	110.0005	72.2055
	$\beta = 0.50$	87.4348	110.9236	101.8908	79.0304	95.4109	78.3339

4.3.6 Effect of mass and flexural rigidity of upper beam on vibration frequencies of non-prismatic EB double-beam system coupled by Pasternak elastic layer

The influence of the mass of the upper beam on the natural frequencies of a non-prismatic EB double-beam system elastically coupled by a Pasternak layer is investigated here. Four cases of variation are considered as follows:

Case 1: $\rho_1 A_1(0)(0) = 0.1 \times \rho A(0)$;

Case 2: $\rho_1 A_1(0) = 0.5 \times \rho A(0)$;

Case 3: $\rho_1 A_1(0) = \rho A(0)$;

Case 4: $\rho_1 A_1(0) = 2 \times \rho A(0)$

where $E = 1 \times 10^{10}\ \mathrm{N\,m^{-2}}$, $I(0) = 4 \times 10^{-4}\ \mathrm{m^4}$, $\rho = 2 \times 10^{3}\ \mathrm{kg\,m^{-3}}$,

$A(0) = 5 \times 10^{-2}\ \mathrm{m^2}$, $E_1 I_1(0) = E_2 I_2(0) = EI(0)$,

$\rho_2 A_2(0) = \rho A_2(0), k = 2 \times 10^{5}\ \mathrm{N\,m^{-2}}$,

$G = 100\ \mathrm{N\,m^{-2}}$, $L = 10\ \mathrm{m}$, and $\beta_1 = \beta_2 = \beta = 0.5$.

The results of the analysis for the effect of the mass of the upper beam on the vibration frequencies of the EB double-beam system for SS-SS, CC-CC and SS-CC boundary conditions are presented in Table 4.9.

The data in Table 4.9 evidently indicate that all the first four natural frequencies of the non-prismatic double-beam system for the three cases of the boundary conditions considered are very sensitive to the mass of the upper beam. Specifically, there is tendency to lower the vibration frequency of the whole double-beam system by increasing the mass of the upper beam.

Table 4.9: Variation of the first four vibration frequencies with mass per unit length of the upper beam of a non-prismatic Euler-Bernoulli double-beam system elastically connected by Pasternak layer for SS-SS, CC-CC and SS-CC boundary conditions

Natural Frequencies	cases	Boundary conditions		
		SS-SS	CC-CC	SS-CC
ω_1	case 1	18.9741	41.7358	34.7902
	case 2	16.4124	37.3353	29.6366
	case 3	14.2431	32.6712	25.1394
	case 4	11.6053	26.4001	19.8849
ω_2	case 1	69.0134	100.4019	97.1956
	case 2	64.8811	97.4295	89.9153
	case 3	57.9037	80.9705	69.1299
	case 4	45.8779	68.8931	50.8641
ω_3	case 1	138.7188	183.3349	175.8171
	case 2	91.4104	100.8411	93.6927
	case 3	74.3212	89.9613	78.7660
	case 4	64.6369	71.3054	70.0452
ω_4	case 1	177.3322	200.7885	184.2698
	case 2	120.0124	151.9237	125.0829
	case 3	95.3683	117.1053	110.2125
	case 4	84.8614	107.4262	98.3224

An investigation on the effect of the flexural rigidity of the upper beam on the natural frequencies of non-prismatic EB double-beam system elastically connected by a Pasternak elastic layer is discussed here. The cases of variation considered are as follows:

Case 1: $E_1I_1(0) = 0.1 \times EI(0)$;

Case 2: $E_1I_1(0) = 0.5 \times EI(0)$;

Case 3: $E_1I_1(0) = EI(0)$;

Case 4: $E_1I_1(0) = 2 \times EI(0)$

where $E = 1 \times 10^{10}\ \mathrm{N\,m^{-2}},\ I(0) = 4 \times 10^{-4}\ \mathrm{m^4},\ \rho = 2 \times 10^3\ \mathrm{kg\,m^{-3}},$

$A(0) = 5 \times 10^{-2}\ \mathrm{m^2}$, $E_2I_2(0) = EI(0)$, $\rho_1A_1(0) = \rho_2A_2(0) = \rho A_2(0)$,

$k = 2 \times 10^5\ \mathrm{N\,m^{-2}},\ G = 100\ \mathrm{N\,m^{-2}},\ L = 10\ \mathrm{m},$ and $\beta_1 = \beta_2 = \beta = 0.5$

The results of the study of the effects of the flexural rigidity of the upper beam on the first four natural frequencies of the non-prismatic EB double-beam system coupled by

Pasternak elastic layer for SS-SS, CC-CC and SS-CC boundary conditions are shown in Table 4.10.

Table 4.10: Effect of flexural rigidity of upper beam on vibration frequencies of a non-prismatic EB double-beam system elastically connected by Pasternak layer for SS-SS, CC-CC and SS-CC boundary conditions

Natural Frequencies	cases	Boundary conditions		
		SS-SS	CC-CC	SS-CC
ω_1	case 1	10.4893	23.3516	22.5807
	case 2	12.3155	28.0649	23.8669
	case 3	17.3895	32.6712	25.1394
	case 4	17.3895	39.3688	27.3853
ω_2	case 1	38.1351	51.2399	46.8402
	case 2	48.8783	73.3947	58.2902
	case 3	57.9037	80.9705	69.1299
	case 4	67.3792	84.5130	73.0224
ω_3	case 1	62.8207	74.8903	64.7111
	case 2	73.8182	79.5717	78.0740
	case 3	74.3212	89.9613	78.7660
	case 4	75.5563	100.1939	86.3076
ω_4	case 1	73.5035	78.3299	78.2700
	case 2	91.3999	111.0436	103.8485
	case 3	95.3683	117.1053	110.2125
	case 4	105.7530	140.9307	114.2948

It is evident from Table 4.10 that the natural frequencies of the double-system generally increase with an increase in the flexural rigidity of the upper beam of the double-beam system considered.

4.4 Vibration characteristics of non-prismatic Rayleigh double-beam system elastically connected by Pasternak elastic layer

The following Section deals with the free vibration analysis of non-prismatic double-beam system elastically connected by Pasternak layer in the case where both beams are based on Rayleigh beam theory. The Rayleigh beam theory considers the effects of rotatory inertia which is neglected in the Euler-Bernoulli beam hypothesis and thus presents a better approximation on the behaviour of the double-beam structure.

4.4.1 Natural Frequencies of Non-prismatic Rayleigh double-beam system composed of identical beams for different boundary conditions

In Table 4.11, the variation of the first four natural frequencies with the taper ratio for a double-beam system composed of two non-prismatic Rayleigh beams having identical material and geometric properties for different arrangements of boundary conditions of interest is displayed. The table is the counterpart of Table 4.4 which in its own sense is based on Euler-Bernoulli beam model.

Table 4.11: The first four natural frequencies of a non-prismatic Rayleigh double-beam system composed of identical beams for different boundary conditions with various values of taper ratio (non-uniformity parameter) and coupled by Pasternak elastic layer

Taper ratio (β)	Freq.	Boundary conditions				
		SS-SS	CC-CC	SS-CC	SS-CF	SS-FF
$\beta = 0$		19.7314	44.7246	32.5911	23.1885	16.9708
$\beta = 0.25$	ω_1	17.1492	38.9526	29.1985	21.7603	15.3088
$\beta = 0.50$		14.2397	32.6622	25.1332	19.7946	13.1707
$\beta = 0$		66.2297	77.4377	72.9311	50.8227	40.2391
$\beta = 0.25$	ω_2	68.7297	78.1763	74.1900	52.6407	40.6027
$\beta = 0.50$		57.8535	80.9474	69.0703	52.9703	39.4356
$\beta = 0$		78.8324	123.1191	88.3310	70.5326	57.9225
$\beta = 0.25$	ω_3	69.7727	107.2440	79.8979	72.9076	58.1684
$\beta = 0.50$		74.2987	89.8720	78.7418	76.1478	58.3457
$\beta = 0$		101.0087	138.3638	132.4941	90.3230	68.3175
$\beta = 0.25$	ω_4	96.9508	126.8927	120.3086	84.3113	70.5580
$\beta = 0.50$		95.2893	116.9894	110.1046	83.1398	74.4839

4.4.2 Effect of taper ratio on the natural frequencies of Rayleigh double-beam system made up of identical beams and connected with Pasternak middle layer

Set of Figures 4.11–4.13 symbolize the effects of taper ratio on the first four natural frequencies of a double-beam system composed of two identical Rayleigh beams with variable cross-section and elastically coupled by a Pasternak elastic layer. The physical properties of the beams used for the calculations are the ones used in Section 4.3.

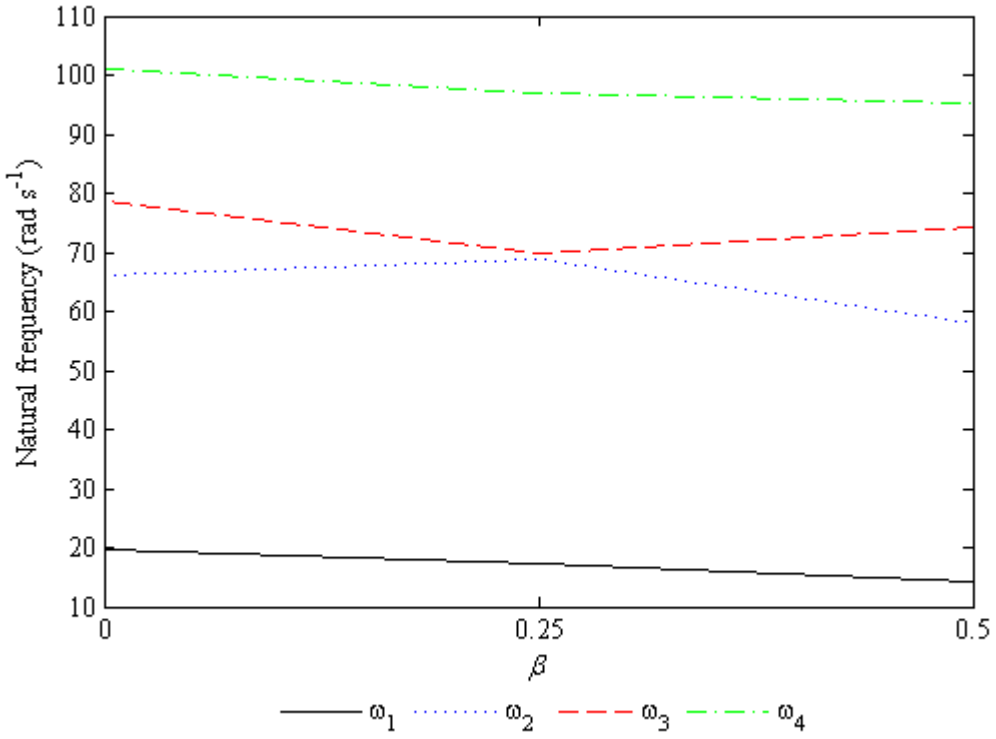

Figure 4.11: Effect of taper ratio on the first four natural frequencies of a non-prismatic Rayleigh double-beam system under SS-SS boundary condition (with the two beams having identical properties)

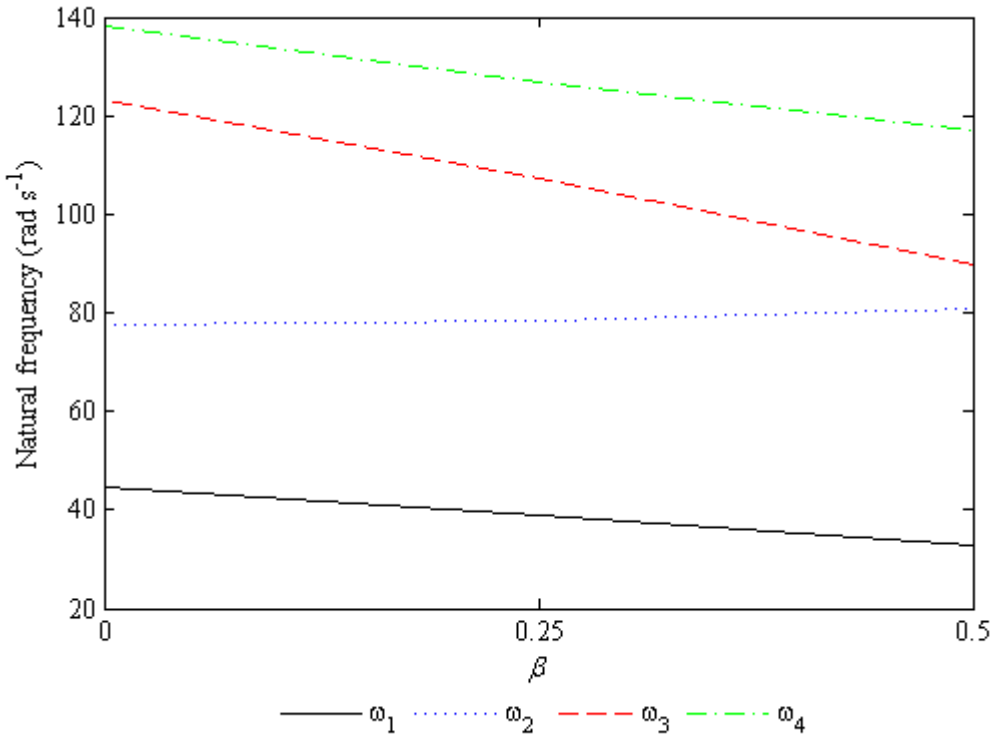

Figure 4.12: Effect of taper ratio on the first four natural frequencies of a non-prismatic Rayleigh double-beam system under CC-CC boundary condition (with the two beams having identical properties)

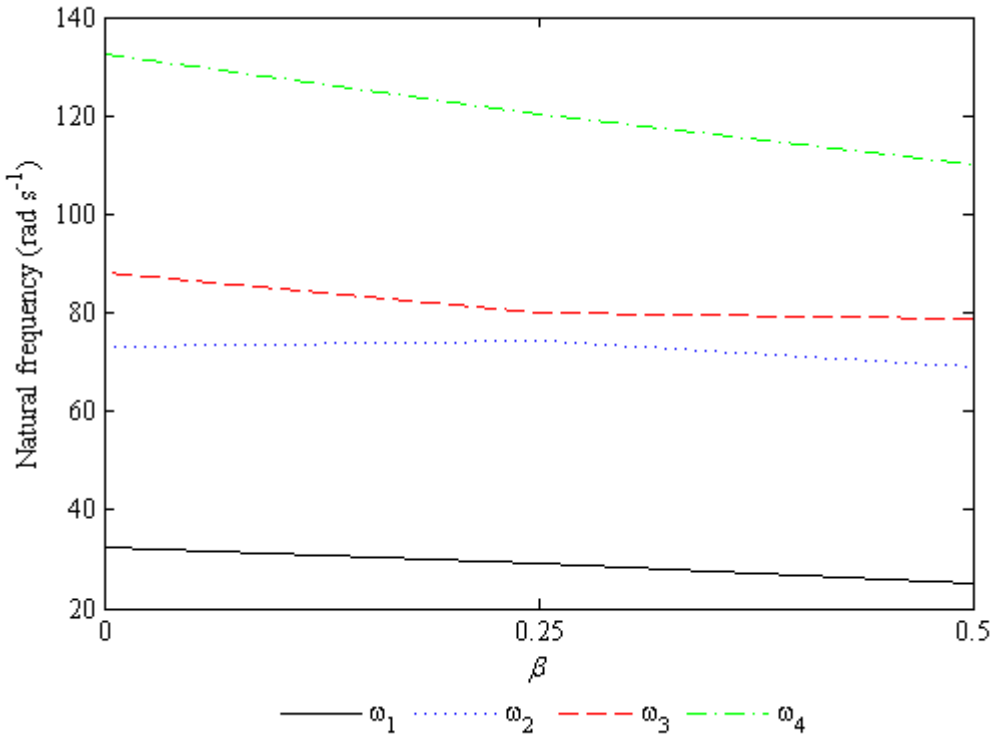

Figure 4.13: Effect of taper ratio on the first four natural frequencies of a non-prismatic Rayleigh double-beam system under SS-CC boundary condition (with the two beams having identical properties)

Obviously, Figures 4.11–4.13 reveal that the influence of taper ratio on the first four natural frequencies of a non-prismatic Rayleigh double-beam system for each of the boundary conditions considered is similar to that of the Euler-Bernoulli double-beam counterpart. The only difference observed is that the frequencies for the Rayleigh double-beam system are lower than the ones for Euler-Bernoulli double-beam system which are apparently due to the effect of the rotatory inertia included in Rayleigh beam theory.

4.4.3 Effect of Winkler modulus and shear modulus of the Pasternak layer on the natural frequencies of non-prismatic double-beam system based on Rayleigh beam theory

Next, the influence of the two moduli relating to the Pasternak elastic layer on the natural frequencies of vibration of non-prismatic double-beam system composed of Rayleigh beams with identical properties is discussed. As earlier done for the Euler-Bernoulli beam theory, the boundary conditions considered are SS-SS, CC-CC and SS-CC. The properties of the beams used in Section 4.3 are used here but with inclusion of the effect of rotatory inertia.

4.4.3.1 Effect of Winkler modulus on the natural frequencies of non-prismatic double-beam system based on Rayleigh beam theory

The effects of Winkler modulus of the springs (at a fixed value of shear modulus) on the natural frequencies of the non-prismatic Rayleigh double-beam system with both beams having the same material and geometric properties are shown in Figures 4.14–4.16.

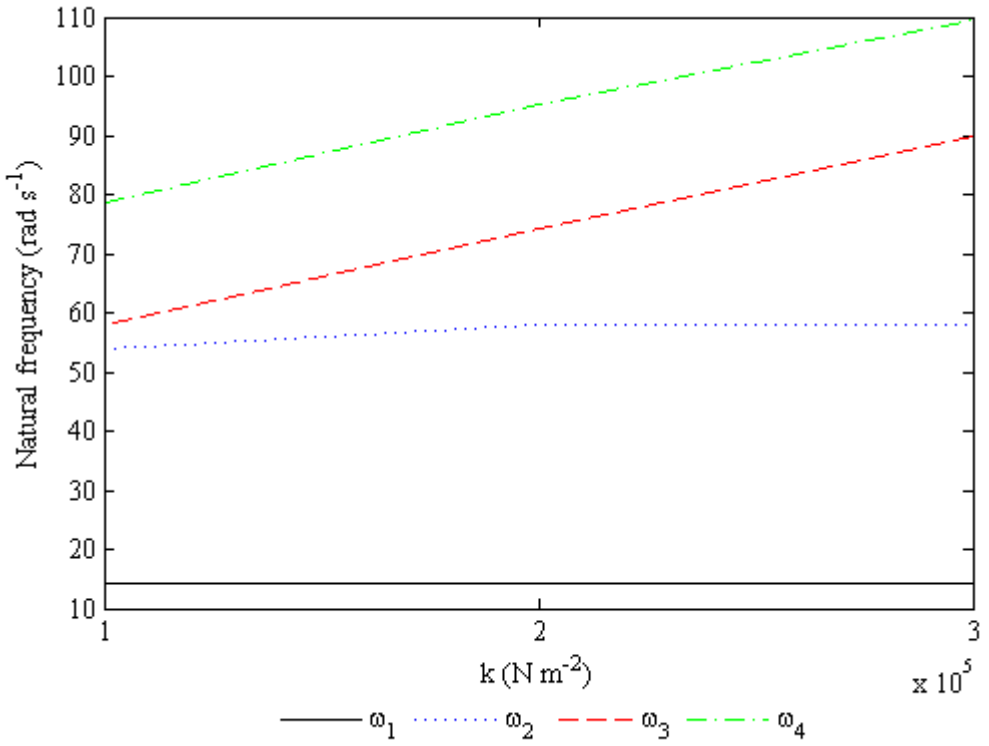

Figure 4.14: Effect of Winkler modulus on the first six natural frequencies of the non-prismatic double-beam system composed of two identical Rayleigh beams under SS-SS boundary condition ($G = 100\ \mathrm{N\,m^{-2}}$)

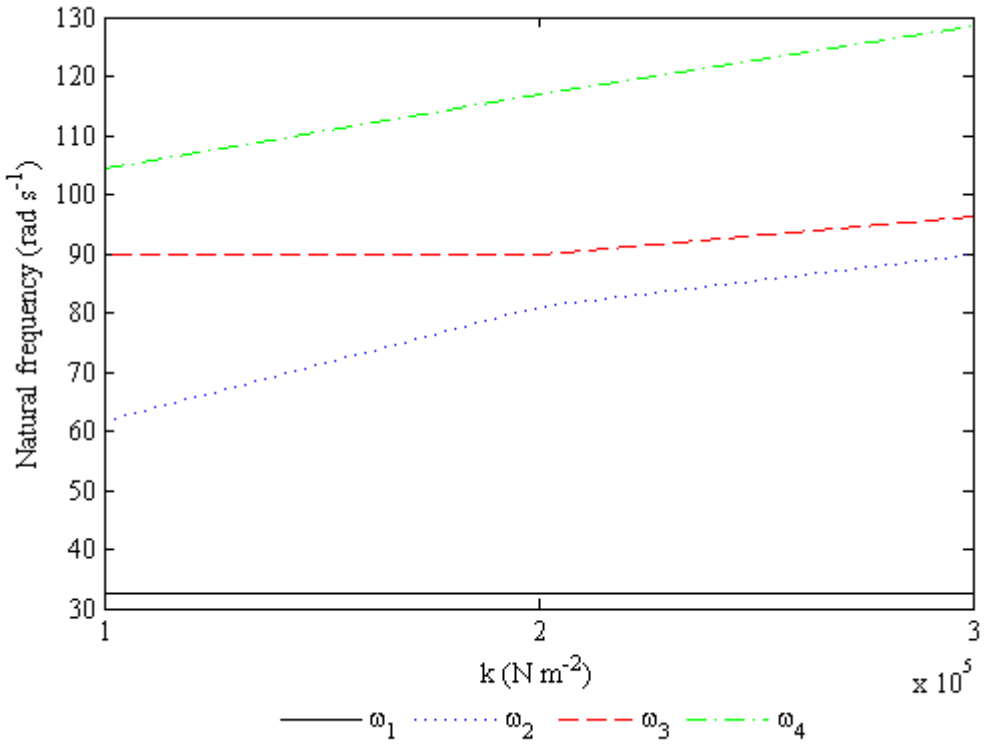

Figure 4.15: Effect of Winkler modulus on the first six natural frequencies of the non-prismatic double-beam system composed of two identical Rayleigh beams under CC-CC boundary condition ($G = 100\ \mathrm{N\,m^{-2}}$)

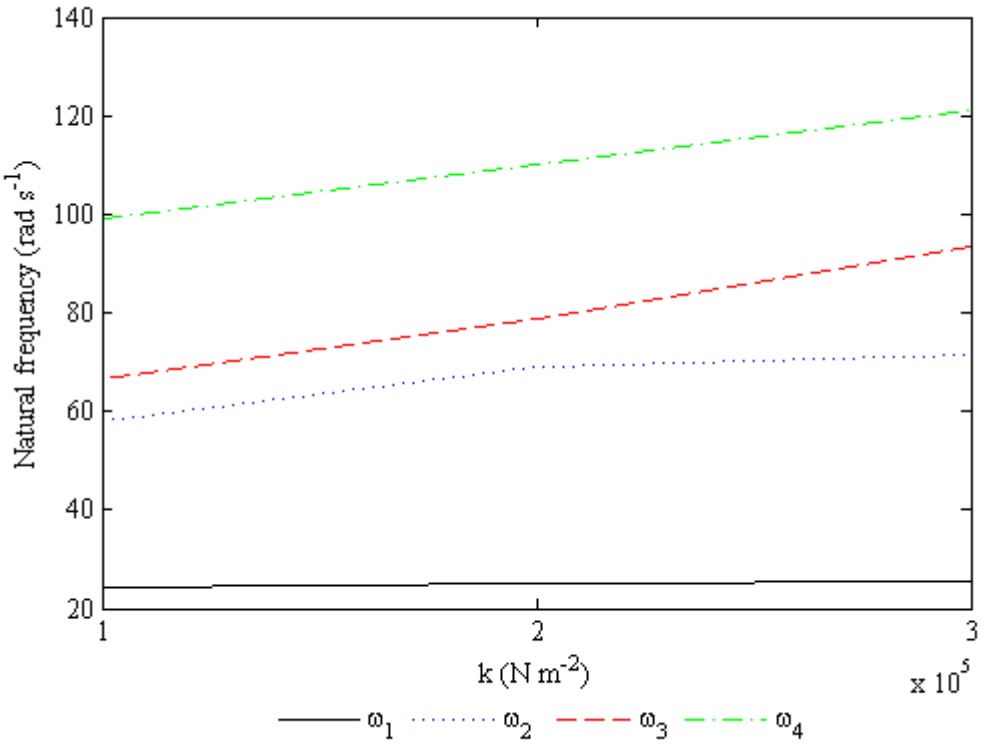

Figure 4.16: Effect of Winkler modulus on the first four natural frequencies of the non-prismatic double-beam system composed of two identical Rayleigh beams under SS-CC boundary condition ($G = 100$ N m^{-2})

4.4.3.2 Effect of shear modulus of the Pasternak layer on the natural frequencies of a non-prismatic double-beam system based on Rayleigh beam theory

The results of the effects of shear modulus of the Pasternak layer on Rayleigh double-beam system for SS-SS, CC-CC and SS-CC boundary conditions are displayed in Tables 4.12–4.14. The values of the parameters of the beams used for the analysis are those previously used for the Euler-Bernoulli case but now with the inclusion of the rotatory inertia term. They are restated here:

$E_1(0) = E_2(0) = 1 \times 10^{10}$ N m^{-2}, $I_1(0) = I_2(0) = 4 \times 10^{-4}$ m^4,

$\rho_1 = \rho_2 = 2 \times 10^3$ kg m^{-3}, $A_1(0) = A_2(0) = 5 \times 10^{-2}$ m^2,

$k = 2 \times 10^5$ N m^{-2}, $L_1 = L_2 = L = 10$ m, and $\beta_1 = \beta_2 = \beta = 0.5$.

Table 4.12: The first four natural frequencies of a non-prismatic Rayleigh double-beam system composed of two identical beams elastically connected by Pasternak layer for different values of shear modulus under simply supported boundary condition (Winkler modulus, $k = 2 \times 10^5$ N m^{-2}, $\beta = 0.50$)

Natural Frequencies	Shear Modulus (N m^{-2})			
	$G = 0$	$G = 100$	$G = 200$	$G = 300$
ω_1	14.2397	14.2397	14.2397	14.2397
ω_2	57.8535	57.8535	57.8535	57.8535
ω_3	74.2969	74.2987	74.3005	74.3023
ω_4	95.2834	95.2893	95.2953	95.3012

Table 4.13: The first four natural frequencies of a non-prismatic Rayleigh double-beam system composed of two identical beams elastically connected by Pasternak layer for different values of shear modulus under CC-CC boundary condition (Winkler modulus, $k = 2 \times 10^5$ N m^{-2}, $\beta = 0.50$)

Natural Frequencies	Shear Modulus (N m^{-2})			
	$G = 0$	$G = 100$	$G = 200$	$G = 300$
ω_1	32.6622	32.6622	32.6622	32.6622
ω_2	80.9453	80.9474	80.9495	80.9516
ω_3	89.8721	89.8719	89.8720	89.8721
ω_4	116.9832	116.9894	116.9952	117.0004

Table 4.14: The first four natural frequencies of a non-prismatic Rayleigh double-beam system composed of two identical beams elastically connected by Pasternak layer for different values of shear modulus under SS-CC boundary condition (Winkler modulus, $k = 2 \times 10^5$ N m^{-2}, $\beta = 0.50$)

Natural Frequencies	Shear Modulus (N m^{-2})			
	$G = 0$	$G = 100$	$G = 200$	$G = 300$
ω_1	25.1329	25.1352	25.1335	25.1337
ω_2	69.0691	69.0703	67.0714	69.0720
ω_3	78.7400	78.7418	78.7435	78.7453
ω_4	110.0997	110.1046	110.1095	110.1141

From the depicted results in Table 4.12, it can be observed that the first and second natural frequencies of the non-prismatic Rayleigh double-beam system under the simply-supported boundary condition remain unchanged when the shear modulus of the Pasternak layer between the beams increases. In line with what was noted for EB double-beam system, the increment of the shear modulus of the Pasternak layer causes an evident increment of the third and fourth natural frequencies of a Rayleigh double-beam system. However, for the CC-CC boundary conditions, it is clearly seen in Table 4.13 that the first and third natural frequencies are generally independent of the Pasternak layer while the second and fourth natural frequencies increase when the shear modulus of the Pasternak layer increase. In Table 4.14 which refers to SS-CC boundary condition, it is shown that the shear modulus of the Pasternak layer has increasing effect on all the four natural frequencies.

4.4.4 Mode shapes of non-prismatic Rayleigh double-beam system composed of two identical beams elastically connected by Pasternak layer for different boundary conditions (Winkler modulus, $k = 2\times10^5$ N m^{-2}, $\beta_1 = \beta_2 = \beta = 0.50$)

Figures 4.17–4.19 show the first four mode shapes of the free vibration of a non-prismatic double-beam system composed of two Rayleigh beams which are elastically coupled by Pasternak layer under the SS-SS, CC-CC and SS-CC boundary conditions.

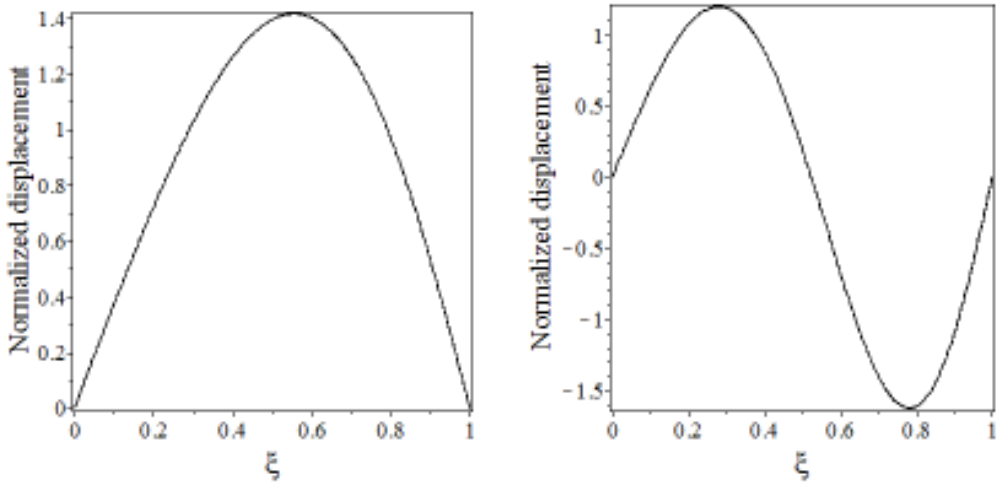

(a) 1st Mode shape: $\omega_1 = 14.2397$

(b) 2nd Mode shape: $\omega_2 = 57.8535$

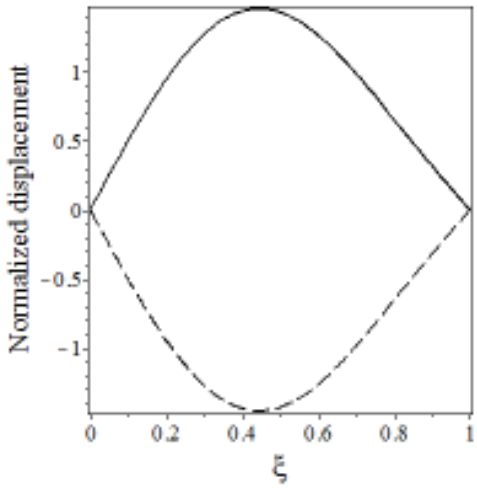

(c) 3rd Mode shape: $\omega_3 = 74.2987$

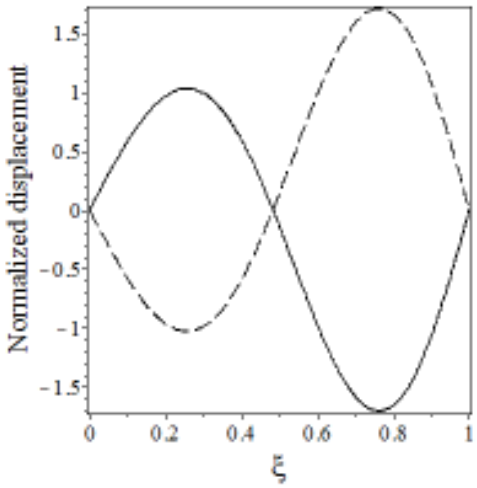

(d) 4th Mode shape: $\omega_4 = 95.2893$

Figure 4.17: The first four mode shapes of the non-prismatic double-beam system composed of a pair of identical Rayleigh beams under simply-supported (SS-SS) boundary condition: $\beta_1 = \beta_2 = \beta = 0.5$, $k = 2 \times 10^5$ N m^{-2}, $G = 100$ N m^{-2}; upper beam (solid line), lower beam (dash)

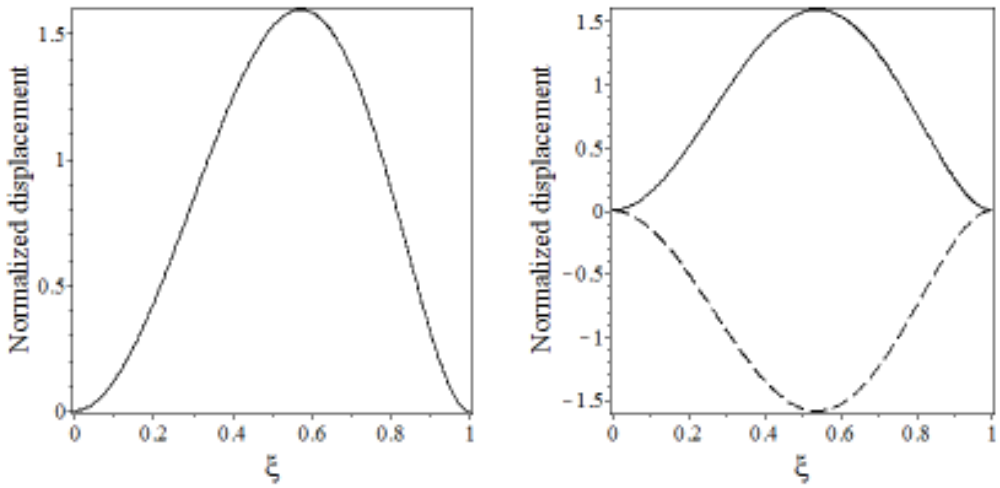

(a) 1st Mode shape: $\omega_1 = 32.6622$ (b) 2nd Mode shape: $\omega_2 = 80.9474$

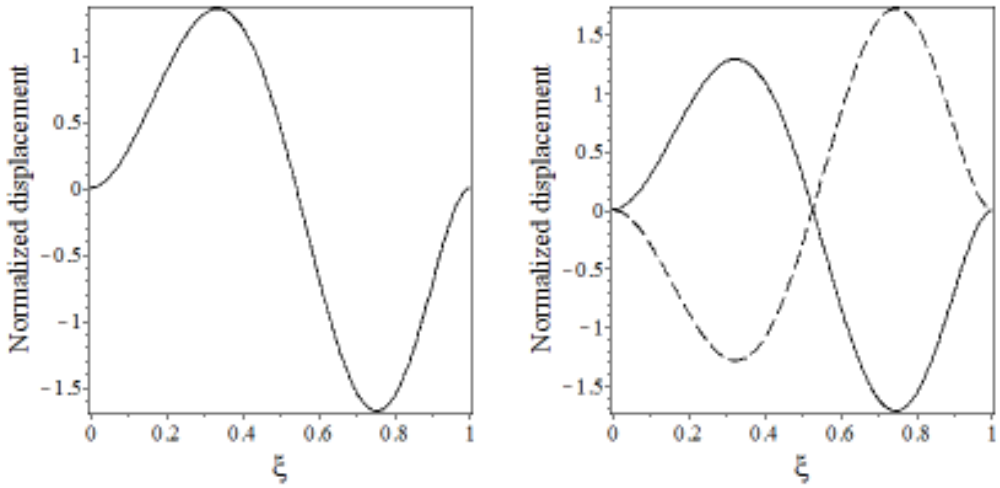

(c) 3rd Mode shape: $\omega_3 = 89.8720$ (d) 4th Mode shape: $\omega_4 = 116.9894$

Figure 4.18: The first four mode shapes of the non-prismatic double-beam system composed of a pair of identical Rayleigh beams under CC-CC boundary condition: $\beta_1 = \beta_2 = \beta = 0.5$, $k = 2 \times 10^5$ N m^{-2}, $G = 100$ N m^{-2}; upper beam (solid line), lower beam (dash)

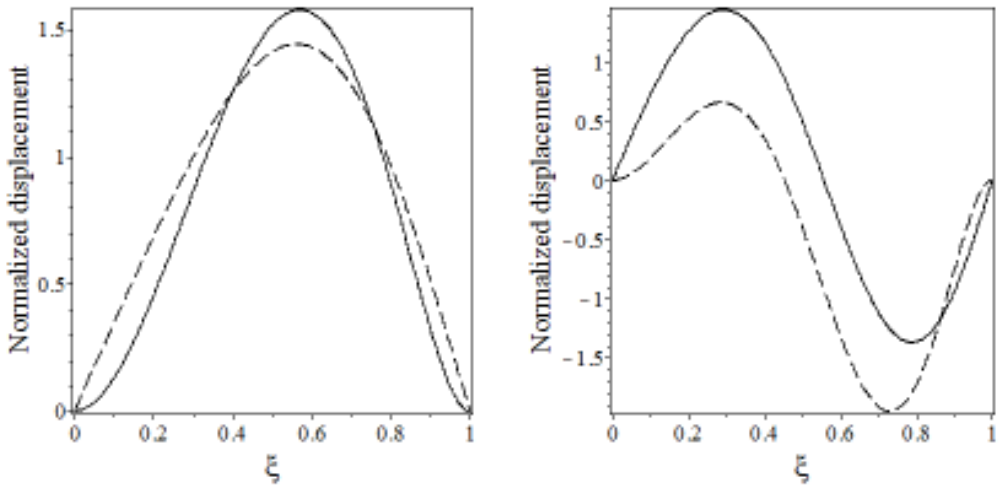

(a) 1st Mode shape: $\omega_1 = 25.1332$

(b) 2nd Mode shape: $\omega_2 = 69.0703$

(c) 3rd Mode shape: $\omega_3 = 78.7418$

(d) 4th Mode shape: $\omega_4 = 10.1046$

Figure 4.19: The first four mode shapes of the non-prismatic double-beam system composed of a pair of identical Rayleigh beams under SC-CC boundary condition: $\beta_1 = \beta_2 = \beta = 0.5$, $k = 2 \times 10^5$ N m^{-2}, $G = 100$ N m^{-2}; upper beam (solid line), lower beam (dash)

The results of the study of the effects of mass per unit length of the upper beam on the first four natural frequencies of the non-prismatic Rayleigh double-beam system coupled by Pasternak elastic layer for SS-SS, CC-CC and SS-CC boundary conditions are shown in Table 4.15.

Table 4.15: Variation of the first four vibration frequencies with mass per unit length of the upper beam of a non-prismatic Rayleigh double-beam system elastically connected by Pasternak layer for SS-SS, CC-CC and SS-CC boundary conditions

Natural Frequencies	cases	Boundary conditions		
		SS-SS	CC-CC	SS-CC
ω_1	case 1	18.9696	41.7244	34.7809
	case 2	16.4085	37.3251	29.6291
	case 3	14.2397	32.6622	25.1332
	case 4	11.6026	26.3928	19.8800
ω_2	case 1	68.9533	100.3020	97.0996
	case 2	64.8248	97.3432	86.8378
	case 3	57.8536	80.9474	69.0703
	case 4	45.8381	68.8319	50.8192
ω_3	case 1	138.4522	182.9469	175.6932
	case 2	91.3839	100.8017	93.6610
	case 3	74.2987	89.8720	78.7418
	case 4	64.6182	71.2777	70.0257
ω_4	case 1	177.2858	200.7347	183.9623
	case 2	119.9098	151.7731	124.9691
	case 3	95.2894	116.9893	110.1046
	case 4	84.7890	107.3195	98.1356

The results of the study of the effects of the flexural rigidity of the upper beam on the first four natural frequencies of the non-prismatic Rayleigh double-beam system coupled by Pasternak elastic layer for SS-SS, CC-CC and SS-CC boundary conditions are shown in Table 4.16.

Table 4.16: Effect of flexural rigidity of upper beam on vibration frequencies of a non-prismatic Rayleigh double-beam system elastically connected by Pasternak layer for SS-SS, CC-CC and SS-CC boundary conditions

Natural Frequencies	cases	Boundary conditions		
		SS-SS	CC-CC	SS-CC
ω_1	case 1	10.4869	23.3452	22.5751
	case 2	12.3126	28.0573	23.8610
	case 3	14.2397	32.6622	25.1332
	case 4	17.3854	39.3581	27.3785
ω_2	case 1	38.1012	51.1881	46.7958
	case 2	48.8359	73.2783	58.2380
	case 3	57.8536	80.9474	69.0703
	case 4	67.3210	84.4887	77.9973
ω_3	case 1	62.6964	74.7357	64.5876
	case 2	73.7944	79.5472	78.0518
	case 3	74.2987	89.8721	78.7418
	case 4	75.5354	100.0951	83.2326
ω_4	case 1	73.4868	78.2941	78.2499
	case 2	91.3215	110.9326	103.6592
	case 3	95.2894	116.9889	110.1046
	case 4	105.6628	140.7903	114.1873

Table 4.16 shows that the natural frequencies of the double-system are increased with increasing the flexural rigidity of the upper beam of the non-prismatic Rayleigh double-beam system. This is similar to what is observed for a non-prismatic Euler-Bernoulli double-beam system in Table 4.10.

CHAPTER FIVE

CONCLUSION AND RECOMMENDATIONS

5.1 Introduction

This chapter summarizes the research described in this thesis. Findings of the study, contributions to the existing body of knowledge on vibration analysis of structures and recommendations for some possible research extensions are also highlighted.

5.2 Summary of the Research Aim and Objectives

Based on the Euler-Bernoulli and Rayleigh beam theories, the free vibration analysis of the characteristics of a non-prismatic double-beam system elastically connected by a Pasternak layer has been studied. Specifically, the following tasks which are captured in the objectives of this study have been accomplished:

(i) The natural frequencies and their corresponding mode shapes for the double-beam system having different boundary conditions, which are combination of simply-supported, clamped and free end supports, have been determined by employing a semi-analytical approach, known as differential transformation method (DTM).

(ii) The effects of the Winkler modulus and shear modulus of the layer connecting the two beams, the taper ratio (often referred to as the non-uniformity parameter of the beams) and the boundary conditions on the vibration characteristics of the double-beam system have been investigated.

(iii) The effects of the mass and flexural rigidity of upper beam on the natural frequencies of the double-beam system have been equally studied.

(iv) Overall, it has been shown that differential transformation method (DTM) has high precision and computational efficiency in the vibration analysis of a system

of two non-prismatic beams which are elastically connected by a Pasternak elastic layer.

Thus, all the objectives of the study stated in Chapter One of this thesis had been successfully accomplished.

5.3 Highlight of Findings

Based on the results of various analyses performed on the non-prismatic double-beam system, the findings are highlighted as follows:

(i) the differential transformation method (DTM) is very proficient in analysing the free vibration of non-prismatic double-beam systems;

(ii) the taper ratio of the beams which accounts for non-uniformity of the beams has significant effect on the natural frequencies of the double-beam system;

(iii) the effects on natural frequencies of the Winkler modulus and shear modulus of the Pasternak layer connecting the beams in the double-beam system largely depend on the type of the boundary conditions;

(iv) non-prismatic double-beam systems have two forms of natural frequencies, known as synchronous and asynchronous natural frequencies. The synchronous natural frequencies are the ones that are independent of the Pasternak layer while asynchronous frequencies are those whose values depend on the Pasternak layer;

(v) the natural frequencies of the simply supported (SS-SS) double-beam systems are smaller than those of the clamped (CC-CC) ones.

(vi) for all the boundary conditions considered, it is found that all the lowest four natural frequencies of the non-prismatic double-beam system are very sensitive to the mass of the upper beam. The mass of the upper beam, in particular, has a decreasing effect on the vibration frequencies of the double-beam system; and

(vii) The natural frequencies of the double-beam system generally increase with an

increase in the flexural rigidity of the upper beam.

5.4 Contributions to Knowledge

The study conducted has led to the following contributions:

(i) extension of differential transformation method to study vibration analysis of elastically connected non-prismatic double-beam systems with a Pasternak middle layer;

(ii) new results on the vibration problem identified above which would be of interest to the scientific and engineering community in the area of multiple-beam structures have been obtained; and

(iii) the natural frequencies and the mode shapes of free vibration analysis of the non-prismatic double-beam system obtained can serve as benchmarks to other researchers who might wish to verify the results using other numerical methods.

5.5 Conclusion

The study taken up in this thesis has developed differential transformation method for solving the vibration problems of elastically connected non-prismatic double-beam system based on Euler-Bernoulli and Rayleigh beam models. The elastic layer joining the two beams in the system has been simulated by Pasternak model. The effects of the structural parameters of the beam and the Pasternak elastic layer on the free vibration characteristics of the system have also been studied.

5.6 Recommendations for future Research

For future development of this research, DTM can be extended to analyse the following vibration problems:

(i) free and forced vibrations of a non-prismatic double-beam system elastically connected by a Pasternak layer subjected to pre-stressed compressive axial load;

(ii) free and forced vibrations of a non-prismatic double-beam system visco-elastically connected by a Pasternak layer;

(iii) further investigation of more complex non-prismatic n-beam systems such as non-prismatic triple-beam systems elastically connected by Pasternak layers;

iv) vibration of two non-prismatic beams partially; connected to each other by a Winkler-type elastic layer; and

(v) free and forced vibrations of non-prismatic cross-beam system.

REFERENCES

Abazari, N., and Abazari, R. (2009). Solution of nonlinear second-order pantograph equations via differential transformation method. *World Academy of Science, Engineering and Technology*, **34**, 1052–1056.

Abbas, L.K., Bestle, D., and Rui, X. (2013). Transfer matrix method for the determination of the free vibration of two elastically coupled beams. *Applied Mechanics and Materials*, **372**, 301–304. doi:10.4028/www.scientific.net/AMM.372.301

Abbas, L.K., Zhou, Q., Hendy, H., and Rui, X. (2015). Transfer matrix method for determination of the natural characteristics of elastically coupled launch vehicle boosters. *Acta Mechanica Sinica*, **31(4)**, 570–580. doi:10.1007/s10409–015–0425–6

Hassan, I.H.A. (2002). On solving some eigenvalue problems by using a differential transformation. *Applied Mathematics and Computation*, **127(1)**, 1–22.

Hassan, I.H.A. (2008). Application to differential transformation method for solving systems of differential equations. *Applied Mathematical Modelling*, **32(12)**, 2552–2559. doi:10.1016/japm.2007.09.025

Abdelghany, S.M., Ewis K.M., Mahmoud A.A., and Nassar, M.M. (2015). Vibration of a circular beam with variable cross sections using differential transformation method, *Beni-Suef University Journal of Basic and Applied Sciences*, **4**, 185–191.

Abrate, S. (1995). Vibratıon of non-unıform rods and beams. *Journal of Sound and Vibration*, **185(4)**, 703–716.

Abu–Hilal, M. (2003). Forced vibration of Euler–Bernoulli beams by means of dynamic Green functions. *Journal of Sound and Vibration*, **267(2)**, 191–207. doi:10.1016/S0022–460X(03)00178–0

Abu–Hilal, M. (2006). Dynamic response of a double Euler–Bernoulli beam due to a moving constant load. *Journal of Sound and Vibration*, **297(3-5)**, 477–491.

Abu–Hilal, M., and Mohsen, M.S. (2000). Vibration of beams with general boundary conditions due to a moving harmonic load. *Journal of Sound and Vibration*, **232(4)**, 703–717. doi:10.1006/jsvi.1999.2771

Abu–Hilal, M., and Zibdeh, H.S. (2000). Vibration analysis of beams with general boundary conditions traversed by a moving force. *Journal of Sound and Vibration*, **229(2)**, 377–388. doi:10.1006/jsvi.1999.2491

Ahmadi, M., and Nikkhoo, A. (2014). Utilization of characteristic polynomials in vibration analysis of non-uniform beams under a moving mass excitation. *Applied Mathematical Modelling*, **38**, 2130–2140. doi:10.1016/j.apm.2013.10.011

Aida, T., Toda, S., Ogawa, N., and Imada, Y. (1992). Vibration control of beams by beam-type dynamic vibration absorbers. *Journal of Engineering Mechanics-ASCE*, **118(2)**, 248–258. doi:10.1061/(ASCE)0733–9399(1992)118:2(248)

Arani, A.G., and Amir, S. (2013). Electro-thermal vibration of visco-elastically coupled BNNT systems conveying fluid embedded on elastic foundation via strain gradient

theory. *Physica B.*, **419**, 1–6.

Arani, A.G., Amir, S., Dashti, P. and Yousefi, M. (2014). Flow-induced vibration of double bonded visco-CNTs under magnetic fields considering surface effect. *Computational Materials Science*, **86**, 144–154. doi:10.1016/j.commatsci.2014.01.047

Ariaei, A., Ziaei-Rad, S., and Ghayour, M. (2011). Transverse vibration of a multiple-Timoshenko beam system with intermediate elastic connections due to a moving load. *Archive of Applied Mechanics*, **81**, 263–281. doi:10.1007/s00419-010-0410-2

Arikoglu, A., and Ozkol, I. (2005). Solution of boundary value problems for integro–differential equations by using differential transform method. *Applied Mathematics and Computation*, **168(2)**, 1145–1158. doi:10.1016/jamc.2004.10.009

Attarnejad, R., and Shahba A. (2008). Application of differential transform method in free vibration analysis of rotating non-prismatic beams. *World Applied Sciences Journal*, **5(4)**, 441–448. Available from: http://www.idosi.org/wasj/wasj5(4)/8.pdf

Attarnejad, R., Jandaghi, S., and Shahba, A. (2010). Basic displacement functions for free vibration of non-prismatic Timoshenko beams. *Finite Elements in Analysis and Design*, **46**, 916–929.

Auciello, N.M., and Maurizi, M.J. (1997). On the natural vibrations of tapered beams with attached inertia elements. *Journal of Sound and Vibration*, **199(3)**, 522–530.

Ayaz, F. (2003). On the two-dimensional differential transform method. *Applied Mathematics and Computation*, **143**, 361–374. doi:10.1016/S0096-3003(02)00368–5

Ayaz, F. (2004). Solutions of the system of differential equations by differential transform method. *Applied Mathematics and Computation*, **147(2)**, 547–567.

Bottega, W.J. (2006). Engineering Vibrations. Boca Raton: Taylor and Francis. ISBN No 13: 978–1–4200–2009–0

Chen, C.K., and Ho, S.H. (1996). Application of differential transformation to eigenvalue problems. *Applied Mathematics and Computation*, **79(2–3)**, 173–188. doi:10.1016/0096-3003(95)00253–7

Chen, C.K., and Ho, S.H. (1999). Transverse vibration of a rotating Timoshenko beam under axial load using differential transform. *International Journal of Mechanical Sciences*, **41(11)**, 1339–1359. doi:10.1016/S0020-7403(98)00095-2

Chonan, S. (1976). Dynamical behaviours of elastically connected double–beam systems subjected to an impulsive load. *Bulletin of JSME*, **19(132)**, 595–603. doi:10.1299/kikai1938.41.2815

Chun, K.R. (1972). Free vibration of a beam with one end spring–hinged and the other free. *Journal of Applied Mechanics*, **39(4)**, 1154–1155. doi:10.1115/1.3422854

De Rosa, M.A., and Lippiello, M. (2007). Non-classical boundary conditions and DQM for double-beams. *Mechanics Research Communications*, **34(7–8)**, 538-544. doi:10.1016/j.mechrescom.2007.08.003

Esmailzadeh, E., and Ghorashi, E. (1995). Vibration analysis of beams traversed by uniform partially distributed moving masses. *Journal of Sound and Vibration*, **184(1)**,

9–17. doi:10.1006/jsvi.1995.0301

Foda, M.A., and Abduljabbar, Z. (1998). A dynamic Green function formulation for the response of a beam structure to a moving mass, *Journal of Sound and Vibration*, **210**, 295–306. doi:10.1006/jsvi.1997.1334

Frýba, L., Fischer, C., and Urushadze, S. (2007). Response of a double system beam and string with an elastic layer to the dynamic excitations. *WIT Transactions on Modelling and Simulation*, **46**, 671–680. Available from: www.witpress.com, ISSN 1743-355X (on-line)e

Fung, R.–F., and Chen, C.–C. (1997). Free and forced vibration of a cantilever beam contacting with a rigid cylindrical foundation. *Journal of Sound and Vibration*, **202(2)**, 161–185. doi:10.1006/jsvi.1996.0831

Gbadeyan, J.A. and Agboola, O.O. (2012). Dynamic behaviour of a double Rayleigh beam–system due to uniform partially distributed moving load. *Journal of Applied Sciences Research*, **8(1)**, 571–581.

Gbadeyan, J.A., Hammed, F.A., and Titiloye, E.O. (2005). Dynamic behavior of visco–elastically connected beams carrying uniform partially distributed moving masses. *Nigeria Journal of Pure and Applied Sciences*, **20**, 1891–1905.

Gbadeyan, J.A., and Oni, S.T. (1994). Dynamic behavior of beams and rectangular plates under moving loads. *Journal of Sound and Vibration*, **182(5)**, 677-695.

Goel, R.P. (1976a). Transverse vibrations of tapered beams. *Journal of Sound and Vibration*, **47(1)**, 1–7. doi:10.1016/0022–460X(76)90403–X

Goel, R.P. (1976b). Free vibrations of a beam–mass system with elastically restrained ends. *Journal of Sound and Vibration*, **47(1)**, 9–14. doi:10.1016/0022–460X(76)90404–1

Grant, D.A. (1975). Vibration frequencies for a uniform beam with one end elastically supported and carrying a mass at the other end. *Journal of Applied Mechanics*, **42(4)**, 878-880. doi:10.1115/1.3423723

Hamada, T.R. (1981). Dynamic analysis of a beam under a moving force: A double Laplace transform solution. *Journal of Sound and Vibration*, **74(2)**, 221–233. doi:10.1016/0022–460X(81)90505–8

Hamarat, M.A., Çalik Karaköse, Ü.H., and Orakdöğen, E. (2012). Seismic analysis of structures resting on two parameter elastic foundation. Proceedings of the 15th World Conference on Earthquake Engineering, 24-28 September. Lisbon, Portugal.

Han, S.M., Benaroya, H., and Wei, T. (1999). Dynamics of transversely vibrating beams using four engineering theories. *Journal of Sound and Vibration*, **225(5)**, 935-988. doi:10.1006/jsvi.1999.2257

Ho, S.H., and Chen, C.K. (1998). Analysis of general elastically end restrained non–uniform beams using differential transform. *Applied Mathematical Modelling*, **22**, 219–234.

Hsu, J.C., Lai, H.Y., and Chen, C.K. (2008). Free vibration of non–uniform Euler–Bernoulli beams with general elastically end constraints using Adomian modified

decomposition method. *Journal of Sound and Vibration*, **318(4–5)**, 965–981.

Huang, M. and Liu, J.K. (2013). Structural method for vibration analysis of the elastically connected double-beam system. *Advances in Structural Engineering*, **16**, 365–377.

Hussein, M.F.M., and Hunt, H.E.M. (2006). Modelling of floating-slab tracks with continuous slabs under oscillating moving loads. *Journal of Sound and Vibration*, **297 (1–2)**, 37–54. doi:10.1016/j.jsv.2006.03.026

Irie, T., Yamada G., and Kobayashi, Y. (1982). The steady-state response of an internally damped double-beam system interconnected by several springs. *The Journal of the Acoustical Society of America*, **71(5)**, 1155—1162.

Jun, L., and Hongxing, H. (2008). Dynamic stiffness vibration analysis of an elastically connected three-beam system. *Applied Acoustics*, **69(7)**, 591-600.

Kaya, M.O. (2006). Free vibration analysis of a rotating Timoshenko beam by differential transform method. *Aircraft Engineering and Aerospace Technology: An International Journal*, **78(3)**, 194–203.

Kelly S.G., and Srinivas, S. (2009). Free vibrations of elastically connected stretched beams. *Journal of Sound and Vibration*, **326(3-5)**, 883–893. doi:10.1016/j.jsv.2009.06.004

Kessel, P.G. (1966). Resonances excited in an elastically connected double–beam system by a cyclic moving load. *The Journal of Acoustical Society of America*, **40**, 684–687.

Kessel, P.G., and Raske, T.F. (1967). Damped response of an elastically connected double-beam system due to a cyclic moving load. *The Journal of the Acoustical Society of America*, **42(4)**, 873–881. doi:10.1121/1.1910661

Kim, H.K., and Kim, M.S. (2001). Vibration of beams with generally restrained boundary conditions using Fourier series. *Journal of Sound and Vibration*, **245(5)**, 771–784. doi:10.1006/jsvi.2001.3615

King, G.C. (2009). Vibrations and Waves. Great Britain: John Wiley Sons Ltd. ISBN No 978-0-470-01188-1

Kukla, S. (1991). The Green function method in frequency analysis of a beam with intermediate elastic supports. *Journal of Sound and Vibration*, **149(1)**, 154–159. doi:10.1016/0022–460X(91)90920–F

Kukla, S., and Posiadala, B. (1994). Free vibrations of beams with elastically mounted masses. *Journal of Sound and Vibration*, **175(4)**, 557–564. doi:10.1006/jsvi.1994.1345

Kukla, S., and Skalmierski, B. (1994). Free vibration of a system composed of two beams separated by an elastic layer. *Journal of Theoretical and Applied Mechanics*, **32**, 581–590.

Lee, J.K., Jeongn, S., and Lee J. (2014). Natural frequencies for flexural and torsional vibrations of beams on Pasternak foundation. *Soils and Foundations*, **54(6)**, 1202–1211. doi:10.1016/j.sandf.2014.11.013

Li, J., and Hua, H. (2007). Spectral finite element analysis of elastically connected double–beam systems. *Finite Elements in Analysis and Design* **43**, 1155–1168.

Li, X.F., Tang, A.Y., and Xi, L.Y. (2013). Vibration of a Rayleigh cantilever beam with axial force and tip mass. *Journal of Construction Steel Research*, **80**, 15–22.

Li, Y.X., Hu, Z.J., and Sun, L.Z. (2016). Dynamical behavior of a double-beam system interconnected by a viscoelastic layer. *International Journal of Mechanical Sciences*, **105**, 291–303. doi:10.1016/j.ijmecsci.2015.11.023

Liu, Y., and Gurram, C.S. (2009), The use of He's variational iteration method for obtaining the free vibration of an Euler–Bernoulli beam. *Mathematical and Computer Modelling*, **50**, 1545—1552. doi:10.1016/j.mcm.2009.09.005

Malik, M., and Dang, H.H. (1998). Vibration analysis of continuous systems by differential transformation. *Applied Mathematics and Computation*, **96(1)**, 17–26.

Mao, Q. (2012). Free vibration analysis of elastically connected multiple-beams by using the Adomian modified decomposition method. *Journal of Sound and Vibration*, **331(11)**, 2532–2542. doi:10.1016/j.jsv.2012.01.028

Mao, Q., and Wattanasakulpong, N. (2015). Vibration and stability of a double-beam system interconnected by an elastic foundation under conservative and nonconservative axial forces. *International Journal of Mechanical Sciences*, **93**, 1–7.

Maurizi, M.J., Rossi, R.E., and Reyes, J.A. (1976). Vibration frequencies for a uniform beam with one end spring–hinged and subjected to a translational restraint at the other end. *Journal of Sound and Vibration*, **48(4)**, 565–568. doi:10.1016/0022–460X(76)90559–9

Mehri, B., Davar, A., and Rahmani, O. (2009). Dynamic Green function solution of beams under a moving load with different boundary conditions. *Transaction B: Mechanical Engineering*, **16(3)**, 273-279.

Meirovitch, L. (2001). Fundamentals of Vibrations. International Edn., Singapore: McGraw–Hill. ISBN No 0–07–288180–1

Michaltsos, G., Sophianopoulos, G., and Kounadis, A.N. (1996). The effect of a moving mass and other parameters on the dynamic response of a simply supported beam. *Journal of Sound and Vibration*, **191(3)**, 357–362. doi:10.1006/jsvi.1996.0127

Mirzabeigy, A. (2014). Semi-analytical approach for free vibration analysis of variable cross-section beams resting on elastic foundation and under axial force. *International Journal of Engineering*, **27(3)**, 385-394.

Mirzabeigy, A., Dabbagh V., and Madoliat R., (2017). Explicit formulation for natural frequencies of double-beam system with arbitrary boundary conditions. *Journal of Mechanical Science and Technology*, **31(2)**, 515–521. doi:10.1007/s12206-017-0104-6

Mirzabeigy, A., Madoliat, R., and Vahabi, M. (2016). Free vibration analysis of two parallel beams connected together through variable stiffness elastic layer with elastically restrained ends. *Advances in Structural Engineering*, **20(3)**, 275–287. doi:10.1177/1369433216649395

Mohammadi, N., and Nasirshoaibi, M. (2015). Forced transverse vibration analysis of a Rayleigh double–beam system with a Pasternak middle layer subjected to compressive axial load. *Journal of Vibroengineering*, **17(8)**, 4545–4559.

Motaghian, S., Mofid, M., and Alanjari, P., (2011). Exact solution to free vibration of beams partially supported by an elastic foundation. *Scientia Iranica*, **18(4)**, 861-866. Available from: http://www.sciencedirect.com/science/article/pii/S1026309811001271

Naguleswaran, S. (1991). Vibration of a vertical cantilever with and without axial freedom at clamped end. *Journal of Sound and Vibration*, **146(2)**, 191–198.

Naguleswaran, S. (2004). Transverse vibration of an uniform Euler–Bernoulli beam under linearly varying axial force. *Journal of Sound and Vibration*, **275(1–2)**, 47–57.

Nasirshoaibi, M, Mohammadi, N., and Nasirshoaibi, M. (2015). Forced transverse vibration of a closed double single–walled Carbon nanotube system containing a fluid with effect of compressive axial load. *Shock and Vibration*, 2015, Article ID 435284, 11 pages. doi:10.1155/2015/435284

Oniszczuk, Z. (2000). Free transverse vibrations of elastically connected simply supported double-beam complex system. *Journal of Sound and Vibration*, **232(2)**, 287–403. doi:10.1006/jsvi.1999.2744

Oniszczuk, Z. (2003). Forced transverse vibrations of an elastically connected complex simply supported double–beam system. *Journal of Sound and Vibration*, **264**, 273–286.

Ozgumus, O.O., and Kaya, M.O. (2006). Flapwise bending vibration analysis of a rotating tapered cantilever Bernoulli–Euler beam by differential transform method. *Journal of Sound and Vibration*, **289**, 413–420.

Palmeri, A., and Adhikari, S. (2011). A Galerkin–type state–space approach for transverse vibrations of slender double–beam systems with viscoelastic inner layer. *Journal of Sound and Vibration*, **330**, 6372–6486.

Palmeri, A., and Ntotsios, E. (2016). Transverse vibrations of viscoelastic sandwich beams via Galerkin-based state-space approach. *Journal of Engineering Mechanics*, **142(7)**, 04016036. doi:10.1061/(ASCE)EM.1943-7889.0001069

Pavlović, R., Kozić, P., and Pavlović, I. (2012). Dynamic stability and instability of a double-beam system subjected to random forces. *International Journal of Mechanical Sciences*, **62**, 111-119. doi:10.1016/j.ijmecsci.2012.06.004

Rao, G.V. (2000). Linear dynamics of an elastic beam under moving loads. *Journal of Vibration and Acoustics-Transactions of the ASME*, **122(3)**, 281-289.

Rao, S.S. (1974). Natural vibrations of systems of elastically connected Timoshenko beams. *The Journal of the Acoustical Society of America*, **55(6)**, 1232–1237.

Rao, S.S. (2004). Mechanical Vibrations, 5th Edn., Upper Saddle River: Prentice Hall. ISBN No. 978–0–13–212819–3

Rezaiee–Pajand, M., and Hozhabrossadati, S.M. (2016). Free vibration analysis of a double–beam system joined by a mass–spring device. *Journal of Vibration and Control*, **22(13)**, 3004-3017. Available from: jvc.sagepub.com doi:10.1177/1077546314557853

Seelig, J.M., and Hoppmann II, W.H. (1964a). Normal mode vibrations of systems of elastically connected parallel bars. *Journal of the Acoustical Society of America*, **36**, 93–99. doi:10.1121/1.1918919

Seelig, J.M., and Hoppmann II, W.H. (1964b). Impact on an elastically connected double-beam system. *Journal of Applied Mechanics*, **31(4)**, 621–626.

Şimşek, M., and Cansiz, S. (2012). Dynamics of elastically connected double-functionally graded beam systems with different boundary conditions under action of a moving harmonic load. *Composite Structures*, **94**, 2861–2878. doi:10.1016/j.compstruct.2012.03.016

Stojanović, V., and Kozić, P. (2012). Forced transverse vibration of Rayleigh and Timoshenko double-beam system with effect of compressive axial load. *International Journal of Mechanical Sciences*, **60**, 59–71.

Sun, L. (2001). A closed-form solution of a Bernoulli-Euler beam on a viscoelastic foundation under harmonic line loads. *Journal of Sound and Vibration*, **242(4)**, 619–627. doi:10.1006/jsvi.2000.3376

Tang, A.–Y, Li, X.–F., Wu, J.–X., and Lee, K.Y. (2015). Flapwise bending vibration of rotating tapered Rayleigh cantilever beams. *Journal of Constructional Steel Research*, **112**, 1–9.

Vu, H.V., Ordóñez, A.M., and Karnopp, B.H. (2000). Vibration of a double-beam system. *Journal of Sound and Vibration*, **229(4)**, 807–822.

Wang, J.T.–S., and Lin, C.–C. (1996). Dynamic analysis of generally supported beams using Fourier series. *Journal of Sound and Vibration*, **196(3)**, 285–293. Available from: http://www.sciencedirect.com/science/article/pii/S0022460X96904848

Wu, J–J, Whittaker, A.R., and Cartmell, M.P. (2001). Dynamic responses of structures to moving bodies using combined finite element and analytical methods. *International Journal of Mechanical Sciences*, **43(11)**, 2555–2579. doi:10.1016/S0020–7403(01)00054–6

Xiaobin, L., Shuangxi, X., Weiguo, W., and Jun, L. (2014). An exact dynamic stiffness matrix for axially loaded double-beam systems. *Sadhana*, **39(3)**, 607-623. doi:10.1007/s12046-013-0214-5

Xin, T., and Gao, L. (2011). Reducing slab track vibration into bridge using elastic materials in high speed railway. *Journal of Sound and Vibration*, **330(10**, 2237-2248.

Yeih, W., Chen, J.T., and Chang, C.M. (1999). Applications of dual MRM for determining the natural frequencies and natural modes of an Euler–Bernoulli beam using the singular value decomposition method. *Engineering Analysis with Boundary Elements*, **23(4)**, 339–360. doi:10.1016/S0955–7997(98)00084–8

Zhang, Y.Q., Lu, Y., and Ma, G.W. (2008a). Effect of compressive axial load on forced transverse vibrations of a double–beam system. *International Journal of Mechanical Sciences*, **50**, 299–305.

Zhang, Y.Q., Y. Lu., Y., Wang, S.L., and Liu, X. (2008b). Vibration and buckling of a double–beam system under compressive axial loading. *Journal of Sound and Vibration*, **318**, 341–352.

Zamorska, I. (2010). Free transverse vibrations of non–uniform beams. *Scientific Research of the Institute of Mathematics and Computer Science*, **9(2)**, 243–249.

APPENDIX I

MAPLE CODE FOR EVALUATION OF NATURAL FREQUENCIES

```
restart;
Typesetting:-Settings(functionassign = false):
with(Physics):
Setup(mathematicalnotation = true):
E[1]:= 10^10: E[2]:= 10^10:
A[1](0):= 5*10^(-2): A[2](0):= 5*10^(-2):
J[1](0):= 4*10^(-4); J[2](0):= 4*10^(-4);
rho[1]:= 2*10^3: rho[2]:= 2*10^3: k:= 2*10^5: G:= 100: L:= 10
J[1](xi):=(1-beta*xi)^(3): J[2](xi):=(1-beta*xi)^(3):
J[1](1):= eval(J[1](xi), xi = 1);
J[2](1):= eval(J[2](xi), xi=1):
kappa[1]:= k*L^4/(E[1]*J[1](0)):
kappa[2]:= k*L^4/(E[2]*J[2](0)):
g[1]:= (G.(L^2))/(E[1]*J[1](0)):
g[2]:= (G.(L^2))/(E[2]*J[2](0)): r[0] := 0:
gamm1:= rho[1]*A[1](0)*L^4/(E[1]*J[1](0)):
gamm2:= rho[2]*A[2](0)*L^4/(E[2]*J[2](0)):
Lambda[1]:= r[0]*J[1](0)/(L^2*A[1](0)):
Lambda[2]:= r[0]*J[2](0)/(L^2*A[2](0)):
J[1](L):=eval(J[1](xi),xi=L):
J[2](L):=eval(J[2](xi),xi=L):
Theta[1]:= (eval(diff(J[1](xi), xi), xi= 1))/J[1](1):
Theta[2]:= (eval(diff(J[2](xi), xi), xi= 1))/J[2](1):
K[1,LT]:= 10^18; K[2, LT]:= 10^18:
K[1,RT]:= 10^18; K[2, RT]:= 10^18:
K[1,LR]:= 0; K[2, LR]:= 0:
K[1,RR]:= 0; K[2, RR]:= 0:
Psi[1,LT]:= K[1, LT]*L^3/(E[1]*J[1](0)):
Psi[2,LT]:= K[2, LT]*L^3/(E[2]*J[2](0)):
Psi[1,RT]:= K[1, RT]*L^3/(E[1]*J[1](L)):
Psi[2,RT]:= K[2, RT]*L^3/(E[2]*J[2](L)):
Psi[1,LR]:= K[1, LR]*L/(E[1]*J[1](0)):
Psi[2,LR]:= K[2, LR]*L/(E[2]*J[2](0)):
Psi[1,RR]:= K[1, RR]*L/(E[1]*J[1](L)):
Psi[2,RR]:= K[2, RR]*L/(E[2]*J[2](L)):
```

```
beta:= 0.50:
Y[1](0), Y[1](1), Y[2](0), Y[2](1):= c[1], c[2], c[3], c[4]:
Y[1](2):= solve(factorial(2)*Y[1](2)-Psi[1,LR]*Y[1](1)=0,
            Y[1](2)):
Y[2](2):= solve(factorial(2)*Y[2](2)-Psi[2,LR]*Y[2](1) = 0,
            Y[2](2)):
Y[1](3):= solve(factorial(3)*Y[1](3)
        +2*(eval(diff(J[1](xi), xi), xi = 0))*Y[1](2)
+gamm1*omega^2*Lambda[1]*Y[1](1)+Psi[1,LT]*Y[1](0) = 0,
    Y[1](3)):
Y[2](3):= solve(factorial(3)*Y[2](3)
        +2*(eval(diff(J[2](xi), xi), xi = 0))*Y[2](2)
        +gamm2*omega^2*Lambda[2]*Y[2](1)+Psi[2,LT]*Y[2](0) = 0,
    Y[2](3)):
B[r-s]:= -beta^3*KroneckerDelta[r, s+3]
        +3*beta^2*KroneckerDelta[r, s+2]
-3*beta*KroneckerDelta[r, s+1]
+KroneckerDelta[r, s]:
B1[r-s]:= beta^2*KroneckerDelta[r, s+2]
         -2*beta*KroneckerDelta[r, s+1]
        +KroneckerDelta[r, s]:
B2[r-s]:= -beta*KroneckerDelta[r, s+1]
          +KroneckerDelta[r, s]:
A1:= sum(B[r-s]*(s+1)*(s+2)*(s+3)*(s+4)*Y[1](s+4),
       s = 0 .. r)-6*beta*(sum(B1[r-s]*(s+1)*(s+2)*(s+3)
 *Y[1](s+3), s = 0 .. r))
   +6*beta^2*(sum(B2[r-s]*(s+1)*(s+2)*Y[1](s+2),
  s = 0 .. r))-gamm1*omega^2*(sum(B2[r-s]*Y[1](s),
s = 0 .. r))+gamm1*omega^2*Lambda[1]
*(sum(B[r-s]*(s+1)*(s+2)*Y[1](s+2), s = 0 .. r)
-3*beta*(sum(B1[r-s]*(s+1)*Y[1](s+1), s = 0 .. r)))
  +kappa[1]*(Y[1](r)-Y[2](r))-g[1]*(r+1)*(r+2)
*(Y[1](r+2)-Y[2](r+2)) = 0:
A2:= sum(B[r-s]*(s+1)*(s+2)*(s+3)*(s+4)*Y[2](s+4), s = 0 .. r)
     -6*beta*(sum(B1[r-s]*(s+1)*(s+2)*(s+3)*Y[2](s+3),
 s = 0 .. r))+6*beta^2*(sum(B2[r-s]*(s+1)*(s+2)
*Y[2](s+2), s = 0 .. r))-gamm2*omega^2*(sum(B2[r-s]
*Y[2](s), s = 0 .. r))+gamm2*omega^2*Lambda[2]
*(sum(B[r-s]*(s+1)*(s+2)*Y[2](s+2), s = 0 .. r)-3*beta
```

```
*(sum(B1[r-s]*(s+1)*Y[2](s+1), s = 0 .. r)))
+kappa[2]*(Y[2](r)-Y[1](r))-g[2]*(r+1)*(r+2)
*(Y[2](r+2)-Y[1](r+2)) = 0:
m:= 46:
for i from 0 to m do
Y[1](i+4):= solve(eval(A1, r = i), Y[1](i+4));
Y[2](i+4):= solve(eval(A2, r = i), Y[2](i+4))
end do:
M:= m+4;
M:= 50
C:= sum(r*(r-1)*Y[1](r), r = 0 .. M-1)
   +Psi[1, RR]*(sum(r*Y[1](r), r = 0 .. M-1)):
C1:= sum(r*(r-1)*Y[1](r), r = 0 .. M)
   +Psi[1, RR]*(sum(r*Y[1](r), r = 0 .. M)):
F:= sum(r*(r-1)*Y[2](r), r = 0 .. M-1)
   +Psi[2, RR]*(sum(r*Y[2](r), r = 0 .. M-1)):
F1:= sum(r*(r-1)*Y[2](r), r = 0 .. M)
   +Psi[2, RR]*(sum(r*Y[2](r), r = 0 .. M)):
G1:= sum(r*(r-1)*(r-2)*Y[1](r), r = 0 .. M-1)
   +Theta[1]*(sum(r*(r-1)*Y[1](r), r = 0 .. M-1))
 +Lambda[1]*gamm1*omega^2*(sum(r*Y[1](r), r = 0 .. M-1))
 -Psi[1, RT]*(sum(Y[1](r), r = 0 .. M-1)):
G2:= sum(r*(r-1)*(r-2)*Y[1](r), r = 0 .. M)
   +Theta[1]*(sum(r*(r-1)*Y[1](r), r = 0 .. M))
 +Lambda[1]*gamm1*omega^2*(sum(r*Y[1](r), r = 0 .. M))
 -Psi[1, RT]*(sum(Y[1](r), r = 0 .. M)):
H:= sum(r*(r-1)*(r-2)*Y[2](r), r = 0 .. M-1)
   +Theta[2]*(sum(r*(r-1)*Y[2](r), r = 0 .. M-1))
 +Lambda[2]*gamm2*omega^2*(sum(r*Y[2](r), r = 0 .. M-1))
 -Psi[2, RT]*(sum(Y[2](r), r = 0 .. M-1)):
H1:= sum(r*(r-1)*(r-2)*Y[2](r), r = 0 .. M)
   +Theta[2]*(sum(r*(r-1)*Y[2](r), r = 0 .. M))
 +Lambda[2]*gamm2*omega^2*(sum(r*Y[2](r), r = 0 .. M))
 -Psi[2, RT]*(sum(Y[2](r), r = 0 .. M)):
f11[M-1], f12[M-1]:= coeff(C, c[1]), coeff(C, c[2]):
f13[M-1], f14[M-1]:= coeff(C, c[3]), coeff(C, c[4]):
f21[M-1], f22[M-1]:= coeff(F, c[1]), coeff(F, c[2]):
f23[M-1], f24[M-1]:= coeff(F, c[3]), coeff(F, c[4]);
f31[M-1], f32[M-1]:= coeff(G1, c[1]), coeff(G1, c[2]):
```

```
f33[M-1], f34[M-1]:= coeff(G1, c[3]), coeff(G1, c[4]):
f41[M-1], f42[M-1]:= coeff(H, c[1]), coeff(H, c[2]):
f43[M-1], f44[M-1]:= coeff(H, c[3]), coeff(H, c[4]):
f11[M], f12[M]:= coeff(C1, c[1]), coeff(C1, c[2]):
f13[M], f14[M]:= coeff(C1, c[3]), coeff(C1, c[4]):
f21[M], f22[M]:= coeff(F1, c[1]), coeff(F1, c[2]):
f23[M], f24[M]:= coeff(F1, c[3]), coeff(F1, c[4]):
f31[M], f32[M]:= coeff(G2, c[1]), coeff(G2, c[2]):
f33[M], f34[M]:= coeff(G2, c[3]), coeff(G2, c[4]):
f41[M], f42[M]:= coeff(H1, c[1]), coeff(H1, c[2]):
f43[M], f44[M]:= coeff(H1, c[3]), coeff(H1, c[4]):
with(Student[LinearAlgebra]):
XticMatrix[M-1]:= <<f11[M-1], f21[M-1], f31[M-1], f41[M-1]>
       |<f12[M-1], f22[M-1], f32[M-1], f42[M-1]>
 |<f13[M-1], f23[M-1], f33[M-1], f43[M-1]>
 |<f14[M-1], f24[M-1], f34[M-1], f44[M-1]>>:
XticMatrix[M]:= <<f11[M], f21[M], f31[M], f41[M]>
       |<f12[M], f22[M], f32[M], f42[M]>
 |<f13[M], f23[M], f33[M], f43[M]>
 |<f14[M], f24[M], f34[M], f44[M]>>:
A2[M-1]:= Determinant(XticMatrix[M-1]) = 0:
A2[M]:= Determinant(XticMatrix[M]) = 0:
omega[M-1]:= fsolve(A2[M-1], omega);
omega[49]:= -6.285557669*10^8, -6.284248984*10^8, -1298.492326,
         -1247.871753, -694.4936865, -355.4439026, -242.0994957,
 -231.0958517, -150.2546743, -129.9596919, -95.36822285,
 -74.32122731, -57.90368216, -14.24306578, 14.24306578,
 57.90368216, 74.32122731, 95.36822285, 129.9596919,
 150.2546743, 231.0958517, 242.0994957, 355.4439026,
 694.4936865, 1247.871753, 1298.492326, 6.284248984*10^8,
 6.285557669*10^8
omega[M]:= fsolve(A2[M], omega);
omega[50]:= -5.254428516*10^8, -5.253114128*10^8, -1734.354468,
         -1726.193667, -563.1193873, -472.9214141, -242.5383188,
 -230.7967972, -150.2584998, -129.9583344, -95.36829888,
 -74.32121786, -57.90368219, -14.24306568, 14.24306568,
 57.90368219, 74.32121786, 95.36829888, 129.9583344,
 150.2584998, 230.7967972, 242.5383188, 472.9214141,
 563.1193873, 1726.193667, 1734.354468, 5.253114128*10^8,
```

```
5.254428516*10^8
```

APPENDIX II

MAPLE CODE FOR PLOTTTING OF MODE SHAPES

```
restart;
Typesetting:-Settings(functionassign = false):
with(Physics):
Setup(mathematicalnotation = true):
E[1]:= 10^10: E[2]:= 10^10:
A[1](0):= 5*10^(-2): A[2](0):= 5*10^(-2):
J[1](0):= 4*10^(-4); J[2](0):= 4*10^(-4);
rho[1]:= 2*10^3: rho[2]:= 2*10^3: k:= 2*10^5: G:= 100: L:= 10
J[1](xi):=(1-beta*xi)^(3): J[2](xi):=(1-beta*xi)^(3):
J[1](1):= eval(J[1](xi), xi = 1);
J[2](1):= eval(J[2](xi), xi=1):
kappa[1]:= k*L^4/(E[1]*J[1](0)):
kappa[2]:= k*L^4/(E[2]*J[2](0)):
g[1]:= (G.(L^2))/(E[1]*J[1](0)):
g[2]:= (G.(L^2))/(E[2]*J[2](0)): r[0] := 0:
gamm1:= rho[1]*A[1](0)*L^4/(E[1]*J[1](0)):
gamm2:= rho[2]*A[2](0)*L^4/(E[2]*J[2](0)):
Lambda[1]:= r[0]*J[1](0)/(L^2*A[1](0)):
Lambda[2]:= r[0]*J[2](0)/(L^2*A[2](0)):
J[1](L):=eval(J[1](xi),xi=L):
J[2](L):=eval(J[2](xi),xi=L):
Theta[1]:= (eval(diff(J[1](xi), xi), xi= 1))/J[1](1):
Theta[2]:= (eval(diff(J[2](xi), xi), xi= 1))/J[2](1):
K[1,LT]:= 10^18; K[2, LT]:= 10^18:
K[1,RT]:= 10^18; K[2, RT]:= 10^18:
K[1,LR]:= 0; K[2, LR]:= 0:
K[1,RR]:= 0; K[2, RR]:= 0:
Psi[1,LT]:= K[1, LT]*L^3/(E[1]*J[1](0)):
Psi[2,LT]:= K[2, LT]*L^3/(E[2]*J[2](0)):
Psi[1,RT]:= K[1, RT]*L^3/(E[1]*J[1](L)):
Psi[2,RT]:= K[2, RT]*L^3/(E[2]*J[2](L)):
Psi[1,LR]:= K[1, LR]*L/(E[1]*J[1](0)):
Psi[2,LR]:= K[2, LR]*L/(E[2]*J[2](0)):
Psi[1,RR]:= K[1, RR]*L/(E[1]*J[1](L)):
Psi[2,RR]:= K[2, RR]*L/(E[2]*J[2](L)):
```

```
beta:= 0.50:
Y[1](0), Y[1](1), Y[2](0), Y[2](1):= c[1], c[2], c[3], c[4]:
Y[1](2):= solve(factorial(2)*Y[1](2)-Psi[1,LR]*Y[1](1)=0,
            Y[1](2)):
Y[2](2):= solve(factorial(2)*Y[2](2)-Psi[2,LR]*Y[2](1) = 0,
            Y[2](2)):
Y[1](3):= solve(factorial(3)*Y[1](3)
        +2*(eval(diff(J[1](xi), xi), xi = 0))*Y[1](2)
+gamm1*omega^2*Lambda[1]*Y[1](1)+Psi[1,LT]*Y[1](0) = 0,
    Y[1](3)):
Y[2](3):= solve(factorial(3)*Y[2](3)
        +2*(eval(diff(J[2](xi), xi), xi = 0))*Y[2](2)
        +gamm2*omega^2*Lambda[2]*Y[2](1)+Psi[2,LT]*Y[2](0) = 0,
    Y[2](3)):
B[r-s]:= -beta^3*KroneckerDelta[r, s+3]
        +3*beta^2*KroneckerDelta[r, s+2]
-3*beta*KroneckerDelta[r, s+1]
+KroneckerDelta[r, s]:
B1[r-s]:= beta^2*KroneckerDelta[r, s+2]
         -2*beta*KroneckerDelta[r, s+1]
        +KroneckerDelta[r, s]:
B2[r-s]:= -beta*KroneckerDelta[r, s+1]
          +KroneckerDelta[r, s]:
A1:= sum(B[r-s]*(s+1)*(s+2)*(s+3)*(s+4)*Y[1](s+4),
       s = 0 .. r)-6*beta*(sum(B1[r-s]*(s+1)*(s+2)*(s+3)
 *Y[1](s+3), s = 0 .. r))
   +6*beta^2*(sum(B2[r-s]*(s+1)*(s+2)*Y[1](s+2),
  s = 0 .. r))-gamm1*omega^2*(sum(B2[r-s]*Y[1](s),
s = 0 .. r))+gamm1*omega^2*Lambda[1]
*(sum(B[r-s]*(s+1)*(s+2)*Y[1](s+2), s = 0 .. r)
-3*beta*(sum(B1[r-s]*(s+1)*Y[1](s+1), s = 0 .. r)))
  +kappa[1]*(Y[1](r)-Y[2](r))-g[1]*(r+1)*(r+2)
*(Y[1](r+2)-Y[2](r+2)) = 0:
A2:= sum(B[r-s]*(s+1)*(s+2)*(s+3)*(s+4)*Y[2](s+4), s = 0 .. r)
     -6*beta*(sum(B1[r-s]*(s+1)*(s+2)*(s+3)*Y[2](s+3),
 s = 0 .. r))+6*beta^2*(sum(B2[r-s]*(s+1)*(s+2)
*Y[2](s+2), s = 0 .. r))-gamm2*omega^2*(sum(B2[r-s]
*Y[2](s), s = 0 .. r))+gamm2*omega^2*Lambda[2]
*(sum(B[r-s]*(s+1)*(s+2)*Y[2](s+2), s = 0 .. r)-3*beta
```

```
*(sum(B1[r-s]*(s+1)*Y[2](s+1), s = 0 .. r)))
+kappa[2]*(Y[2](r)-Y[1](r))-g[2]*(r+1)*(r+2)
*(Y[2](r+2)-Y[1](r+2)) = 0:
m:= 46:
for i from 0 to m do
Y[1](i+4):= solve(eval(A1, r = i), Y[1](i+4));
Y[2](i+4):= solve(eval(A2, r = i), Y[2](i+4))
end do:
M:= m+4;
M:= 50
C:= sum(r*(r-1)*Y[1](r), r = 0 .. M-1)
   +Psi[1, RR]*(sum(r*Y[1](r), r = 0 .. M-1)):
C1:= sum(r*(r-1)*Y[1](r), r = 0 .. M)
   +Psi[1, RR]*(sum(r*Y[1](r), r = 0 .. M)):
F:= sum(r*(r-1)*Y[2](r), r = 0 .. M-1)
   +Psi[2, RR]*(sum(r*Y[2](r), r = 0 .. M-1)):
F1:= sum(r*(r-1)*Y[2](r), r = 0 .. M)
   +Psi[2, RR]*(sum(r*Y[2](r), r = 0 .. M)):
G1:= sum(r*(r-1)*(r-2)*Y[1](r), r = 0 .. M-1)
   +Theta[1]*(sum(r*(r-1)*Y[1](r), r = 0 .. M-1))
 +Lambda[1]*gamm1*omega^2*(sum(r*Y[1](r), r = 0 .. M-1))
 -Psi[1, RT]*(sum(Y[1](r), r = 0 .. M-1)):
G2:= sum(r*(r-1)*(r-2)*Y[1](r), r = 0 .. M)
   +Theta[1]*(sum(r*(r-1)*Y[1](r), r = 0 .. M))
 +Lambda[1]*gamm1*omega^2*(sum(r*Y[1](r), r = 0 .. M))
 -Psi[1, RT]*(sum(Y[1](r), r = 0 .. M)):
H:= sum(r*(r-1)*(r-2)*Y[2](r), r = 0 .. M-1)
   +Theta[2]*(sum(r*(r-1)*Y[2](r), r = 0 .. M-1))
 +Lambda[2]*gamm2*omega^2*(sum(r*Y[2](r), r = 0 .. M-1))
 -Psi[2, RT]*(sum(Y[2](r), r = 0 .. M-1)):
H1:= sum(r*(r-1)*(r-2)*Y[2](r), r = 0 .. M)
   +Theta[2]*(sum(r*(r-1)*Y[2](r), r = 0 .. M))
 +Lambda[2]*gamm2*omega^2*(sum(r*Y[2](r), r = 0 .. M))
 -Psi[2, RT]*(sum(Y[2](r), r = 0 .. M)):
f11[M-1], f12[M-1]:= coeff(C, c[1]), coeff(C, c[2]):
f13[M-1], f14[M-1]:= coeff(C, c[3]), coeff(C, c[4]):
f21[M-1], f22[M-1]:= coeff(F, c[1]), coeff(F, c[2]):
f23[M-1], f24[M-1]:= coeff(F, c[3]), coeff(F, c[4]);
f31[M-1], f32[M-1]:= coeff(G1, c[1]), coeff(G1, c[2]):
```

```
f33[M-1], f34[M-1]:= coeff(G1, c[3]), coeff(G1, c[4]):
f41[M-1], f42[M-1]:= coeff(H, c[1]), coeff(H, c[2]):
f43[M-1], f44[M-1]:= coeff(H, c[3]), coeff(H, c[4]):
f11[M], f12[M]:= coeff(C1, c[1]), coeff(C1, c[2]):
f13[M], f14[M]:= coeff(C1, c[3]), coeff(C1, c[4]):
f21[M], f22[M]:= coeff(F1, c[1]), coeff(F1, c[2]):
f23[M], f24[M]:= coeff(F1, c[3]), coeff(F1, c[4]):
f31[M], f32[M]:= coeff(G2, c[1]), coeff(G2, c[2]):
f33[M], f34[M]:= coeff(G2, c[3]), coeff(G2, c[4]):
f41[M], f42[M]:= coeff(H1, c[1]), coeff(H1, c[2]):
f43[M], f44[M]:= coeff(H1, c[3]), coeff(H1, c[4]):
with(Student[LinearAlgebra]):
XticMatrix[M-1]:= <<f11[M-1], f21[M-1], f31[M-1], f41[M-1]>
       |<f12[M-1], f22[M-1], f32[M-1], f42[M-1]>
 |<f13[M-1], f23[M-1], f33[M-1], f43[M-1]>
 |<f14[M-1], f24[M-1], f34[M-1], f44[M-1]>>:
XticMatrix[M]:= <<f11[M], f21[M], f31[M], f41[M]>
       |<f12[M], f22[M], f32[M], f42[M]>
 |<f13[M], f23[M], f33[M], f43[M]>
 |<f14[M], f24[M], f34[M], f44[M]>>:
A2[M-1]:= Determinant(XticMatrix[M-1]) = 0:
A2[M]:= Determinant(XticMatrix[M]) = 0:
omega[M-1]:= fsolve(A2[M-1], omega);
omega[49]:= -6.285557669*10^8, -6.284248984*10^8, -1298.492326,
         -1247.871753, -694.4936865, -355.4439026, -242.0994957,
 -231.0958517, -150.2546743, -129.9596919, -95.36822285,
 -74.32122731, -57.90368216, -14.24306578, 14.24306578,
 57.90368216, 74.32122731, 95.36822285, 129.9596919,
 150.2546743, 231.0958517, 242.0994957, 355.4439026,
 694.4936865, 1247.871753, 1298.492326, 6.284248984*10^8,
 6.285557669*10^8
omega[M]:= fsolve(A2[M], omega);
omega[50]:= -5.254428516*10^8, -5.253114128*10^8, -1734.354468,
         -1726.193667, -563.1193873, -472.9214141, -242.5383188,
 -230.7967972, -150.2584998, -129.9583344, -95.36829888,
 -74.32121786, -57.90368219, -14.24306568, 14.24306568,
 57.90368219, 74.32121786, 95.36829888, 129.9583344,
 150.2584998, 230.7967972, 242.5383188, 472.9214141,
 563.1193873, 1726.193667, 1734.354468, 5.253114128*10^8,
```

```
 5.254428516*10^8
f11[M]:= eval(coeff(C1, c[1]), omega = 14.2431):
f12[M]:= eval(coeff(C1, c[2]), omega = 14.2431):
f13[M]:= eval(coeff(C1, c[3]), omega = 14.2431):
f14[M]:= eval(coeff(C1, c[4]), omega = 14.2431):
f21[M]:= eval(coeff(F1, c[1]), omega = 14.2431):
f22[M]:= eval(coeff(F1, c[2]), omega = 14.2431):
f23[M]:= eval(coeff(F1, c[3]), omega = 14.2431):
f24[M]:= eval(coeff(F1, c[4]), omega = 14.2431):
f31[M]:= eval(coeff(G2, c[1]), omega = 14.2431):
f32[M]:= eval(coeff(G2, c[2]), omega = 14.2431):
f33[M]:= eval(coeff(G2, c[3]), omega = 14.2431):
f34[M]:= eval(coeff(G2, c[4]), omega = 14.2431):
f41[M]:= eval(coeff(H1, c[1]), omega = 14.2431):
f42[M]:= eval(coeff(H1, c[2]), omega = 14.2431):
f43[M]:= eval(coeff(H1, c[3]), omega = 14.2431):
f44[M]:= eval(coeff(H1, c[4]), omega = 14.2431);
Delta := eval(Determinant(<<f11[M], f21[M], f31[M])>
|<f12[M], f22[M], f32[M]>
|<f13[M], f23[M], f33[M]>>), omega = 14.2431):
y[1](xi)[M]:= subs([omega = 14.2431,
    c[1] = (Determinant(<<-f14[M], -f24[M], -f34[M]>
|f12[M], f22[M], f32[M]>|<f13[M], f23[M], f33[M]>>))/Delta,
c[2] = (Determinant(<<f11[M], f21[M], f31[M]>
|<-f14[M], -f24[M], -f34[M]>
|<f13[M], f23[M], f33[M]>>))/Delta,
c[3] = (Determinant(<<f11[M], f21[M], f31[M]>
|f12[M], f22[M], f32[M]>
|-f14[M], -f24[M], -f34[M]>>))/Delta, c[4] = 1],
sum(xi^r*Y[1](r), r = 0 .. M));
y[2](xi)[M]:= subs([omega = 14.2431,
    c[1] = (Determinant(<<-f14[M], -f24[M], -f34[M]>
|f12[M], f22[M], f32[M]>|<f13[M], f23[M], f33[M]>>))/Delta,
c[2] = (Determinant(<<f11[M], f21[M], f31[M]>
|<-f14[M], -f24[M], -f34[M]>|<f13[M], f23[M], f33[M]>>))/Delta,
c[3] = (Determinant(<<f11[M], f21[M], f31[M]>
|f12[M], f22[M], f32[M]>
|-f14[M], -f24[M], -f34[M]>>))/Delta, c[4] = 1],
sum(xi^r*Y[2](r), r = 0 .. M));
```

```
ynormalizedmodeshapefunction[upperbeam]:=
    y[1](xi)[M]/(int(y[1](xi)[M]^2, xi = 0 .. 1)):
ynormalizedmodeshapefunction[lowerbeam]:=
    y[1](xi)[M]/(int(y[1](xi)[M]^2, xi = 0 .. 1)):
plot([ynormalizedmodeshapefunction[upperbeam],
   ynormalizedmodeshapefunction[lowerbeam]], xi = 0 .. 1,
 axes = boxed, legend = ["Upper beam", "Lower beam"],
 labels = ["xi", "1st mode shape: omega = 14.2431"],
 labeldirections = ["horizontal", "vertical"],
 labelfont = ["ROMAN", 18], linestyle = [solid, longdash],
 axesfont = ["ROMAN", "ROMAN", 12],
 legendstyle = [font = ["ROMAN", 12], location = top])
```